
SPECTRAL ESTIMATION FOR POINT PROCESSES AND RANDOM FIELDS

A PREPRINT

✉ **J. P. GRAINGER**^{*1}, ✉ **T. A. RAJALA**^{†2}, ✉ **D. J. MURRELL**^{‡3}, and ✉ **S. C. OLHEDE**^{§1}

¹Institute of Mathematics, École Polytechnique Fédérale de Lausanne, Station 8, 1015 Lausanne, Switzerland

²Natural Resources Institute Finland, 00790 Helsinki, Finland

³Research Department of Genetics, Evolution and Environment, Centre for Biodiversity and Environment Research, University College London, UK

September 3, 2025

ABSTRACT

Spatial variables can be observed in many different forms, such as regularly sampled random fields (lattice data), point processes, and randomly sampled spatial processes. Joint analysis of such collections of observations is clearly desirable, but complicated by the lack of an easily implementable analysis framework. We fill this gap by providing a multitaper analysis framework using coupled discrete and continuous data tapers, combined with the discrete Fourier transform for inference. Using this set of tools is important, as it forms the backbone for practical spectral analysis. In higher dimensions it is important not to be constrained to Cartesian product domains, and so we develop the methodology for spectral analysis using irregular domain data tapers, and the tapered discrete Fourier transform. We discuss its fast implementation, and the asymptotic as well as large finite domain properties. Estimators of partial association between different spatial processes are provided as are principled methods to determine their significance, and we demonstrate their practical utility on a large-scale ecological dataset.

Keywords Spatial point pattern · random field · spectral representation · spatial multitapering · coherence · partial coherence.

1 Introduction

Collections of spatial variables studied in geostatistics, ecology and other spatial sciences involve complex interactions between a variety of different components. Often we need to jointly analyze data of different types, such as spatial point patterns, marked point patterns and realizations of random fields. We therefore need a common framework to include all data types in our analysis. Spectral analysis provides a convenient way to construct notions of correlation and partial correlation between these different types of processes. In this paper, we develop methodology to estimate such quantities for any combination of point patterns, marked point patterns and realizations of random fields, when the processes may be recorded with differing sampling methods, and when the observational region is not necessarily rectangular, but common to all observed spatial variables. Existing methodology, with the exception of that for univariate Gaussian random fields (Andén and Romero, 2020), cannot handle arbitrary observational regions or different sampling mechanisms (including Rajala et al. 2023), and the existing spectral estimation methodology for marked point processes can be seen to be biased. All of these issues are resolved by the novel methodology that we propose in this paper.

Probabilistically, a spectral representation for general multivariate random measures is available (Brillinger, 1972; Daley and Vere-Jones, 2003), providing the theoretical background for our work. However, statistical estimation of

^{*}jake.grainger@epfl.ch

[†]tuomas.rajala@iki.fi

[‡]d.murrell@ucl.ac.uk

[§]sofia.olhede@epfl.ch

the spectral density matrix function for such processes has not yet been developed. Our introduction of multitapering is a necessary step to develop statistical methodology for the spectral analysis of multivariate spatial data. We show in simulations that the large sample theory developed in this paper is applicable to data which is similar to data of practical interest, on which we also illustrate our methodology. This enables us to use principled thresholds to determine significance, and gives confidence in the quality of the proposed methodology.

Although methodology for spectral estimation exists for spatial point processes (Bartlett, 1964; Diggle et al., 1987; Mugglestone and Renshaw, 1996b,a; Rajala et al., 2023) and random fields (Bandyopadhyay and Lahiri, 2009; Matsuda and Yajima, 2009) separately, the extension to multivariate spatial data is more challenging. Kanaan et al. (2008) proposed an estimator for the cross-spectral density function between a random field and an unmarked point pattern, that is limited to random fields continuously sampled in a rectangular region. Eckardt and Mateu (2019c) proposed a periodogram when the random field is recorded on an integer grid within a rectangular domain, but do not study its properties or discuss smoothing or tapering. In reality, random fields can never be sampled continuously, and often we have multiple random fields recorded on different grids. Handling this is not trivial, and getting it wrong can result in substantial bias in the estimated spectra. We also consider marked point processes, where each point is associated with an additional random variable called a mark (e.g. size of a tree). A periodogram estimator has been proposed in the marked setting (Renshaw, 2002; Eckardt and Mateu, 2019b), however, this estimator is biased (see Appendix S7.1 for details). Hence, several key issues must be resolved to develop a practical, unified framework for spectral analysis of multivariate spatial data.

Whilst Andén and Romero (2020) consider spectral estimation for univariate Gaussian random fields on non-rectangular domains, performing such analysis in the case of multivariate random measures is more challenging. In particular, one first needs to construct continuous families of taper functions, in order to analyse the point processes, and then also build discrete families of taper sequences which are appropriate for each grid used to record the random fields, but that are related to the continuous tapers (otherwise estimates of cross statistics will be biased). We start from the discrete tapers of Simons and Wang (2011) and use these to generate continuous tapers, utilising the low wavenumber concentration already required to retain the same desirable properties. We then construct discrete taper sequences from these continuous tapers, again exploiting the low wavenumber concentration. As a result, we can combine all of these different kinds of data together, with no need for aggregation or interpolation, and requiring no additional tuning parameters beyond the single bandwidth parameter already used for multitaper estimation in the case of time series and random fields (Walden, 2000). This results in a methodology which neatly handles all of these additional complexities presented by the richer class of spatial processes.

Understanding dependence between spatial processes is challenging, making it valuable to have diverse tools for analysing observations. However, existing exploratory methods may fail to clearly reveal underlying processes. A common approach is to model point processes given some covariates and then examines pairwise residual dependence, but this ignores interactions with other point processes in the system. Partial coherence (see Section 2.3) offers a measure of dependence that accounts for all other processes, not just covariates.

Consider an inhomogeneous Poisson process (PP) and two cluster processes (CP1, CP2) that share the Poisson process as a parent but are otherwise independent. Suppose the Poisson process intensity (Λ) is observed as a covariate (see the Appendix for details). Figure 1 illustrates a sample process on an irregular domain (see Section 4.1), along with the inhomogeneous cross-L function (Baddeley et al., 2000), and the partial coherence between processes. These statistics are standardized to zero when no interaction remains after accounting for other processes. Pointwise extrema over 100 replications are shown as bands; the lines correspond to the realization in the top row. The inhomogeneous cross-L function incorrectly suggests interactions among all processes, while partial coherence (which we estimate in this paper) correctly identifies the independence of the cluster processes once the Poisson process is accounted for. Partial coherence also captures the association between the covariate (Λ) and the Poisson process (PP), but not with the cluster processes (CP1, CP2), as expected. This toy example highlights how partial coherence complements existing spatial statistics tools, and why its accurate estimation is essential.

In this paper, we provide a single unified multitaper framework for estimation of the spectra and cross-spectra of random fields, point processes and marked point processes. The methodology is discussed in detail, and we provide theoretical justifications for the proposed estimators. We verify the properties of the proposed estimator through simulation studies, the first of their kind for spectral analysis of multivariate spatial data, and apply the methodology to forest ecology data from Barro Colorado Island (Condit et al., 2019). Several outstanding issues, long eluding the successful development of spectral analysis in this setting are resolved, including the extension to non-rectangular regions, the bias in the marked case, and handling different kinds of grid sampling. We then discuss how to use this framework to compute estimates of coherence and partial coherence between the different processes, with principled significance thresholds. We further demonstrate the promise of spectral analysis to summarize dependence in complex systems, and provide methodology to perform inference.

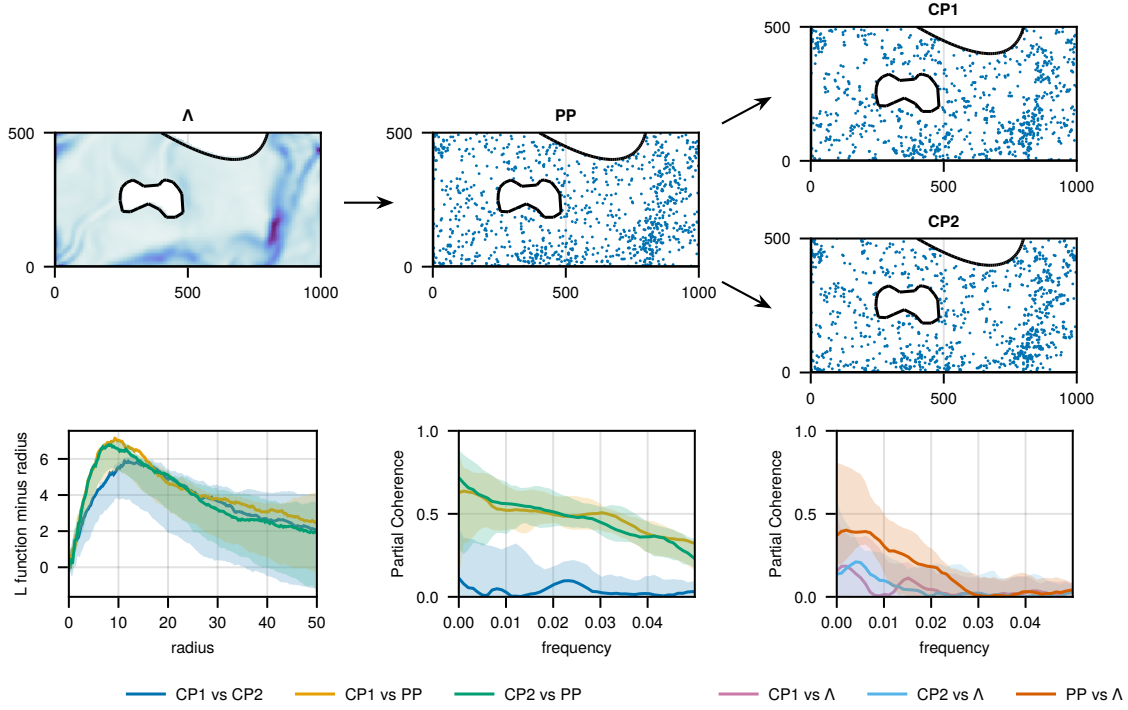


Figure 1: Simulated patterns (top), the inhomogeneous cross-L function (bottom left), and the partial coherence between the point processes (bottom middle) and between the covariate and the processes (bottom right).

For readers from a point process background, Percival and Walden (1993) provide an introduction to spectral analysis and, in particular, the multitaper method. For readers from a time series background, Illian et al. (2008) provide an introduction to point processes. In either case, Chapter 8 of Daley and Vere-Jones (2003) provides a detailed treatment of the spectra of random measures, which is the most relevant theoretical background for this paper.

2 Background

2.1 Basic notation

We write $\mathbb{N} = \{1, 2, \dots\}$ and for $n \in \mathbb{N}$, $[n] = \{1, \dots, n\}$. Given a set A , and a binary operator on A , say $*$, then for $a \in A$ we write $A * a = \{b * a \mid b \in A\}$ for the right coset and $a * A$ for the left coset. For two vectors a and b , we will write $a \circ b$ for the elementwise (Hadamard) product, $a \oslash b$ for elementwise division, and $a \cdot b$ for the dot product. Furthermore, we will write $\prod(a) = \prod_{j=1}^d a_j$ for the product of elements of $a = (a_1, \dots, a_d)^\top$.

2.2 Random measures and spectral density functions

A *point process* is a random set of locations in some space, say \mathbb{R}^d , such that there are finitely many points within a given bounded Borel set (Møller and Waagepetersen, 2003). A point process is said to be *simple* if points do not occur in the same location almost surely. A *marked point process* is a point process with additional information at each of the points, called a *mark*, which we shall take to be real-valued and non-negative. For a marked point process, the point process without the marks is often referred to as the *ground process*. The unmarked case is recovered when the marks are independent and where the conditional distribution of the mark given a point is present at a location, the *mark kernel*, is just a point mass at 1. Let X be the set of random point locations, and $W(x)$ be the mark at x , the point location. The *mark-sum measure*, or *count measure* in the unmarked case (setting $W(x) = 1$), is

$$\xi(A) = \sum_{x \in X \cap A} W(x), \quad A \in \mathcal{B}(\mathbb{R}^d),$$

where $\mathcal{B}(\mathbb{R}^d)$ denotes the Borel sets of \mathbb{R}^d (Daley and Vere-Jones, 2003).

A *random field* is a random function, say Y , on \mathbb{R}^d (Adler, 2010). Assuming the random field is almost surely continuous and non-negative, we can define a random measure from Y by

$$\xi(A) = \int_A Y(u) du, \quad A \in \mathcal{B}(\mathbb{R}^d).$$

The two preceding equations show that random measures provide a unified framework in which to study these different spatial processes (Daley and Vere-Jones, 2003).

Assume that we have P such processes, and augment our previous notation by writing ξ_p for the p th random measure. We assume that these processes are homogeneous (Daley and Vere-Jones, 2007, Chapter 12) and that their second-order moment measures exist and are finite (the equivalent of finite variance for time series). From Daley and Vere-Jones (2003), for $1 \leq p, q \leq P$ the first and second moment measures are given for $A, B \in \mathcal{B}(\mathbb{R}^d)$ by

$$M_p(A) = E \{ \xi_p(A) \}, \quad M_{p,q}(A \times B) = E \{ \xi_p(A) \xi_q(B) \},$$

with the appropriate extension of $M_{p,q}$ to $\mathcal{B}(\mathbb{R}^{2d})$. Under stationarity these moment measures have reduced forms so that for any $A \in \mathcal{B}(\mathbb{R}^d)$ and any g a bounded measurable function of bounded support

$$M_p(A) = \lambda_p \ell(A), \quad \int_{\mathbb{R}^{2d}} g(x, y) M_{p,q}(dx \times dy) = \int_{\mathbb{R}^d} \int_{\mathbb{R}^d} g(s+u, s) \ell(ds) \check{M}_{p,q}(du),$$

where λ_p is called the mean density and $\check{M}_{p,q}$ is the reduced second-order moment measure and ℓ is the Lebesgue measure (Daley and Vere-Jones, 2003, Chapter 8).⁵

If ξ_p is a simple point process, then λ_p is the intensity, which describes the average number of points per unit area. If ξ_p is a random field λ_p is the mean at any given location. If ξ_p is a marked point process with a simple ground process, then λ_p is the product of the mean mark and the intensity of the ground process (Illian et al., 2008, Equation 5.1.19).

The reduced covariance (signed) measure between the p th and q th process is

$$\check{C}_{p,q}(A) = \check{M}_{p,q}(A) - \lambda_p \lambda_q \ell(A), \quad A \in \mathcal{B}(\mathbb{R}^d).$$

Whilst the reduced covariance measures do not necessarily have densities, we write the reduced covariance density, $\check{c}_{p,q}$, a generalized density (which may have point masses), satisfying

$$\check{C}_{p,q}(A) = \int_A \check{c}_{p,q}(u) du, \quad A \in \mathcal{B}(\mathbb{R}^d).$$

If $p = q$ and the process in question is a simple point process with a reduced factorial moment measure that admits a density, which we call $\rho_{p,p}$, then, $\check{c}_{p,p}(\cdot) = \rho_{p,p}(\cdot) - \lambda_p^2 + \lambda_p \delta(\cdot)$ where $\delta(\cdot)$ is the Dirac delta function. This is referred to as the complete covariance function by Bartlett (1963), who first introduced the spectra of point processes. If the processes in question are both random fields, then $\check{c}_{p,q}(\cdot) = \text{cov}(Y_p(\cdot), Y_q(0))$ the usual autocovariance function.

The notion of spectra exists in a more general form than the one given here (Daley and Vere-Jones, 2003), but we are interested in processes for which the spectral density function exists. To ensure this existence, we require that reduced covariance measure $\check{C}_{p,q}$ is totally finite. In the random field case, this corresponds to the standard assumption that $\check{c}_{p,q}$ is integrable, e.g. Brillinger (1974). In the point process case, this corresponds to assuming that $\rho_{p,q}(\cdot) - \lambda_p \lambda_q$ is integrable, as in Rajala et al. (2023) for example.

The (cross) spectral density function between the p th and q th processes is defined as

$$f_{p,q}(k) = \int_{\mathbb{R}^d} e^{-2\pi i k \cdot u} \check{C}_{p,q}(du), \quad k \in \mathbb{R}^d.$$

We call the matrix-valued function $f(\cdot) = [f_{p,q}(\cdot)]_{1 \leq p,q \leq P}$ the spectral density matrix function. At a given wavenumber, $f(k)$ plays the role of a wavenumber domain covariance matrix (Brillinger, 1972; Daley and Vere-Jones, 2003).

This definition generalizes the usual notion of spectral density matrix function from time series and random fields, as well as including the point process case as introduced by Bartlett (1963). However, in the marked case this differs slightly from the definition introduced by Renshaw (2002). In particular, Renshaw (2002) defines the spectral density to be proportional to the Fourier transform of the reduced factorial moment density of the mark-sum measure, whereas we define it to be the Fourier transform of the reduced covariance measure. Importantly, our definition corresponds

⁵We write the lag in the first index to match the notation used in the time series literature, in contrast to Daley and Vere-Jones (2003).

to a special case of the definition for random measures, so we inherit all the properties of the spectral density matrix function listed by Daley and Vere-Jones (2003), such as positive semi-definiteness. In addition, setting the mark kernel to a point mass at one recovers the unmarked case, in that the spectral densities as we define them are the same. For a more thorough discussion, see Appendix S7.2.

In order to handle sampling of the random fields, we will need an additional assumption on the decay of their covariance function and spectral density function.

Assumption 1 (Covariance decay). *The reduced covariance measure $\check{C}_{p,q}$ is totally finite. In the case where both processes are random fields, the covariance density (function) $\check{c}_{p,q}$ is continuous and there exists $C, \delta > 0$ such that for all $x \in \mathbb{R}^d$, $|\check{c}_{p,q}(x)| + |f_{p,q}(x)| \leq C(1 + \|x\|_2)^{-d-\delta}$.*

This latter condition ensures that we have an aliasing relation between the spectral density function of the continuous process and its sampled counterpart. For example, random fields with Matérn (cross-)covariance functions satisfy Assumption 1.

So far, we only considered almost-surely non-negative random fields; however, this condition can be relaxed by viewing everything as random-signed measures. Not all of the theory necessarily follows, see Section 8.4 of Daley and Vere-Jones (2003) for details. However, if these random signed measures do have reduced covariance measures satisfying Assumption 1, then we can also perform estimation with our framework (e.g. for many Gaussian processes).

2.3 Coherence and partial coherence

Typically, we standardise the cross spectral density functions to complex *coherence*, which is the wavenumber-domain correlation between the two processes. Because coherence is complex-valued, we take the magnitude, which is called magnitude coherence, and argument, which is called phase (Carter, 1987). In particular, for $k \in \mathbb{R}^d$ define the coherence and phase as

$$r_{p,q}(k) = \frac{|f_{p,q}(k)|}{\{f_{p,p}(k)f_{q,q}(k)\}^{1/2}}, \quad \theta_{p,q}(k) = \arg f_{p,q}(k).$$

Coherence has both benefits and limitations in this setting. One benefit is that the coherence between a random field and a point process is natural to define. In contrast, when considering spatial-domain cross-statistics between a random field and a point process, the random field needs to be made into a point process (or vice versa) and then standard spatial cross statistics for point processes (or random fields) can be computed (Illian et al., 2008, Section 6.11.2). This requires choices around how we convert one process into the other, which is not necessary with the wavenumber-domain approach. However, there are some clear limitations. In particular, the coherence assumes that the processes in question are pairwise homogeneous, and does not account for potential confounding from other observed processes.

One way to address both limitations is to consider partial coherence, which is the wavenumber-domain equivalent of partial correlation. This is equivalent to computing the coherence of residual processes, after first removing the linear effect of the other processes (Eichler et al., 2003). In other words, this approach can account for inhomogeneity in the mean of the processes, as is also the case with the intensity reweighted stationary approaches introduced by Baddeley et al. (2000), and the parametric approach proposed by Waagepetersen et al. (2016).

More formally, define $\mathcal{V}_{p,q} = [P] \setminus \{p, q\}$ and let $f_{p,q \bullet \mathcal{V}_{p,q}}$ be the cross-spectral density function of two residual processes formed by producing the best linear prediction of ξ_p and ξ_q from the other processes $\{\xi_r \mid r \in \mathcal{V}_{p,q}\}$. As with partial correlation, the magnitude partial coherence and partial phase for $k \in \mathbb{R}^d$ are

$$r_{p,q \bullet \mathcal{V}_{p,q}}(k) = \frac{|f_{p,q \bullet \mathcal{V}_{p,q}}(k)|}{\{f_{p,p \bullet \mathcal{V}_{p,q}}(k)f_{q,q \bullet \mathcal{V}_{p,q}}(k)\}^{1/2}}, \quad \theta_{p,q \bullet \mathcal{V}_{p,q}}(k) = \arg f_{p,q \bullet \mathcal{V}_{p,q}}(k),$$

respectively (Dahlhaus, 2000; Eckardt and Mateu, 2019b). Importantly the magnitude partial coherence (and phase) can be computed efficiently by inverting the spectral matrix and making appropriate transformations (Dahlhaus, 2000). This approach is then able to account for conditional inhomogeneity in the processes, which is not possible with coherence alone. As demonstrated in Fig. 1, it is easy to account for the other observed point processes as well as the random fields.

3 Estimation

3.1 Multitapering

Assume we observe the random measures ξ_1, \dots, ξ_P on some bounded region $\mathcal{R} \subset \mathbb{R}^d$. Given a single realisation, we aim to construct estimators of the spectral density matrix function. Of course, when the processes are random fields we cannot observe them everywhere in \mathcal{R} , but must instead sample them discretely in space. In Section 3.4, we discuss irregular sampling approaches, however, here we will assume that the random fields have been recorded on a regular grid. In particular, if the p th process is a random field, assume it is observed on the intersection between \mathcal{R} and the grid $\mathcal{G}_p = \mathbb{Z}^d \circ \Delta_p + v_p$ where $\Delta_p \in \mathbb{Q}_{>0}^d$ denotes the sampling interval and $v_p \in \mathbb{Q}^d$ the offset of the grid.

To estimate the spectral density function, we first construct multiple tapered Fourier transforms, whose covariance matrix is asymptotically $f(k)$, and then compute their sample covariance matrix. All of the process in which we are interested can be thought of generally as random measures (Daley and Vere-Jones, 2003). Similarly, all of the tapered Fourier transforms can be seen as special cases of the tapered Fourier transform of a general random measure.

Consider a function $h : \mathbb{R}^d \rightarrow \mathbb{R}$, bounded in magnitude and zero outside \mathcal{R} , which we will call a taper. Then the tapered Fourier transform of ξ_p is defined as

$$J_p(k; h) = \int_{\mathbb{R}^d} h(s) e^{-2\pi i k \cdot s} \xi_p^0(ds), \quad k \in \mathbb{R}^d$$

where ξ_p^0 denotes the centred random measure, i.e. $\xi_p^0(A) = \xi_p(A) - \lambda_p \ell(A)$. Because h is only non-zero inside \mathcal{R} , it is possible to compute the tapered Fourier transform from our observations.

If the p th process is a (marked) point process, with locations X_p and marks W_p , then

$$J_p(k; h) = \sum_{x \in X_p} h(x) W_p(x) e^{-2\pi i k \cdot s} - \lambda_p H(k), \quad k \in \mathbb{R}^d,$$

where for $k \in \mathbb{R}^d$, $H(k) = \int_{\mathbb{R}^d} h(s) e^{-2\pi i k \cdot s} ds$ is the Fourier transform of h . When the process is not marked ($W_p(x) = 1$ a.s.) this is the tapered Fourier transform proposed in Rajala et al. (2023). When the process is marked, our approach represents a generalisation to the marked setting.

If the p th process is a random field, with the field denoted by Y_p , then

$$J_p(k; h) = \int_{\mathbb{R}^d} h(s) \{Y_p(s) - \lambda_p\} e^{-2\pi i k \cdot s} ds, \quad k \in \mathbb{R}^d.$$

However, computing this would require us to record the random field everywhere in \mathcal{R} . For some function g , let the grid sampled function $g^{(\mathcal{G}_p)}$ be $g^{(\mathcal{G}_p)}(s) = g(s) \prod (\Delta_p) \sum_{z \in \mathcal{G}_p} \delta(s - z)$, for $s \in \mathbb{R}^d$, where $\delta(\cdot)$ is the Dirac delta function. Then if we instead consider

$$J_p(k; h^{(\mathcal{G}_p)}) = \prod (\Delta_p) \sum_{s \in \mathcal{G}_p} h(s) \{Y_p(s) - \lambda_p\} e^{-2\pi i k \cdot s}, \quad k \in \mathbb{R}^d$$

we see that this is essentially the usual tapered Fourier transform for random fields (Andén and Romero, 2020, for example). It is important that the tapers h and $h^{(\mathcal{G}_p)}$ behave similarly, see Assumption 3, and this is easiest to achieve when the tapers used for the random fields are subsampled from the continuous base taper (with appropriate rescaling).

The tapered periodogram between processes p and q is

$$I_{p,q}(k; h_p, h_q) = J_p(k; h_p) \overline{J_q(k; h_q)}, \quad k \in \mathbb{R}^d,$$

for the appropriate choices of h_p and h_q . The periodogram is the sample variance of one observation (with known mean zero). The rational for this choice being that the tapered Fourier transform has a variance related to f . However, the clear issue is that the sample variance of one observation is a very poor estimate of the population variance. One technique to resolve this problem is multitapering, first proposed for the time series setting by Thomson (1982), which constructs multiple different tapered Fourier transforms, and then computes the sample variance of this collection. In particular, consider a family of tapers for each process $\{h_{p;m}\}_{m \in [M]}$, and define the shorthands

$$J_{p;m}(k) = J_p(k; h_{p;m}), \quad I_{p,q;m}(k) = I_{p,q}(k; h_{p;m}, h_{q;m}), \quad k \in \mathbb{R}^d,$$

where $h_{p;m}$ is the appropriate taper for the given sampling regime, i.e. if the p th process is a (marked) point process $h_{p;m} = h_m$ and if the p th process is a random field sampled on the grid \mathcal{G}_p then $h_{p;m} = h_m^{(\mathcal{G}_p)}$. For a given m , the taper

is always the same for two point processes, but for random fields will depend on the sampling grid. Then the multitaper estimator is

$$\hat{f}_{p,q}(k) = \frac{1}{M} \sum_{m=1}^M I_{p,q;m}(k), \quad k \in \mathbb{R}^d.$$

The estimator performs well if the family of vectors of tapered Fourier transforms $J_m(k) = [J_{p;m}(k)]_{p \in [P]}$ are iid across m , which is true asymptotically (see Theorem 3).

3.2 A general characterisation for growing observational regions

Whilst we can make stronger statements about specific region shapes and asymptotic regimes, we start with the generic setting in which we have a sequence of increasing regions, and ask what properties we would need tapers to satisfy in order to construct consistent estimators. Such properties will place some implicit constraints on the kinds of sequences of regions for which we can use multitapering. In Appendix S1.2, we give explicit forms of growing domain and taper choice that satisfy all of the assumptions we introduce here. In general these properties are useful, firstly to abstract some of the proofs, and secondly because they give a good indication of the desirable taper properties in practice, when given a single region.

Consider a sequence of regions $\{\mathcal{R}_n\}_{n \in \mathbb{N}}$ such that for $n \in \mathbb{N}$, $\mathcal{R}_n \subset \mathcal{R}_{n+1}$, and $\ell(\bigcup_{n=1}^{\infty} \mathcal{R}_n) = \infty$. We aim to construct a sequence of families of tapers $\{h_{m,n}\}_{m \in [M_n]}$, where the number of tapers M_n may depend on n . For consistency of the multitaper estimate (Theorem 2), we will need M_n to grow with n , but for the asymptotic normality of the tapered Fourier transform (Theorem 3), we will need M_n to be fixed. This will be made clear in the relevant results.

Assumption 2 (Finite sample taper properties). *The family of tapers $\{h_{m,n}\}_{m \in [M_n]}$ are such that for all $n \in \mathbb{N}$, for all $m \in [M_n]$, $h_{m,n} : \mathbb{R}^d \rightarrow \mathbb{R}$ is bounded, continuous, supported on a subset of \mathcal{R}_n with $\|h_{m,n}\|_2^2 = 1$ and $\|H_{m,n}\|_1 < \infty$, where $H_{m,n}$ is the Fourier transform of $h_{m,n}$.*

Boundedness and continuity ensure the tapered Fourier transforms are well defined. The L^2 norm assumption ensures that the tapers are normalized. The finite L^1 norm allows us to rearrange the order of integration in the proof of some results and to invert various Fourier transforms, and is satisfied by all taper families constructed in this paper.⁶

There are two forms of bias present in spectral estimation, which we will refer to as leakage bias and aliasing bias. The leakage bias results from the boundary effects, and is importantly a property of the taper which we control. The aliasing bias comes from the sampling of the random fields, and is a property of both the sampling grid and the underlying random field. Intuitively, aliasing results from only being able to sample a function on some regular grid. In this case, we are thinking about this function being the autocovariance of a random field (or between two random fields). The impact of such sampling in space is clear: we cannot observe the covariance at all possible lags, but just on a subset of them. In wavenumber, grid sampling results in aliasing, which is a more complicated phenomena, where the Fourier transform we observe is the Fourier transform we care about plus some erroneous values from higher wavenumbers.

The bias effects of tapers are most easily understood in terms of a smoothing in the wavenumber domain. To understand this, we will need to consider the Fourier transform of the taper, and the aliased spectral density function. In particular, write $H_{p;m,n}$ for the Fourier transform of the taper so that if the p th process is a point process

$$H_{p;m,n}(k) = H_{m,n}(k) = \int_{\mathbb{R}^d} h_{m,n}(s) e^{-2\pi i k \cdot s} ds,$$

and for a random field is

$$H_{p;m,n}(k) = H_{m,n}^{(\mathcal{G}_p)}(k) = \prod (\Delta_p) \sum_{s \in \mathcal{G}_p} h_{m,n}(s) e^{-2\pi i k \cdot s},$$

for any $k \in \mathbb{R}^d$. In the latter case, $|H_{p;m,n}|$ is periodic on $K_p = [-1/2, 1/2]^d \oslash \Delta_p$, which we will call the Nyquist box. For convenience, if the process is sampled continuously we set $K_p = \mathbb{R}^d$. Aliasing for processes on a single grid (Percival and Walden, 1993) is simpler compared to multiple processes sampled in different ways. Therefore we need a more general notion of aliased spectra.

Definition 1 (The aliased spectral density). *Introduce a set of aliasing wavenumbers Ψ_p and a phase adjustment function $w_p : \mathbb{R}^d \rightarrow \mathbb{C}$, so that if the p th process is sampled on a grid, then $\Psi_p = \mathbb{Z}^d \oslash \Delta_p$ and $w_p(x) = e^{-2\pi i v_p \cdot x}$*

⁶Using no taper (a scaled indicator function), we would not satisfy this assumption. However, due to the substantial leakage bias (Percival and Walden, 1993), we never use no taper.

and otherwise $\Psi_p = \{0\}$ and $w_p(x) = 1$. Let the aliased spectral density function be

$$\tilde{f}_{p,q}(k) = \sum_{\psi \in \Psi_p \cap \Psi_q} f_{p,q}(k + \psi) w_p(\psi) \overline{w_q(\psi)}, \quad k \in \mathbb{R}^d.$$

Aliasing is not always present, but it is notationally convenient to define the aliased spectral density function in all cases. Since zero is always in the set $\Psi_p \cap \Psi_q$, we have $f_{p,q}(k) = \tilde{f}_{p,q}(k)$ if there is no aliasing, in particular, if one of the processes is sampled continuously in space. When both processes p and q are sampled on a grid, $|\tilde{f}_{p,q}|$ is periodic on the set $K_{p,q} = [-1/2, 1/2]^d \otimes \Delta_{p,q}$ where $\Delta_{p,q}$ is elementwise the largest number such that both $\Delta_p \otimes \Delta_{p,q} \in \mathbb{N}^d$ and $\Delta_q \otimes \Delta_{p,q} \in \mathbb{N}^d$. For example, if $\Delta_p = (4, 1/3)^\top$ and $\Delta_q = (6, 1/2)^\top$, then $\Delta_{p,q} = (2, 1/6)^\top$. When one or both of the processes are sampled continuously in space, then we write $K_{p,q} = \mathbb{R}^d$. The product $H_{p;m,n}(k) \overline{H_{q;m,n}(k)}$, which is important for leakage bias, is also periodic in magnitude on $K_{p,q}$.

The left half of Fig. 2 shows an example taper and its discrete counterparts on two different grids. The right half of Fig. 2 shows the products of the different Fourier transforms of the taper and its discrete counterparts. In particular, we see from the diagonal terms that the discrete version repeat on different intervals. In addition, from the off-diagonals we see that pairs including the continuous taper do not repeat, and the cross term between the two discrete tapers is periodic with a longer period than either of the originals, specifically $K_{p,q} \supseteq K_p$ for all $p, q \in [P]$.

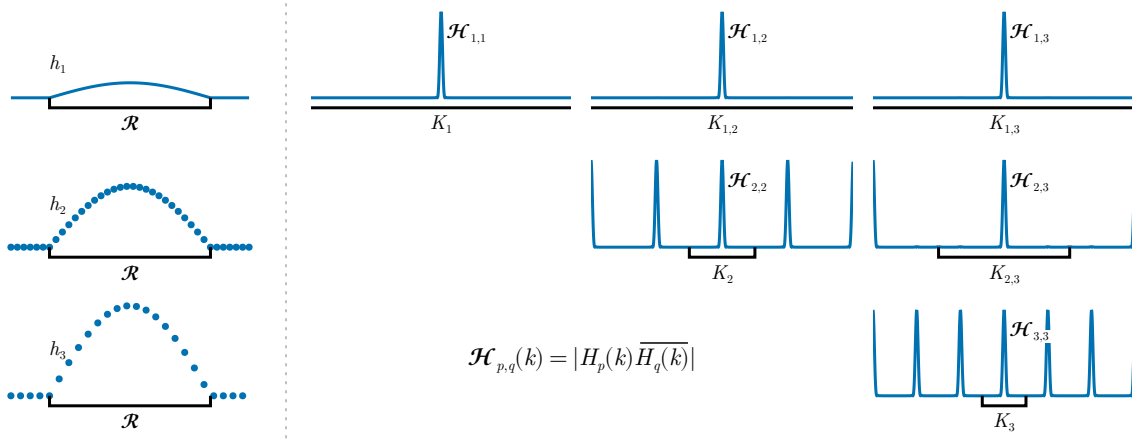


Figure 2: An illustration of the aliasing effects in one dimension, assuming the first process was recorded continuously, and the second and third recorded on grids with sampling intervals of 4 and 6 respectively. The taper in question is a minimum bias taper (Riedel and Sidorenko, 1995).

Unless specified otherwise, we shall assume for simplicity that the intensity/mean λ_p is known, which we refer to as the ‘‘oracle case’’. Estimating the intensity has a negligible effect, except near zero wavenumber. However, the finite sample equations become more complicated, and so we consider the oracle case here, and the non-oracle case is discussed in Appendix S5. We can now obtain a general expression for the effect of the tapers and grid sampling on the bias of the periodogram. This generalizes the standard result for multivariate time series (Walden, 2000), random fields (Guillaumin et al., 2022) and univariate point processes (Rajala et al., 2023).

Proposition 1 (Expectation of the periodogram). *Given the processes satisfy Assumption 1 and the tapers satisfy Assumption 2, the expectation of the periodogram is*

$$E \{ I_{p,q;m,n}(k) \} = \int_{K_{p,q}} H_{p;m,n}(k') \overline{H_{q;m,n}(k')} \tilde{f}_{p,q}(k - k') dk',$$

for all n , for all $m \in [M_n]$, $k \in \mathbb{R}^d$.

Proof. See Appendix S2.1. □

The only way to reduce aliasing bias is to sample the process at a higher resolution, or to sample it randomly and treat it as a marked point process (see Appendix S8). Since we typically do not control the sampling mechanism, we

cannot control the aliasing bias, and should just be aware that it exists. However, since the expectation is a convolution between the aliased spectral density function and a property of the taper, we can control leakage bias by constraining the behaviour of the taper.

The underlying idea is to construct the tapers such that their Fourier transforms concentrate within a bandwidth around zero, and that this concentration increases appropriately with growing domain (Walden, 2000). Combined with continuity of the spectral density function, this will yield asymptotic unbiasedness (up to an aliasing effect).

Assumption 3 (Taper concentration). *Let $b_n \rightarrow 0$ as $n \rightarrow \infty$ be the taper bandwidth, and B_{b_n} be a ball centred at zero of radius b_n . Then we assume that for all $p, q \in [P]$ as $n \rightarrow \infty$,*

$$\max_{m \in [M_n]} \left| 1 - \int_{B_{b_n}} H_{p;m,n}(k) \overline{H_{q;m,n}(k)} dk \right| \rightarrow 0, \quad \max_{m \in [M_n]} \int_{K_p \setminus B_{b_n}} |H_{p;m,n}(k)|^2 dk \rightarrow 0.$$

In the case when every process is sampled continuously, the latter condition is not necessary, as $\|H_{m,n}\|_2 = \|h_{m,n}\|_2 = 1$. However, for the processes sampled on a grid it is necessary. If the former condition holds, then for the grid sampled cases the latter condition is equivalent to $\max_{m \in [M_n]} |1 - \prod(\Delta_p) \sum_{u \in \mathcal{G}_p} h_{m,n}(u)^2| \rightarrow 0$ as $n \rightarrow \infty$.

Theorem 1 (Asymptotic bias of the periodogram). *Let the processes satisfy Assumption 1, and the tapers satisfy assumptions 2 and 3 for some fixed number of tapers M . For all $k \in \mathbb{R}^d$, $p, q \in [P]$, for all fixed $m \in [M]$,*

$$E \{ I_{p,q;m,n}(k) \} \rightarrow \tilde{f}_{p,q}(k),$$

as $n \rightarrow \infty$.

Proof. See Appendix S2.2. □

Theorem 1 shows that the only asymptotic bias of the periodogram is due to aliasing. Importantly, in the case where at least one of the processes is not sampled on a grid, the periodogram is asymptotically unbiased. This includes marked point processes, meaning that we have resolved the bias present in the current state-of-the-art estimator (Renshaw, 2002). The two main results we will establish are consistency of the multitaper periodogram under a growing number of tapers, and asymptotic normality of the tapered discrete Fourier transform under a finite number of tapers. In both cases, we need the tapers to be asymptotically orthogonal.

Assumption 4 (Asymptotic orthogonality). *For all $p, q \in [P]$, as $n \rightarrow \infty$,*

$$\max_{m \in [M_n]} \max_{m' \in [M_n] \setminus \{m\}} \left| \int_{B_{b_n}} H_{p;m,n}(k) \overline{H_{q;m',n}(k)} dk \right| \rightarrow 0.$$

In general, we will construct tapers that are close to being orthogonal, but not quite, in particular when constructing tapers for unusual region shapes. In practice, assumptions 3 and 4 can be checked numerically, as will be discussed in Section 3.3. As well as yielding variance reduction for consistency, this assumption also ensures that the different tapered Fourier transforms are asymptotically uncorrelated when we study asymptotic normality. We also assume that the L^1 norms of the Fourier transforms of the tapers shrink to zero as the observational region grows.

Assumption 5 (Shrinking taper Fourier transform). *For all $p \in [P]$, there is $C_p < \infty$ such that*

$$\max_{m \in [M_n]} \int_{K_p} |H_{p;m,n}(k)| dk \rightarrow 0, \quad \max_{m \in [M_n]} \sum_{\psi \in \Psi_p} \left(\int_{K_p + \psi} |H_{m,n}(k)|^2 dk \right)^{1/2} \rightarrow C_p$$

as $n \rightarrow \infty$.

The first part of Assumption 5 is commonly used when dealing with spectral estimation on unusual domains or more abstract settings (Brillinger, 1982). The second part is a technical condition to handle the grid sampled processes. See Appendix S1.2 for examples of constructions where both conditions are satisfied. In particular, both conditions are implied if we assume that the Fourier transform of the taper is bounded by a decreasing function with appropriate tail decay.

Finally we need to make an assumption about the higher-order cumulants of the processes. At a high level, we just need to ensure that fourth order terms that appear in the variance of the periodogram (due to the periodogram being a product of two tapered Fourier transforms) are negligible. It will be convenient for the theory to embed all of the grids on one fine grid. In particular, let $\mathcal{G} = \Delta \circ \mathbb{Z}^d$ to be a grid which contains all of the other grids we consider (e.g. by taking Δ

to be one over the product of the denominators of all Δ_p and v_p in each dimension). Weighted sums on the original grid can always be constructed by multiplying the desired weights by $\mathbb{1}_{\mathcal{G}_p}$. Now it is easier to work with the sampled random measures, which will include the potential effect of the grid sampling. Define the sampled random measures ζ_p for $A \in \mathcal{B}(\mathbb{R}^d)$ by $\zeta_p(A) = \xi_p(A)$ if the p th process is sampled continuously, and $\zeta_p(A) = \sum_{u \in \mathcal{G} \cap A} Y_p(u)$ if the p th process is sampled on a grid.

Let $\mathcal{C}[X_1, \dots, X_r]$ denote the r th-order cumulant of some random variables X_1, \dots, X_r . Define the r th-order cumulant measure of the sampled process as

$$C_{p_1, \dots, p_r}^{(\zeta)}(A_1 \times \dots \times A_r) = \mathcal{C}[\zeta_{p_1}(A_1), \dots, \zeta_{p_r}(A_r)],$$

for $A_1, \dots, A_r \in \mathcal{B}(\mathbb{R}^d)$, appropriately extended to $\mathcal{B}(\mathbb{R}^{rd})$ (Daley and Vere-Jones, 2007). Now we need a minor extension of Proposition 12.6.III in Daley and Vere-Jones (2007) to include the grid sampling.

Lemma 1 (Reduced cumulant measure). *For $p_1, \dots, p_r \in [P]$, assume that the r th joint moment measures of $\xi_{p_1}, \dots, \xi_{p_r}$ exist and are finite. Say that either all of the processes are sampled continuously, or they are enumerated so that at least ξ_p is sampled on a grid. For any bounded measurable function of bounded support $g : \mathbb{R}^{rd} \rightarrow \mathbb{R}$ there exists a reduced cumulant measure $\check{C}_{p_1, \dots, p_r}^{(\zeta)}$ such that*

$$\begin{aligned} & \int_{\mathbb{R}^{rd}} g(x_1, \dots, x_r) C_{p_1, \dots, p_r}^{(\zeta)}(dx_1 \times \dots \times dx_r) \\ &= \int_{\mathbb{R}^d} \int_{\mathbb{R}^{(r-1)d}} g(x + u_1, \dots, x + u_{r-1}, x) \check{C}_{p_1, \dots, p_r}^{(\zeta)}(du_1 \times \dots \times du_{r-1}) \ell_{p_r}(dx), \end{aligned}$$

where ℓ_{p_r} is the Lebesgue measure on \mathbb{R}^d if ξ_p is sampled continuously (meaning all the processes are sampled continuously), and ℓ_{p_r} is the counting measure on \mathcal{G} if ξ_p is sampled on a grid.

Proof. See Appendix S2.3. □

More concretely, when all of the processes are sampled on a grid, in the fourth-order case

$$\check{C}_{p,q,r,s}^{(\zeta)}(A_1 \times A_2 \times A_3) = \sum_{u_1 \in \mathcal{G} \cap A_1} \sum_{u_2 \in \mathcal{G} \cap A_2} \sum_{u_3 \in \mathcal{G} \cap A_3} \mathcal{C}[Y_p(u_1), Y_q(u_2), Y_r(u_3), Y_s(0)].$$

so that in particular, the summand is the usual cumulant function of a stationary multivariate time series or random field, see for example Brillinger (1974).

Assumption 6 (Fourth-order cumulants). *For $p, q \in [P]$, the first four joint moment measures of ζ_p, ζ_q exist and are finite, and the reduced cumulant measure $\check{C}_{p,p,q,q}^{(\zeta)}$ is totally finite.*

Assumption 6 corresponds to standard integrability/absolute summability of higher-order cumulant function in the time series case (Brillinger, 1965), analogously to Assumption 1.

Theorem 2 (Consistency of the multitaper periodogram). *If the processes satisfy assumptions 1 and 6 and the tapers satisfy assumptions 2 to 5 and in addition $M_n \rightarrow \infty$ as $n \rightarrow \infty$, then for all $k \in \mathbb{R}^d$, for all $p, q \in [P]$,*

$$E \left\{ \hat{f}_{p,q;n}(k) \right\} \rightarrow \tilde{f}_{p,q}(k), \quad \text{var} \left\{ \hat{f}_{p,q;n}(k) \right\} \rightarrow 0,$$

as $n \rightarrow \infty$.

Proof. See Appendix S2.4. □

As a result, we see that if we grow the number of tapers with appropriate control on their behaviour, then we obtain an estimator which is mean-square consistent, which is not true when using a single taper.

There are two main approaches to establishing asymptotic normality of the tapered Fourier transform. The first is to use Brillinger mixing conditions (Brillinger, 1982), which assume that all of the higher-order cumulant measures exist and are totally finite. The second is to use an α -mixing condition (Yang and Guan, 2024, for example), typically with the assumption that at least finitely many moments exist and are finite (see e.g. Biscio and Coeurjolly (2016) for a discussion of the two assumptions in the point process setting). In Appendix S1.1, we give a result using the general α -mixing central limit theorem from Biscio and Waagepetersen (2019). However, we will use Brillinger mixing here as we already introduced higher-order cumulants.

Assumption 7 (Brillinger mixing). *For all $r \in \mathbb{N}$, for all $p_1, \dots, p_r \in [P]$, the joint moment measures of $\zeta_{p_1}, \dots, \zeta_{p_r}$ up to order r exist and are finite, and $\check{C}_{p_1, \dots, p_r}^{(\zeta)}$ is totally finite.*

Assumption 7 will be used for asymptotic normality of the tapered Fourier transforms. Since the tapered Fourier transforms are complex-valued, convergence will be to a complex normal distribution. We write $\mathcal{CN}(\mu, S, R)$ for a multivariate complex-normal distribution mean vector μ , covariance matrix S and relation matrix R . Furthermore, since we transform real-valued processes, the tapered Fourier transforms are symmetric. In addition, for certain wavenumbers, the tapered Fourier transforms are real valued (at zero, and multiple of the Nyquist wavenumbers). This is the same as the time series case, see Brillinger (1974), with a slightly more complicated formulation due to the different kind of sampling present. For this reason, we restrict attention to wavenumbers where these issues do not occur.

Theorem 3 (Asymptotic normality of tapered Fourier transforms). *Let the processes satisfy assumptions 1 and 7 and the tapers satisfy assumptions 2 to 5. Consider $k_1, \dots, k_r \in \mathbb{R}^d$ such that, for all $i, j \in [r]$ with $i \neq j$, $2k_i, 2k_j, k_i \pm k_j \notin \bigcup_{p \in [P]} \Psi_p$. Then for all $i \in [r]$*

$$J_{m,n}(k_i) = [J_{p;m,n}(k_i)]_{1 \leq p \leq P} \xrightarrow{d} \mathcal{CN}(0, \tilde{f}(k_i), 0)$$

as $n \rightarrow \infty$. In addition, for any two distinct m, m' , the vectors $J_{m,n}(k_i)$ and $J_{m',n}(k_i)$ are asymptotically independent, so the matrix $J_n(k_i) = [J_{m,n}(k_i)]_{1 \leq m \leq M}^T$ is asymptotically complex normal with uncorrelated rows. Finally, for $i \neq j$, $J_n(k_i)$ and $J_n(k_j)$ are asymptotically independent.

Proof. See Appendix S2.5. □

3.3 Practical construction of tapers on a region of interest

For a general region which we observe (including non-convex regions) we can construct a family of tapers which satisfy the finite sample conditions in Assumption 2, and for which we can check how well asymptotic conditions in the remaining assumptions are satisfied. We do this by first taking (multidimensional) Slepian sequences on some grid which can be constructed numerically using the methodology of Simons and Wang (2011). Then we multilinearly interpolate these taper sequences to construct a family of continuous tapers on the region of interest.

Proposition 2. *Let g_1, \dots, g_M be a family of discrete space tapers on a grid $\mathcal{G} = \Delta \circ \mathbb{Z}^d + v$, only non-zero on the bounded region $\tilde{\mathcal{R}} = \{s \in \mathcal{R} \mid s + \Delta \circ [-1, 1]^d \subseteq \mathcal{R}\}$. Then if we construct a family of tapers via multilinear interpolation of g_1, \dots, g_m , then the interpolated family satisfies Assumption 2, provided they are correctly normalised. Furthermore, their Fourier transform is*

$$H_m(k) = G_m^{(\mathcal{G})}(k) \prod_{j=1}^d \text{sinc}^2(\pi \Delta_j k_j)$$

where k_j and Δ_j are the j th components of k and Δ respectively, and $\text{sinc}(x) = \sin(x)/x$.

Proof. See Appendix S2.6. □

The construction on the smaller region $\tilde{\mathcal{R}}$ is to ensure that the interpolated tapers are zero outside \mathcal{R} , avoiding linear interpolation across holes not fully covered by the grid, for example. In order to correctly normalize the tapers, we need their L^2 norm, which can be computed exactly with finite sums using the results in Appendix S6.2. We can then check the conditions of assumptions 3 and 4 numerically.

Additional specific details of the taper construction and effect of the linear interpolation are given in Appendix S6. In the case of random fields sampled on a regular grid, the tapered Fourier transforms can be computed efficiently using Fast Fourier Transforms (Cooley and Tukey, 1965), as is well known. For point patterns, we can use Non-Uniform Fast Fourier Transforms, the properties of which were studied by Dutt and Rokhlin (1993). We use the NUFFT implementation from Barnett et al. (2019).

A subset of the tapers we will use for the Barro Colorado Island data (see Section 4.1) is shown in Fig. 3. Whilst any given taper concentrates on a certain region of the spatial domain, the total weight is approximately uniform across the spatial domain, except at the borders (Fig. 3, top row). Similarly, in the wavenumber domain we see that the spectral windows are concentrated on different regions within the bandwidth of zero (denoted by the white circle), but together they cover this region evenly (Fig. 3, bottom row). This points to the major benefit of multitapering, as if we were to use a single taper and kernel smoothing, we would be focusing on a small part of the observational region whereas multitapering uses most of the region evenly.

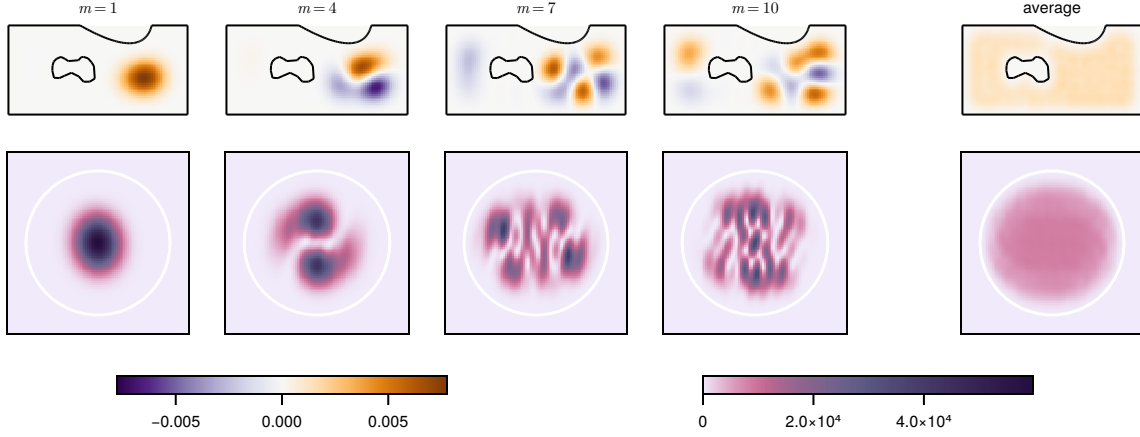


Figure 3: Four of the tapers and the total average absolute taper for an irregular region (top), and the corresponding spectral windows (bottom). The spatial data has axes 0 to 1000 and 0 to 500, and the wavenumber domain plots range from -0.01 to 0.01 in each dimension.

3.4 Irregular sampling

So far, we have only considered the case where the processes are sampled on a regular grid. However, we may also want to handle situations in which they are not. This specific case has been considered previously in the literature, for example Masry (1978, 2003); Matsuda and Yajima (2009). In fact, this also fits into the framework we introduce in this paper. Say we have a mean-zero random field Y which we sample at the now random locations given by the point process X . Then we can regard this sampled process as a mark sum measure, say ξ , corresponding to the marked point process with marks $Y(x)$ for $x \in X$. Then, if the marks are independent of the locations, from Daley and Vere-Jones (2003), page 338, we have

$$f_{\xi\xi}(k) = \int_{\mathbb{R}^d} f_{YY}(k - k') f_{XX}(k') dk' + \lambda_X f_{YY}(k), \quad k \in \mathbb{R}^d$$

where $f_{\xi\xi}$ is the spectral density function of the marked process, f_{YY} is the spectral density function of the random field, f_{XX} is the spectral density function of the point process, and λ_X is the intensity of the point process. If the point process used for sampling is Poisson, then

$$f_{\xi\xi}(k) = \lambda_X \text{var}(Y(0)) + \lambda_X^2 f_{YY}(k), \quad k \in \mathbb{R}^d.$$

The spectra of the random field f_{YY} can then be estimated by plug-in and appropriate rearrangement. That estimator would be identical to the one we would obtain if the sample locations were uniform over the region and we used the methodology proposed by Matsuda and Yajima (2009). For more details, see Appendix S8.

3.5 Coherence and partial coherence

As usual for spectral estimation, we use a plug-in estimator for the magnitude coherence, phase and their partial counterparts. This requires the estimated spectral density matrix at a given frequency to be invertible, so we need to have more tapers than processes, a necessary but not sufficient condition (Walden, 2000). In particular, we cannot use the periodogram as a plug-in estimator for the magnitude partial coherence as the periodogram is not invertible (Walden, 2000).

The probability density function of the absolute value of the sample correlation of a bivariate complex proper normal random vector with absolute correlation ρ and N observations is

$$f(r; \rho, N) = 2(N-1)(1-\rho^2)^N r(1-r^2)^{N-2} {}_2F_1(N, N, 1; \rho^2 r^2) \quad (1)$$

if $0 < r < 1$ and zero otherwise (Miller, 1980). Provided the assumptions of Theorem 3 hold, the matrix $J_n(k)$ is asymptotically complex normal. Therefore, the plug in estimator for $r_{p,q}$, which is the absolute value of the sample correlation of the matrix $J_n(k)$, has an asymptotic distribution with probability density function given by Eq. (1), with $\rho = \tilde{r}_{p,q}$ and $N = M$, as in the case of segment averaging (Goodman, 1957; Carter et al., 1973).

The plug-in estimator for the magnitude partial coherence is the sample partial correlation of $J_n(k)$ (with known zero mean). This partial correlation is the sample correlation of the residuals of the linear regressions of $J_p(k)$ and $J_q(k)$ with $\{J_r(k) \mid r \in [P] \setminus \{p, q\}\}$ (Whittaker, 2009). If the number of tapers M is small, this approximation may be poor, however, in the spatial setting the number of tapers is typically large and thus this approximation performs well (see the simulations in Appendix S11).

4 Application and simulation study

4.1 Barro Colorado Island data

The Barro Colorado Island study records the locations of every individual tree of at least 10mm in trunk diameter within a 1000 by 500 metre rectangle of tropical rainforest, along with additional measurements, such as the diameter and species name of each individual tree (Condit et al., 2019). In addition, they record topological features and the concentration of various soil chemicals, all sampled on regular grids.

Whilst the study records data on a rectangular domain, it is known that the forest is not homogeneous. In particular, there is a region near the northern border of the plot known to consist of a much younger forest dominated by the pioneer tree species *Gustavia superba* (Hubbell and Foster, 1983, 1986), which we therefore remove from all of our analyses to make homogeneity a more reasonable assumption. Similarly, we also remove a swamp region in the centre of the plot where the soil has much higher moisture content and the associated flora is more typical of a riparian habitat (Harms et al., 2001).

There are around 200 species present in the plot, and many additional covariates. To fully analyse such data, we would need to develop methodology to handle that high-dimensional setting. This is beyond the scope of this paper, so for the sake of illustration we will consider a small subset of the available species in our analysis. In particular, Harms et al. (2001) list five species which are known to be associated with the gradient of the terrain.⁷ We take the three most abundant species from this list, *Beilschmiedia tovarensis*, *Poulsenia armata* and *Unonopsis pittieri*, and consider the gradient of the terrain as the fourth process.

To test the significance of magnitude (partial) coherence we use the distribution in Eq. (1) and a Bonferroni correction (Bonferroni, 1936). In particular, we correct as if we perform $K_n P(P - 1)/2$ tests, where $P = 4$ is the number of processes and K_n are the approximate number of wavenumbers on which the multitaper estimate is uncorrelated. Approximately, the multitaper estimate is uncorrelated when wavenumbers are spaced two bandwidths apart and when we use only wavenumbers where the first coordinate is non-negative (as there is a symmetry), see Appendix S1.3 for details. We display more than K_n wavenumbers for visualization purposes, but the threshold is based on K_n , because correcting for all displayed wavenumbers would be overly conservative. It would be preferable to utilise envelope approaches, e.g. Mrkvička and Myllymäki (2023), but they require resampling from the null distribution, which is difficult when the region shape is irregular, and is beyond the scope of this paper.

Figure 4 shows the coherence and partial coherence between each of the four processes from the BCI, alongside the observed data. We have thresholded the coherence and partial coherence based on the marginal asymptotic null distribution with the correction described above. As expected, we can see that there is (statistically) significant coherence between each of the three species locations and the gradient (Fig. 4, plot matrix upper-right triangle). In addition, there is also significant coherence between each of the pairs of species. When we consider partial coherence, thus correcting to some extent for the other processes, we see that there is still residual coherence between the gradient and each of the species' locations. (Fig. 4, plot matrix lower-left triangle). However, *B. tovarensis* and *P. armata* do not have significant partial coherence whereas *U. pittieri* has significant partial coherence with both other species. From the phase, shown in the Appendix S11, we see that all significant associations have a positive sign. Although this example is a preliminary analysis that could change when all other processes and covariates are considered, this example highlights the utility of partial coherence and how it is likely to lead to new inferences compared to existing methods.

4.2 Simulation study

To investigate the asymptotic properties of the proposed method, we conduct a simulation study, examining the distribution of magnitude coherence and partial coherence between two point processes and a random field, and comparing it to the asymptotic distribution given in Eq. (1). In the following models, we always have and two point processes (PP1 and PP2) and a random field (RF). In each case, the random field is a log-Gaussian process, where the Gaussian process has mean -6 and a Matérn covariance function with length scale 20 m, smoothness 3 and variance 1,

⁷Strictly speaking this list is based partially on the BCI dataset, and therefore this selection criteria is to some extent double dipping, though the list is based on an older census.

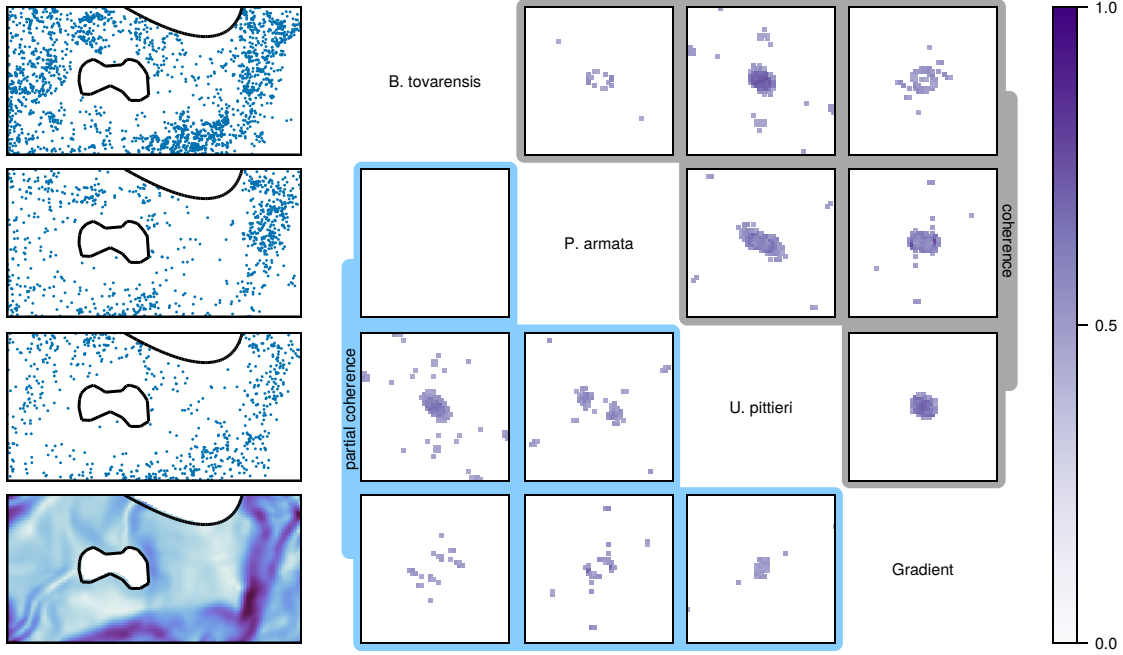


Figure 4: The results of computing the magnitude coherence (upper triangle) and magnitude partial coherence (lower triangle) between *B. tovarensis*, *P. armata*, *U. pittieri* and the gradient of the terrain. The data is shown on the left. The spectral plots are shown from -0.05 to 0.05 in each axis, and the data is shown from 0 to 1000 and 0 to 500.

and is recorded on a grid with spacing every 5 m starting from (0 m, 0 m) as in the case of the gradient data from Barro Colorado Island. The specific details of the three models are:

- Model 1: The two point processes are independent log-Gaussian Cox processes with the Gaussian process described above driving them (independently of the recorded random field).
- Model 2: The two point processes are independently Cox processes with the random intensity driven by the field (i.e. they are log-Gaussian Cox processes, see Møller et al. (1998)).
- Model 3: The second point process (PP2) is a Cox process with the random intensity driven by the field, and the first point process (PP1) is the result of random clustering around the second point process, where for each point in the first process, there are Poisson(1) offspring, who are placed randomly around the parent with a $\text{Normal}(0, 5^2)$ distribution in each direction.

For each case, we generate 1000 replications, and compute estimates of the spectral density matrix function. All simulations use the region from the Barro Colorado Island data with the swamp removed. It is not possible to visualize all of the results, so we show a subset. In particular, we focus on two wavenumbers which illustrate different areas of the spectrum. The first is at a low wavenumber on the slope (so we expect smoothing effects to degrade the quality of the approximation), the second is at a high wavenumber, exploring the effects in the tails. At each of these wavenumbers, we show the empirical and asymptotic distributions of magnitude coherence and magnitude partial coherence between the point processes (processes 1 and 2) and between one of the point processes and the field (processes 2 and 3). The left hand column of Fig. 5 shows the true spectral matrix for each model, with the magnitude (partial) coherence in the upper (lower) triangle, respectively. The locations at which we compare the empirical to asymptotic distributions are marked with a point labelled so that it corresponds to the appropriate panel in the right hand column. For model 1 (the null model), the empirical distribution of the magnitude coherence and magnitude partial coherence align well with the asymptotic distribution (Fig. 5, top section). In models 2 and 3, the asymptotic distributions begin to break down in some of the non-null cases (Fig. 5, middle and bottom sections). However, we would still detect the effect as being significant when compared to the null asymptotic distribution. Whilst not perfect, the results are promising and suggest that the asymptotic distribution is a good approximation for the magnitude coherence and magnitude partial coherence in many cases.

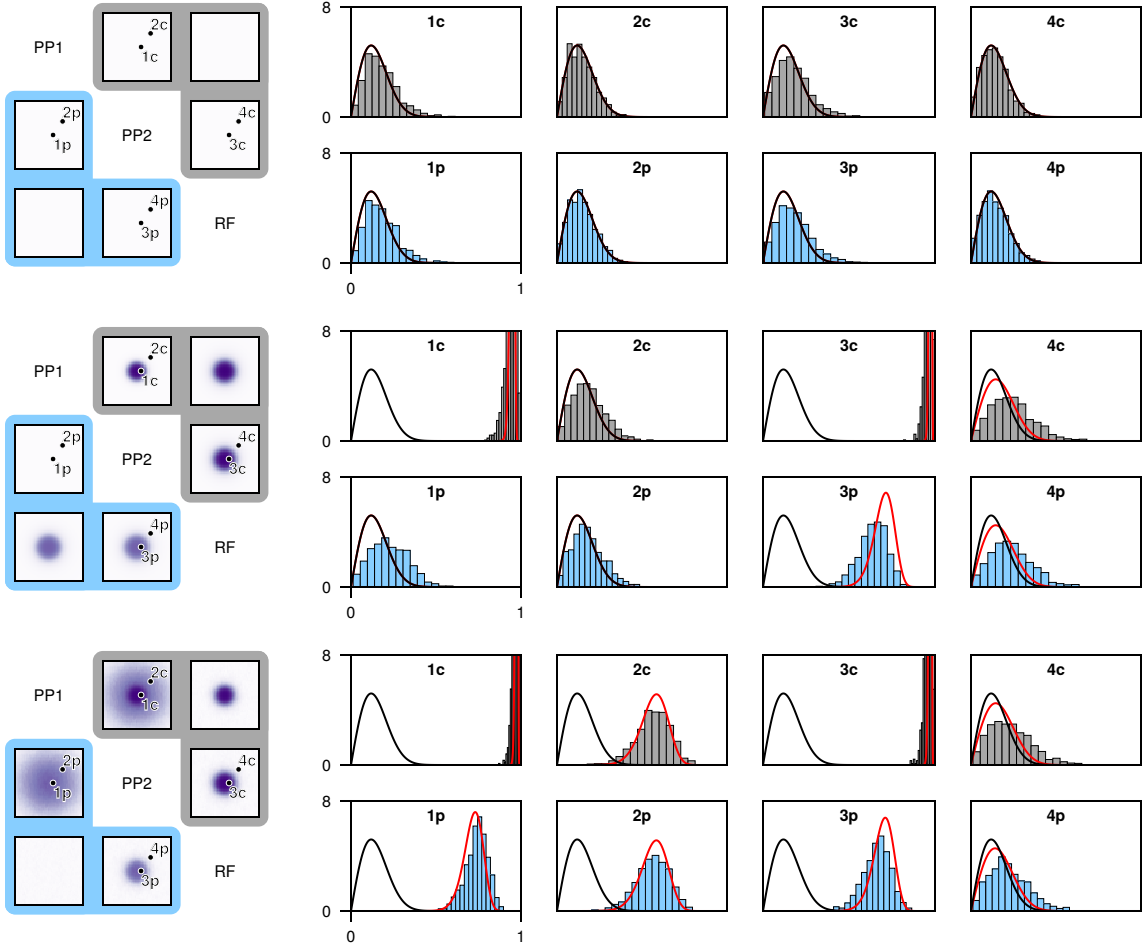


Figure 5: Results of the simulation study. The left column shows for each model the true magnitude (partial) coherence in the upper (lower) triangle where both wavenumber components k_1 and k_2 range from -0.05 to 0.05. The right hand column shows the estimated magnitude (partial) coherence on top (bottom), and asymptotic distribution (red line) and null distribution (black line). The rows correspond to models one to three from top to bottom. The result is optimal when the asymptotic (red line) matches the simulation-based histogram.

Acknowledgement

Sofia Olhede would like to thank the European Research Council under Grant CoG 2015-682172NETS, within the Seventh European Union Framework Program.

Simulation details

In the example constructed in Section 1, each cluster process was generated by placing a cluster at every point in the parent process, where the number of children N and location relative to the parent X were given by $N \sim \text{Poisson}(1)$, $X \sim \text{Normal}(0, 5^2 I_2)$ where I_2 is the identity matrix. The intensity for the inhomogeneous Poisson was specified by $\log(\lambda(x)) = 9Y(x) - 7$ where Y is the gradient of the Barro Colorado Island terrain. The choice of coefficients was based roughly on fitting a model for the intensity of *P. armata* based on the gradient.

SUPPLEMENTARY MATERIAL FOR SPECTRAL ESTIMATION FOR POINT PROCESSES AND RANDOM FIELDS

S1 Additional results

S1.1 Asymptotic normality under α -mixing

To prove asymptotic normality under α -mixing, we need an additional assumption on the tapers, and a condition on the mixing of the processes.

Assumption S1 (Additional taper regularity). *For all $m \in \mathbb{N}$, $\sup_{n \in \mathbb{N}} \ell(\mathcal{R}_n) \|h_{m,n}\|_\infty^2 < \infty$, and letting $D_n = \{x \in \mathbb{Z}^d \mid x + [-1/2, 1/2]^d \cap \mathcal{R}_n \neq \emptyset\}$, $\liminf_{n \rightarrow \infty} \ell(\mathcal{R}_n) |D_n|^{-1} > 0$.*

The first of these conditions just ensures that the largest value of the taper goes to zero sufficiently fast relative to the area of the observational window. In the time series case, one usually scales the tapers by the square root of the length of the time series, which satisfies this condition. The second condition is required because the construction in Biscio and Waagepetersen (2019) breaks up space into a grid, and the region needs to not become too concentrated around the grid centres. This condition is also satisfied when we grow a convex region.

To directly utilise the central limit theorem from Biscio and Waagepetersen (2019), we need to construct a marked point process from which all statistics can be computed. In particular define the marked point processes on $\mathbb{R}^d \times \mathcal{M}$ where $\mathcal{M} = [0, \infty) \times [P]$ by $U = \cup_{p \in [P]} U_p$ where $U_p = \{(x, W_p(x), p) \mid x \in X_p\}$ if the p th process is sampled continuously, and $U_p = \{(x, Y_p(x), p) \mid x \in \mathcal{G}_p\}$ if the p th process is sampled on a grid. Now for $A \subset \mathbb{R}^d$ and $B \subset \mathcal{M}$ let $U_{A,B} = U \cap A \times B$. Then the α -mixing coefficient from Biscio and Waagepetersen (2019) is defined as

$$\alpha_{c_1, c_2}^U = \sup \{ \alpha(\sigma(U_{E_1, \mathcal{M}}), \sigma(U_{E_2, \mathcal{M}})) \mid E_1 \subset \mathbb{R}^d, E_2 \subset \mathbb{R}^d, \ell(E_1) < c_1, \ell(E_2) < c_2, d(E_1, E_2) > 0 \},$$

for $c_1, c_2 \geq 0$ where d denotes the infimum of a distance between points in the sets and $\alpha(\cdot, \cdot)$ is the mixing coefficient for random variables, see Biscio and Waagepetersen (2019) for details.

Assumption S2 (Mixing conditions). *Assume $f(k)$ is positive definite for all $k \in \mathbb{R}^d$. Furthermore, there exists $\epsilon > 0$ such that $\sup_{n \in \mathbb{N}} \alpha_{2, \infty}^U(s) = O(1/s^{d+\epsilon})$, and there exists $\tau > 2d/\epsilon$ such that*

$$\mathbb{E} \left[\left(\sum_{p=1}^P |Z_p|^2 \right)^{1+\tau/2} \right] < \infty$$

where

$$Z_p = \begin{cases} \xi_p([0, 1]^d) & \text{if } \xi_p \text{ corresponds to a point process,} \\ Y_p(0) & \text{if } \xi_p \text{ corresponds to a random field.} \end{cases}$$

Theorem S1 (Asymptotic normality under α -mixing). *We can replace the taper Assumption 5 with Assumption S1 and the process Assumption 7 with Assumption S2 in Theorem 3. Then the result of Theorem 3 continues to hold.*

Proof. See Appendix S3.1. □

S1.2 Growing a template region

One common way to construct a sequence of regions is to start with some bounded convex template region \mathcal{R} , and then grow it by scaling all of the dimensions by some factor $l_n \in \mathbb{R}_{>0}^d$, so that $\mathcal{R}_n = l_n \circ \mathcal{R}$. In this case, we can be more specific about the construction of the tapers. Note the convexity assumption is required so that we satisfy the previous nesting assumption that $\mathcal{R}_n \subset \mathcal{R}_{n+1}$. We will also assume without loss of generality that the template region contains zero for the same reason (one can always shift it to zero and shift it back again).

Proposition S1 (Growing a template region). *Let \mathcal{R} be some bounded convex region in \mathbb{R}^d which contains zero. Let $\{l_n\}_{n \in \mathbb{N}}$ be a sequence taking elements in $\mathbb{R}_{>0}^d$ such that l_n is elementwise strictly increasing and tend to infinity as $n \rightarrow \infty$. Say we have a family of tapers $\{h_m\}_{m \in \mathbb{N}}$ on \mathcal{R} that are bounded, continuous and orthonormal. Furthermore, for all $m \in \mathbb{N}$ there exists $\delta > 0$ and $C_m > 0$ such that for all $x \in \mathbb{R}^d$, $|h_m(x)| + |H_m(x)| \leq C_m(1 + \|x\|_2)^{-d-\delta}$. These constants scale so $\max_{m \in [M_n]} C_m \prod (l_n)^{1/2} (\min l_n)^{-d-\delta} \rightarrow 0$ and $\max_{m \in [M_n]} C_m \prod (l_n)^{-1/2} \rightarrow 0$ as $n \rightarrow \infty$. Choose the bandwidth b_n so that $b_n \rightarrow 0$ and*

$$\min_{m \in [M_n]} \int_{B_{b_n \circ l_n}} |H_m(k)|^2 dk \rightarrow 1, \quad (1)$$

as $n \rightarrow \infty$. Then the family of tapers on \mathcal{R}_n given by $h_{m,n}(x) = \prod (l_n)^{-1/2} h_m(x \otimes l_n)$ satisfies assumptions 2 to 5 and Assumption S1.

Proof. See Appendix S3.2. □

Here we take $\min l_n$ to mean the smallest element of the vector l_n for a given n . When $M_n = M$ is fixed, then $b_n \min l_n \rightarrow \infty$ as $n \rightarrow \infty$ is sufficient for Eq. (1), but Eq. (1) is slightly stronger when M_n is allowed to grow, which is required for consistency. In this case, the ordering of the tapers then matters, as we want to introduce new tapers sufficiently slowly relative to the growth of their concentration. This is discussed explicitly in Proposition S3. The condition on the decay of the tapers is required to use aliasing results and ensure that the errors when growing the number of tapers are controlled. Proposition S1 is however reassuring, in that the natural extension of multitapering to a growing region when one does have a reasonable family of tapers will satisfy our various assumptions.

For completeness, we can also consider the case where the template region is rectangular. In this case, we can construct a family of tapers on this region by taking the outer product of one-dimensional tapers. This will also give an existence proof for a family of tapers satisfying the conditions of Proposition S1, as we can simply make a family on a rectangle contained in \mathcal{R} (which is possible due to convexity), and then set the family to be zero on the rest of the region. This is of course not the most efficient way to construct tapers, and is intended only to show that such a family exists.

Proposition S2 (Growing a rectangular region). *Let $\mathcal{R} = \prod_{j=1}^d [a_j, b_j]$, where $a_j < 0 < b_j$. Say $\{g_m\}_{m \in \mathbb{N}}$ is an orthonormal family tapers supported on a subset of $[0, 1]$ that are bounded and continuous. Let γ be a bijection from \mathbb{N} to \mathbb{N}^d so that $\gamma(m)$ maps from a taper index m to a d -dimensional vector of indices from which we select the one-dimensional tapers. Writing $M_{n,j} = \max_{m \in [M_n]} \gamma(m)_j$ and $l_{n,j}$ for the j th element of l_n , assume that*

$$\min_{m \in [M_{n,j}]} \int_{-b_n l_{n,j} / \sqrt{d}}^{b_n l_{n,j} / \sqrt{d}} |g_m(x)|^2 dx \rightarrow 1.$$

Furthermore, for all $m \in \mathbb{N}$ there exists $\delta > 0$ and $C_m > 0$ such that for all $x \in \mathbb{R}^d$, $|g_m(x)| + |G_m(x)| \leq C_m(1 + |x|)^{-1-\delta}$, where $\max_{m \in [M_{n,j}]} C_m l_{n,j}^{-1/2} \rightarrow 0$ as $n \rightarrow \infty$.

Now define

$$h_m(x) = \prod_{j=1}^d \frac{1}{\sqrt{b_j - a_j}} g_{\gamma(m)_j} \left(\frac{x_j - a_j}{b_j - a_j} \right)$$

Then using the family of tapers $\{h_m\}_{m \in \mathbb{N}}$ in the construction in Proposition S1 satisfies assumptions 2 to 5 and Assumption S1.

Proof. See Appendix S3.3. □

Note here that the choice of bijection γ is not arbitrary, as it determines how quickly $M_{n,j}$ grows in each dimension. Typically, one would use $M = \prod_{j=1}^d M_j$ tapers in practice, using the first M_j tapers in each dimension. In this separable case, we have a slight relaxation of the condition on the decay of the tapers and their Fourier transforms, as we only require that they decay at a rate of $1 + \delta$ in each dimension. The factor of $1/\sqrt{d}$ modifying the bandwidth is because the previous assumptions were made for concentration on a ball, but now it is easier to work with a box when a separable structure is present. Since d is fixed and b_n is chosen this does not matter.

Finally, we need to check that a univariate family satisfying the required conditions exists. The minimum bias tapers proposed by Riedel and Sidorenko (1995), and used the point process setting by Rajala et al. (2023), satisfy these conditions.

Proposition S3 (Minimum bias tapers). *The minimum bias tapers, i.e. given for all $m \in \mathbb{N}$ by $g_m(x) = \sqrt{2} \sin(\pi mx) \mathbb{1}_{[0,1]}(x)$, $x \in \mathbb{R}$, satisfy the conditions of Proposition S2 if for all $n \in \mathbb{N}$, $b_n l_{n,j} \geq M_{n,j} \sqrt{d}$ and there exists some $\delta > 0$ such that $M_{n,j}^{1+\delta} l_{n,j}^{-1/2} \rightarrow 0$ as $n \rightarrow \infty$.*

Proof. See Appendix S3.4. \square

The assumption $b_n l_{n,j} \geq M_{n,j} \sqrt{d}$ is the usual choice of bandwidth versus number of tapers for the minimum bias tapers (Riedel and Sidorenko, 1995), provided that we view b_n / \sqrt{d} as the bandwidth. The assumption $M_{n,j}^{1+\delta} l_{n,j}^{-1/2} \rightarrow 0$ is required to ensure that the tapers satisfy Assumption 5, which in turn is needed for the consistency result in the non-Gaussian setting. All of these assumptions can be easily satisfied as we are free to choose the bandwidth b_n and the largest taper index in each dimension $M_{n,j}$ (as we choose M_n and γ).

S1.3 Covariance across wavenumbers

One useful additional result is that fixed $M_n = M$, we have a covariance given by

$$\text{cov} \left(\hat{f}_{p,q;n}(k), \hat{f}_{p',q';n}(k') \right) = o(1) + \sum_{m=1}^{M_n} \sum_{m'=1}^{M_n} \left\{ \int_{K_{p,p'}} H_{p;m,n}(k - k'') \overline{H_{p';m',n}(k' - k'')} \tilde{f}_{p,p'}(k'') dk'' \right. \\ \times \int_{K_{q,q'}} \overline{H_{q;m,n}(k' - k'')} H_{q';m',n}(k' - k'') \overline{\tilde{f}_{q,q'}(k'')} dk'' \\ + \int_{K_{p',q'}} H_{p;m,n}(k - k'') H_{q';m',n}(k' - k'') \tilde{f}_{p,q'}(k'') dk' \\ \left. \times \int_{K_{p',q}} \overline{H_{q;m,n}(k - k'')} H_{q';m',n}(k' - k'') \tilde{f}_{q,q'}(k'') dk'' \right\}.$$

where the $o(1)$ term comes from the fourth order cumulants, and is negligible as $n \rightarrow \infty$. Importantly, provided that the wavenumbers are not too close to each other (modulo some details related to aliasing), this covariance is negligible. In particular, we should space wavenumbers such that the distance between them is at least $2b_n$, so that the tapers do not overlap in wavenumber space.

S2 Proofs of main results

S2.1 Proposition 1

Recall the definitions of Ψ_p and w_p given in Definition 1.

Lemma S1. *For all $k \in \mathbb{R}^d$, for all $\psi \in \Psi_p$,*

$$H_{p;m,n}(k + \psi) = H_{p;m,n}(k) w_p(\psi),$$

and for all $\psi \in \Psi_p \cap \Psi_q$

$$H_{p;m,n}(k + \psi) \overline{H_{q;m,n}(k + \psi)} = H_{p;m,n}(k) \overline{H_{q;m,n}(k)} w_p(\psi) \overline{w_q(\psi)}.$$

Proof. For a process sampled on a grid, then for some $\psi \in \Psi_p$, recall $\psi = z' \oslash \Delta_p$ for some $z' \in \mathbb{Z}^d$. Then

$$H_{p;m,n}(k + \psi) = \prod (\Delta_p) \sum_{s \in \mathcal{G}_p} h_{p;m,n}(s) e^{-2\pi i (k + \psi) \cdot s} \\ = \prod (\Delta_p) \sum_{z \in \mathbb{Z}^d} h_{p;m,n}(z \circ \Delta_p + v_p) e^{-2\pi i k \cdot (z \circ \Delta_p + v_p)} e^{-2\pi i \psi \cdot z \circ \Delta_p} e^{-2\pi i \psi \cdot v_p} \\ = \prod (\Delta_p) \sum_{z \in \mathbb{Z}^d} h_{p;m,n}(z \circ \Delta_p + v_p) e^{-2\pi i k \cdot (z \circ \Delta_p + v_p)} e^{-2\pi i \psi \cdot z \circ \Delta_p} e^{-2\pi i \psi \cdot v_p} \\ = H_{p;m,n}(k) w_p(\psi)$$

where the last line holds because and $w_p(\psi) = e^{-2\pi i \psi \cdot v_p}$. In particular, this means we have $\psi \cdot z \circ \Delta_p = z' \cdot z \in \mathbb{Z}$ and hence $e^{-2\pi i \psi \cdot z \circ \Delta_p} = 1$. If one of the processes is sampled continuously, then $\Psi_p \cap \Psi_q = \{0\}$ and $w_p(0) = w_q(0) = 1$, so the second result is trivially true. If both processes are sampled on a grid then as $\Psi_p \cap \Psi_q$ is contained in Ψ_p and Ψ_q the result continues to hold. \square

We will prove a more general result than Proposition 1 which will also be useful for quantifying covariance over wavenumbers and tapers in Theorem 3.

Lemma S2. *Given assumptions 1 and 2,*

$$\text{cov}(J_{p;m,n}(k_1), J_{q;m,n}(k_2)) = \int_{K_{p,q}} H_{p;m,n}(k') \overline{H_{q;m',n}(k' - k_2 + k_1)} f_{p,q}(k_1 - k') dk' \quad (2)$$

for any $k_1, k_2 \in \mathbb{R}^d$.

Proof. Assumption 2 implies that we may use Lemma S6, setting $\phi_p(s) = h_{p;m}(s)e^{-2\pi i s \cdot k_1}$ and $\phi_q(s) = h_{q;m'}(s)e^{-2\pi i s \cdot k_2}$. Note

$$\begin{aligned} \Phi_p(k) &= \int_{\mathbb{R}^d} h_{p;m}(s)e^{-2\pi i s \cdot k_1} e^{-2\pi i s \cdot k} dk \\ &= H_{p;m}(k_1 + k). \end{aligned}$$

From Lemma S6 we have

$$\begin{aligned} \text{cov}(J_{p;m,n}(k_1), J_{q;m,n}(k_2)) &= \int_{\mathbb{R}^d} H_{p;m,n}(k_1 - k') \overline{H_{q;m',n}(k_2 - k')} f_{p,q}(k') dk' \\ &= \int_{\mathbb{R}^d} H_{p;m,n}(k'') \overline{H_{q;m',n}(k'' - k_1 + k_2)} f_{p,q}(k_1 - k'') dk''. \end{aligned}$$

Now breaking this up

$$\begin{aligned} &\text{cov}(J_{p;m,n}(k_1), J_{q;m,n}(k_2)) \\ &= \int_{\mathbb{R}^d} H_{p;m,n}(k') \overline{H_{q;m',n}(k' - k_1 + k_2)} f_{p,q}(k_1 - k') dk' \\ &= \sum_{\psi \in \Psi_p \cap \Psi_q} \int_{K_{p,q} + \psi} H_{p;m,n}(k') \overline{H_{q;m',n}(k' - k_1 + k_2)} f_{p,q}(k_1 - k') dk' \\ &= \sum_{\psi \in \Psi_p \cap \Psi_q} \int_{K_{p,q}} H_{p;m,n}(k' + \psi) \overline{H_{q;m',n}(k' - k_1 + k_2 + \psi)} f_{p,q}(k_1 - k' + \psi) dk' \\ &= \sum_{\psi \in \Psi_p \cap \Psi_q} \int_{K_{p,q}} H_{p;m,n}(k') \overline{H_{q;m',n}(k' - k_1 + k_2)} f_{p,q}(k_1 - k' + \psi) w_p(\psi) \overline{w_q(\psi)} dk' \end{aligned}$$

from the periodicity result in Lemma S1. Finally we have that

$$\begin{aligned} &\int_{K_{p,q}} \sum_{\psi \in \Psi_p \cap \Psi_q} \left| H_{p;m,n}(k') \overline{H_{q;m',n}(k' - k_1 + k_2)} f_{p,q}(k_1 - k') \right| dk' \\ &= \int_{K_{p,q}} \left| H_{p;m,n}(k') \overline{H_{q;m',n}(k' - k_1 + k_2)} \right| \sum_{\psi \in \Psi_p \cap \Psi_q} |f_{p,q}(k_1 - k' + \psi)| dk' \\ &< \infty \end{aligned}$$

by Lemma S9 and Assumption 2. Therefore, we may interchange the sum and integral by Fubini's theorem to obtain

$$\begin{aligned} &\text{cov}(J_{p;m,n}(k_1), J_{q;m,n}(k_2)) \\ &= \int_{K_{p,q}} H_{p;m,n}(k') \overline{H_{q;m',n}(k' - k_1 + k_2)} \sum_{\psi \in \Psi_p \cap \Psi_q} f_{p,q}(k_1 - k' + \psi) w_p(\psi) \overline{w_q(\psi)} dk' \\ &= \int_{K_{p,q}} H_{p;m,n}(k') \overline{H_{q;m',n}(k' - k_1 + k_2)} \tilde{f}_{p,q}(k_1 - k') dk'. \end{aligned}$$

as required. \square

Proof of Proposition 1. Follows from Lemma S2, by setting $k_1 = k_2 = k$ and $m' = m$. \square

S2.2 Theorem 1

In the process of proving Theorem 1 we will prove a stronger proposition which will also be useful for the correlation between the tapered Fourier transforms in Theorem 3, and for the consistency results when growing M_n .

Proposition S4. *Given that the process satisfies Assumption 1, and the tapers satisfy assumptions 2 and 3 we have for any $k_1, k_2 \in \mathbb{R}^d$*

$$\max_{m, m' \in [M_n]} |\text{cov}(J_{p; m, n}(k_1), J_{q; m', n}(k_2)) - Q_{p, q}(m, m', k_1, k_2)| \rightarrow 0$$

as $n \rightarrow \infty$, where

$$Q_{p, q}(m, m', k_1, k_2) = \begin{cases} \tilde{f}_{p, q}(k_1) \overline{w_q(k_2 - k_1)} & \text{if } m = m' \text{ and } k_1 - k_2 \in \Psi_q \\ \tilde{f}_{p, q}(k_2) \overline{w_p(k_1 - k_2)} & \text{if } m = m' \text{ and } k_1 - k_2 \in \Psi_p \setminus \Psi_q \\ 0 & \text{otherwise.} \end{cases}$$

Proof. Fix some $k_1, k_2 \in \mathbb{R}^d$ and fix some $n \in \mathbb{N}$ and $m, m' \in [M_n]$. We will establish bounds to show the desired convergence. We can without loss of generality assume that $k_1 - k_2 \notin \Psi_p \setminus \Psi_q$, as the case $k_1 - k_2 \in \Psi_p \setminus \Psi_q$ can be recovered from conjugate symmetry, because we have

$$\begin{aligned} \text{cov}(J_{q; m, n}(k_1), J_{p; m, n}(k_2)) &= \overline{\text{cov}(J_{p; m, n}(k_2), J_{q; m, n}(k_1))} \\ Q_{p, q}(m, m, k_1, k_2) &= \overline{Q_{q, p}(m, m, k_2, k_1)}. \end{aligned}$$

So without loss of generality assume that $k_1 - k_2 \notin \Psi_p$. From Lemma S2

$$\begin{aligned} \text{cov}(J_{p; m, n}(k_1), J_{q; m', n}(k_2)) &= \int_{K_{p, q}} H_{p; m, n}(k') \overline{H_{q; m', n}(k' - k_1 + k_2)} \tilde{f}_{p, q}(k_1 - k') dk' \\ &= \int_{B_{b_n}} H_{p; m, n}(k') \overline{H_{q; m', n}(k' - k_1 + k_2)} [\tilde{f}_{p, q}(k_1 - k') - \tilde{f}_{p, q}(k_1)] dk' \\ &\quad + \int_{K_{p, q} \setminus B_{b_n}} H_{p; m, n}(k') \overline{H_{q; m', n}(k' - k_1 + k_2)} \tilde{f}_{p, q}(k_1 - k') dk' \\ &\quad + \tilde{f}_{p, q}(k_1) \int_{B_{b_n}} H_{p; m, n}(k') \overline{H_{q; m', n}(k' - k_1 + k_2)} dk'. \end{aligned}$$

To consider each of these in turn, define

$$\begin{aligned} T_{p, q; n}^{(1)}(m, m', k_1, k_2) &= \int_{B_{b_n}} H_{p; m, n}(k') \overline{H_{q; m', n}(k' - k_1 + k_2)} [\tilde{f}_{p, q}(k_1 - k') - \tilde{f}_{p, q}(k_1)] dk' \\ T_{p, q; n}^{(2)}(m, m', k_1, k_2) &= \int_{K_{p, q} \setminus B_{b_n}} H_{p; m, n}(k') \overline{H_{q; m', n}(k' - k_1 + k_2)} \tilde{f}_{p, q}(k_1 - k') dk' \\ T_{p, q; n}^{(3)}(m, m', k_1, k_2) &= \tilde{f}_{p, q}(k_1) \int_{B_{b_n}} H_{p; m, n}(k') \overline{H_{q; m', n}(k' - k_1 + k_2)} dk' - Q_{p, q}(m, m', k_1, k_2) \end{aligned}$$

then to complete the proof we need only show that

$$\begin{aligned} \max_{m, m' \in [M_n]} |T_{p, q; n}^{(1)}(m, m', k_1, k_2)| &\rightarrow 0 \\ \max_{m, m' \in [M_n]} |T_{p, q; n}^{(2)}(m, m', k_1, k_2)| &\rightarrow 0 \\ \max_{m, m' \in [M_n]} |T_{p, q; n}^{(3)}(m, m', k_1, k_2)| &\rightarrow 0 \end{aligned}$$

as $n \rightarrow \infty$.

The $T^{(1)}$ term.

Firstly

$$\begin{aligned}
& \left| T_{p,q;n}^{(1)}(m, m', k_1, k_2) \right| \\
& \leq \int_{B_{b_n}} \left| H_{p;m,n}(k') \overline{H_{q;m',n}(k' - k_1 + k_2)} \right| \left| \tilde{f}_{p,q}(k_1 - k') - \tilde{f}_{p,q}(k_1) \right| dk' \\
& \leq \int_{B_{b_n}} \left| H_{p;m,n}(k') \overline{H_{q;m',n}(k' - k_1 + k_2)} \right| dk' \sup_{k'' \in B_{b_n}} \left| \tilde{f}_{p,q}(k_1 - k'') - \tilde{f}_{p,q}(k_1) \right|
\end{aligned}$$

and furthermore

$$\begin{aligned}
& \int_{B_{b_n}} \left| H_{p;m,n}(k') \overline{H_{q;m',n}(k' - k_1 + k_2)} \right| dk' \\
& \leq \left(\int_{B_{b_n}} |H_{p;m,n}(k')|^2 dk' \int_{B_{b_n}} |H_{q;m',n}(k' - k_1 + k_2)|^2 dk' \right)^{1/2} \\
& \leq \left(\int_{K_p} |H_{p;m,n}(k')|^2 dk' \int_{K_q} |H_{q;m',n}(k')|^2 dk' \right)^{1/2}.
\end{aligned}$$

In addition, by the triangle inequality

$$\begin{aligned}
& \max_{m \in [M_n]} \int_{K_p} |H_{p;m,n}(k')|^2 dk' \\
& \leq 1 + \max_{m \in [M_n]} \left| \int_{K_p} |H_{p;m,n}(k')|^2 dk' - 1 \right| \\
& \leq 1 + \max_{m \in [M_n]} \left| \int_{B_n} |H_{p;m,n}(k')|^2 dk' - 1 \right| + \max_{m \in [M_n]} \left| \int_{K_p \setminus B_n} |H_{p;m,n}(k')|^2 dk' \right| \\
& = 1 + o(1)
\end{aligned}$$

as $n \rightarrow \infty$ by Assumption 3. Putting this together we have

$$\max_{m \in [M_n]} \left| T_{p,q;n}^{(1)}(m, m', k_1, k_2) \right| \leq \sup_{k'' \in B_{b_n}} \left| \tilde{f}_{p,q}(k_1 - k'') - \tilde{f}_{p,q}(k_1) \right| (1 + o(1)) \rightarrow 0$$

as $n \rightarrow \infty$ by continuity of $\tilde{f}_{p,q}$ from Lemma S9 and the assumption that $b_n \rightarrow 0$ as $n \rightarrow \infty$.

The $T^{(3)}$ term.

We deal with the third term next, as we will need to use the result for processes sampled on grids to prove the second term goes to zero when only one process is sampled on a grid. Recall that

$$T_{p,q;n}^{(3)}(m, m', k_1, k_2) = \tilde{f}_{p,q}(k_1) \int_{B_{b_n}} H_{p;m,n}(k') \overline{H_{q;m',n}(k' - k_1 + k_2)} dk' - Q_{p,q}(m, m', k_1, k_2).$$

Firstly, if $k_1 - k_2 \notin \Psi_q$, then we note $Q_{p,q}(m, m', k_1, k_2) = 0$ and

$$\begin{aligned}
& \max_{m, m' \in [M_n]} \left| T_{p,q;n}^{(3)}(m, m', k_1, k_2) \right| \\
& \leq \left\| \tilde{f}_{p,q} \right\|_{\infty} \max_{m, m' \in [M_n]} \left| \int_{B_{b_n}} H_{p;m,n}(k') \overline{H_{q;m',n}(k' - k_1 + k_2)} dk' \right| \\
& \leq \left\| \tilde{f}_{p,q} \right\|_{\infty} \left(\max_{m \in [M_n]} \int_{B_{b_n}} |H_{p;m,n}(k')|^2 dk' \max_{m' \in [M_n]} \int_{B_{b_n}} |H_{q;m',n}(k' - k_1 + k_2)|^2 dk' \right)^{1/2}.
\end{aligned}$$

Firstly

$$\max_{m \in [M_n]} \int_{B_{b_n}} |H_{p;m,n}(k')|^2 dk' \rightarrow 1$$

by Assumption 3 and the triangle inequality. Secondly, take $\psi \in \Psi_q$ such that $k_1 - k_2 + \psi \in K_q$. Since $k_1 - k_2 \notin \Psi_q$, we have that $B_{b_n} + k_1 - k_2 + \psi \subseteq K_q \setminus B_n$ for sufficiently large n . Therefore, by periodicity of $H_{q;m;;n}$

$$\begin{aligned} \max_{m' \in [M_n]} \int_{B_{b_n}} |H_{q;m',n}(k' - k_1 + k_2)|^2 dk' &= \max_{m' \in [M_n]} \int_{B_{b_n}} |H_{q;m',n}(k' - k_1 + k_2 + \psi)|^2 dk' \\ &= \max_{m' \in [M_n]} \int_{B_{b_n} - k_1 + k_2 + \psi} |H_{q;m',n}(k'')|^2 dk'' \\ &\leq \max_{m' \in [M_n]} \int_{K_q \setminus B_n} |H_{q;m',n}(k'')|^2 dk'' \\ &\rightarrow 0 \end{aligned}$$

as $n \rightarrow \infty$ by Assumption 3. Therefore in this case $\max_{m,m' \in [M_n]} |T_{p,q;n}^{(3)}(m, m', k_1, k_2)| \rightarrow 0$ as $n \rightarrow \infty$.

Now consider the case where $k_1 - k_2 \in \Psi_q$. In this case from Lemma S1

$$T_{p,q;n}^{(3)}(m, m', k_1, k_2) = \tilde{f}_{p,q}(k_1) \int_{B_{b_n}} H_{p;m,n}(k') \overline{H_{q;m',n}(k') w_q(-k_1 + k_2)} dk' - Q_{p,q}(m, m', k_1, k_2).$$

Now further differentiating the cases based on whether $m = m'$ or $m \neq m'$, we have

$$\max_{m,m' \in [M_n]} |T_{p,q;n}^{(3)}(m, m', k_1, k_2)| \leq \max_{m \in [M_n]} |T_{p,q;n}^{(3)}(m, m, k_1, k_2)| + \max_{m \in [M_n]} \max_{m' \in [M_n] \setminus \{m\}} |T_{p,q;n}^{(3)}(m, m', k_1, k_2)|$$

Consider the second term first. In this case, since $m \neq m'$, $Q_{p,q}(m, m', k_1, k_2) = 0$. Therefore, since for sufficiently large n , $B_{b_n} \subseteq K_p \cap K_q$

$$|T_{p,q;n}^{(3)}(m, m', k_1, k_2)| \leq \|\tilde{f}_{p,q}\|_\infty \left| \int_{B_{b_n}} H_{p;m,n}(k') \overline{H_{q;m',n}(k')} dk' \right| \rightarrow 0$$

as $n \rightarrow 0$ by Assumption 4, since $m \neq m'$.

Finally, we have the last term, when $k_1 - k_2 \in \Psi_p$ and $m = m'$. In this case,

$$\begin{aligned} T_{p,q;n}^{(3)}(m, m', k_1, k_2) &= \tilde{f}_{p,q}(k_1) \int_{B_{b_n}} H_{p;m,n}(k') \overline{H_{q;m',n}(k') w_q(-k_1 + k_2)} dk' - \tilde{f}_{p,q}(k_1) \overline{w_q(k_2 - k_1)} \\ &= \tilde{f}_{p,q}(k_1) \overline{w_q(k_2 - k_1)} \left(\int_{B_{b_n}} H_{p;m,n}(k') \overline{H_{q;m',n}(k')} dk' - 1 \right). \end{aligned}$$

Therefore

$$\max_{m \in [M_n]} |T_{p,q;n}^{(3)}(m, m', k_1, k_2)| \leq \|\tilde{f}_{p,q}\|_\infty \max_{m \in [M_n]} \left| \int_{B_{b_n}} H_{p;m,n}(k') \overline{H_{q;m,n}(k')} dk' - 1 \right| \rightarrow 0$$

as $n \rightarrow \infty$ by Assumption 3. Therefore, we have shown that

$$\max_{m,m' \in [M_n]} |T_{p,q;n}^{(3)}(m, m', k_1, k_2)| \rightarrow 0$$

as $n \rightarrow \infty$.

The $T^{(2)}$ term.

Now for the second term, recall

$$T_{p,q;n}^{(2)}(m, m', k_1, k_2) = \int_{K_{p,q} \setminus B_{b_n}} H_{p;m,n}(k') \overline{H_{q;m',n}(k' - k_1 + k_2)} \tilde{f}_{p,q}(k_1 - k') dk'.$$

Therefore

$$|T_{p,q;n}^{(2)}(m, m', k_1, k_2)| \leq \int_{K_{p,q} \setminus B_{b_n}} |H_{p;m,n}(k') \overline{H_{q;m',n}(k' - k_1 + k_2)}| dk' \|\tilde{f}_{p,q}\|_\infty.$$

This is easiest dealt with by considering the different special cases for the processes p, q . Begin by assuming that both processes are sampled on grids. Potentially, $H_{p;m,n}$ and $H_{q;m,n}$ can repeat within $K_{p,q}$, however, the important observation is that this happens finitely many times, and they never repeat in the same way (so that they are only at most both large at zero), because we assumed that $k_1 - k_2 \notin \Psi_p \setminus \Psi_q$. The proof proceeds by splitting the integral into parts where one of $H_{p;m,n}$ or $H_{q;m,n}$ are large, and a remaining set where they are both small.

More formally, note that $\Psi_p \cap K_{p,q}$ and $\Psi_q \cap K_{p,q}$ are both finite sets. Also, by construction, $\Psi_p \cap \Psi_q \cap K_{p,q} = \{0\}$. This means that for sufficiently large n (and thus small b_n) we can partition $K_{p,q} \setminus B_{b_n}$ into the finite union of

$$\bigcup_{\psi \in \Psi_p \cap K_{p,q} \setminus \{0\}} B_{b_n} + \psi, \quad \bigcup_{\psi \in \Psi_q \cap K_{p,q} \setminus \{0\}} B_{b_n} + \psi \text{ and } K_{p,q} \setminus \left(\bigcup_{\psi \in \Psi_p \cup \Psi_q} B_{b_n} + \psi \right). \text{ This means}$$

$$\begin{aligned} \left| T_{p,q;n}^{(2)}(m, m', k_1, k_2) \right| &\leq \left\| \tilde{f}_{p,q} \right\|_{\infty} \sum_{\psi \in \Psi_p \cap K_{p,q} \setminus \{0\}} \int_{B_{b_n} + \psi} \left| H_{p;m,n}(k') \overline{H_{q;m',n}(k' - k_1 + k_2)} \right| dk' \\ &\quad + \left\| \tilde{f}_{p,q} \right\|_{\infty} \sum_{\psi \in \Psi_q \cap K_{p,q} \setminus \{0\}} \int_{B_{b_n} + \psi} \left| H_{p;m,n}(k') \overline{H_{q;m',n}(k' - k_1 + k_2)} \right| dk' \\ &\quad + \left\| \tilde{f}_{p,q} \right\|_{\infty} \int_{K_{p,q} \setminus \left(\bigcup_{\psi \in \Psi_p \cup \Psi_q} B_{b_n} + \psi \right)} \left| H_{p;m,n}(k') \overline{H_{q;m',n}(k' - k_1 + k_2)} \right| dk' \end{aligned}$$

The two sums are finite, so if we can bound the maximum over m, m' of their summands we are done. In particular, for some $\psi \in \Psi_p \cap K_{p,q} \setminus \{0\}$ we have

$$\begin{aligned} &\int_{B_{b_n} + \psi} \left| H_{p;m,n}(k') \overline{H_{q;m',n}(k' - k_1 + k_2)} \right| dk' \\ &\leq \left(\int_{B_{b_n} + \psi} |H_{p;m,n}(k')|^2 dk' \int_{B_{b_n} + \psi} |H_{q;m',n}(k' - k_1 + k_2)|^2 dk' \right)^{1/2} \\ &\leq \left(\underbrace{\int_{K_p \setminus B_{b_n}} |H_{p;m,n}(k')|^2 dk'}_{(a)} \underbrace{\int_{K_q + \psi} |H_{q;m',n}(k' - k_1 + k_2)|^2 dk'}_{(b)} \right)^{1/2} \end{aligned}$$

for sufficiently large n , where (a) comes from $B_{b_n} + \psi \cap B_{b_n} = \emptyset$ and (b) follows from $B_{b_n} \subseteq K_q$ (which is independent of m, m'). By periodicity,

$$\int_{B_{b_n} + \psi} \left| H_{p;m,n}(k') \overline{H_{q;m',n}(k' - k_1 + k_2)} \right| dk' \leq \left(\int_{K_p \setminus B_{b_n}} |H_{p;m,n}(k')|^2 dk' \int_{K_q} |H_{q;m',n}(k')|^2 dk' \right)^{1/2}$$

as $n \rightarrow \infty$ by the taper assumptions. Now to finish we see that

$$\begin{aligned} \max_{m \in [M_n]} \int_{K_p \setminus B_{b_n}} |H_{p;m',n}(k')|^2 dk' \int_{K_q} |H_{q;m,n}(k')|^2 dk' &= o(1)(1 + o(1)) \\ &= o(1) \end{aligned}$$

as $n \rightarrow \infty$ by Assumption 3. The argument for the second term is similar, except that we note either $k_1 - k_2 \in \Psi_q$, in which case we use periodicity, or $k_1 - k_2 \notin \Psi_q$, in which case we have that $B_{b_n} + \psi - k_1 + k_2 \cap B_{b_n} = \emptyset$ for sufficiently large n . Then the argument is the same.

Finally then

$$\begin{aligned} &\int_{K_{p,q} \setminus \left(\bigcup_{\psi \in \Psi_p \cup \Psi_q} B_{b_n} + \psi \right)} \left| H_{p;m,n}(k') \overline{H_{q;m',n}(k' - k_1 + k_2)} \right| dk' \\ &\leq \left(\int_{K_{p,q} \setminus \left(\bigcup_{\psi \in \Psi_p \cup \Psi_q} B_{b_n} + \psi \right)} |H_{p;m,n}(k')|^2 dk' \int_{K_{p,q} \setminus \left(\bigcup_{\psi \in \Psi_p \cup \Psi_q} B_{b_n} + \psi \right)} |H_{q;m',n}(k' - k_1 + k_2)|^2 dk' \right)^{1/2}. \end{aligned}$$

Consider the first of these terms. We will increase the domain of integration by removing only certain balls. In particular,

$$\begin{aligned}
\int_{K_{p,q} \setminus \left(\bigcup_{\psi \in \Psi_p \cup \Psi_q} B_{b_n} + \psi \right)} |H_{p;m,n}(k')|^2 dk' &\leq \int_{K_{p,q} \setminus \left(\bigcup_{\psi \in \Psi_p} B_{b_n} + \psi \right)} |H_{p;m,n}(k')|^2 dk' \\
&= \sum_{\psi' \in \Psi_p \cap K_{p,q}} \int_{(K_p + \psi') \setminus \left(\bigcup_{\psi \in \Psi_p} B_{b_n} + \psi \right)} |H_{p;m,n}(k')|^2 dk' \\
&\leq \sum_{\psi' \in \Psi_p \cap K_{p,q}} \int_{(K_p + \psi') \setminus (B_{b_n} + \psi')} |H_{p;m,n}(k')|^2 dk' \\
&= \sum_{\psi' \in \Psi_p \cap K_{p,q}} \int_{K_p \setminus B_{b_n}} |H_{p;m,n}(k' + \psi')|^2 dk' \\
&= \sum_{\psi' \in \Psi_p \cap K_{p,q}} \int_{K_p \setminus B_{b_n}} |H_{p;m,n}(k')|^2 dk'
\end{aligned}$$

by periodicity. Because $\Psi_p \cap K_{p,q}$ is a finite set and by Assumption 3,

$$\max_{m \in [M_n]} \int_{K_{p,q} \setminus \left(\bigcup_{\psi \in \Psi_p \cup \Psi_q} B_{b_n} + \psi \right)} |H_{p;m,n}(k')|^2 dk' \rightarrow 0$$

as $n \rightarrow \infty$. Now the second term satisfies

$$\begin{aligned}
\max_{m' \in [M_n]} \int_{K_{p,q} \setminus \left(\bigcup_{\psi \in \Psi_p \cup \Psi_q} B_{b_n} + \psi \right)} |H_{q;m',n}(k' - k_1 + k_2)|^2 dk' &\leq \max_{m' \in [M_n]} \int_{K_{p,q}} |H_{q;m',n}(k')|^2 dk' \\
&\rightarrow |\Psi_q \cap K_{p,q}| < \infty
\end{aligned}$$

as $n \rightarrow \infty$ by Assumption 3, the triangle inequality (as we detailed before), and periodicity. Therefore, when both processes are sampled on grids

$$\max_{m, m' \in [M_n]} |T_{p,q;n}^{(2)}(m, m', k_1, k_2)| \rightarrow 0$$

as $n \rightarrow \infty$.

When at least one of the processes, say p (wlog) is recorded continuously but the other is not, then $K_{p,q} = \mathbb{R}^d$, $\tilde{f}_{p,q} = f_{p,q}$ and $H_{p;m,n} = H_{m,n}$ so

$$\begin{aligned}
|T_{p,q;n}^{(2)}(m, m', k_1, k_2)| &= \left| \int_{\mathbb{R}^d \setminus B_{b_n}} H_{m,n}(k') \overline{H_{q;m',n}(k' - k_1 + k_2)} f_{p,q}(k_1 - k') dk' \right| \\
&\leq \int_{\mathbb{R}^d \setminus B_{b_n}} \left| H_{m,n}(k') \overline{H_{q;m',n}(k' - k_1 + k_2)} f_{p,q}(k_1 - k') \right| dk' \\
&\leq \left(\int_{\mathbb{R}^d \setminus B_{b_n}} |H_{m,n}(k')|^2 dk' \int_{\mathbb{R}^d \setminus B_{b_n}} \left| \overline{H_{q;m',n}(k' - k_1 + k_2)} f_{p,q}(k_1 - k') \right|^2 dk' \right)^{1/2}
\end{aligned}$$

the maximum over m, m' of which tends to zero provided that the second term converges to something finite. Indeed by Cauchy–Schwarz

$$\begin{aligned}
& \max_{m' \in [M_n]} \int_{\mathbb{R}^d \setminus B_{b_n}} \left| \overline{H_{q;m',n}(k' - k_1 + k_2)} f_{p,q}(k_1 - k') \right|^2 dk' \\
& \leq \max_{m' \in [M_n]} \int_{\mathbb{R}^d \setminus B_{b_n}} \left| \overline{H_{q;m',n}(k' - k_1 + k_2)} \right|^2 f_{q,q}(k_1 - k') f_{p,p}(k_1 - k') dk' \\
& \leq \max_{m' \in [M_n]} \int_{\mathbb{R}^d} |H_{q;m',n}(k' - k_1 + k_2)|^2 f_{q,q}(k_1 - k') dk' \|f_{p,p}\|_\infty \\
& = \max_{m' \in [M_n]} \int_{K_q} |H_{q;m',n}(k' - k_1 + k_2)|^2 \tilde{f}_{q,q}(k_1 - k') dk' \|f_{p,p}\|_\infty \quad (\text{by Definition 1}) \\
& \leq \max_{m' \in [M_n]} \int_{K_q} |H_{q;m',n}(k')|^2 dk' \left\| \tilde{f}_{q,q} \right\|_\infty \|f_{p,p}\|_\infty \\
& \rightarrow \left\| \tilde{f}_{q,q} \right\|_\infty \|f_{p,p}\|_\infty \\
& < \infty
\end{aligned}$$

by Assumption 3.

Finally, when both processes are sampled continuously

$$\begin{aligned}
& \max_{m, m' \in [M_n]} \left| T_{p,q;n}^{(2)}(m, m', k_1, k_2) \right| \\
& \leq \|f_{p,q}\|_\infty \max_{m, m' \in [M_n]} \int_{\mathbb{R}^d \setminus B_{b_n}} \left| H_{m,n}(k') \overline{H_{m',n}(k')} \right| dk' \\
& \leq \|f_{p,q}\|_\infty \left(\max_{m \in [M_n]} \int_{\mathbb{R}^d \setminus B_{b_n}} |H_{m,n}(k')|^2 dk' \right)^{1/2} \left(\max_{m' \in [M_n]} \int_{\mathbb{R}^d \setminus B_{b_n}} |H_{m',n}(k')|^2 dk' \right)^{1/2} \\
& \rightarrow 0
\end{aligned}$$

as $n \rightarrow \infty$ by Assumption 3. \square

Proof of Theorem 1. Noting we assume that λ_p is known, we have

$$\mathbb{E}[I_{p,q;m,n}(k)] = \text{cov}(J_{p;m,n}(k), J_{q;m,n}(k))$$

and so

$$\begin{aligned}
\left| \mathbb{E}[I_{p,q;m,n}(k)] - \tilde{f}_{p,q}(k) \right| &= \left| \text{cov}(J_{p;m,n}(k), J_{q;m,n}(k)) - \tilde{f}_{p,q}(k) \right| \\
&\leq \max_{m \in [M_n]} \left| \text{cov}(J_{p;m,n}(k), J_{q;m,n}(k)) - \tilde{f}_{p,q}(k) \right| \\
&\rightarrow 0
\end{aligned}$$

as $n \rightarrow \infty$ by Proposition S4 with $k_1 = k_2 = k$. \square

S2.3 Lemma 1

Proof of Lemma 1. If all of the processes are sampled continuously, then this is simply Proposition 12.6.III of Daley and Vere-Jones (2007), and so we consider the case when the last process is not sampled continuously, and is instead sampled on $\mathcal{G} = \Delta \circ \mathbb{Z}^d$. Differently from Daley and Vere-Jones (2007), we put the lags in the first arguments, not the last, but this is really just a cosmetic change here because the groups we use for the shift invariance are abelian.

The argument is essentially the same as Lemma 12.1.IV of Daley and Vere-Jones (2007), except that we need to handle the grid sampling. In particular, the original argument in Daley and Vere-Jones (2007) uses a shift invariance to diagonal shifts on the group $D_x^{(r)}$, for $r \in \mathbb{N}$ and $x \in \mathbb{R}^d$ where

$$D_x^{(r)}(y_1, \dots, y_r) = (y_1 + x, \dots, y_r + x)$$

for $y_1, \dots, y_r \in \mathbb{R}^d$. In particular, that the r th order cumulant measure is invariant to such shifts.

However, when at least one process is sampled on a grid this is no longer the case, as the grid is fixed, and thus not invariant to shifts, even when the underlying process is homogeneous (as a shift could change the number of included grid points). However, we still do have an invariance to diagonal shifts on the grid, provided all processes are sampled on the same grid (or can be embedded on the same grid). In particular, define the diagonal grid shifts by $\tilde{D}_x^{(r)}$ for $x \in \mathcal{G}$, where

$$\tilde{D}_x^{(r)}(y_1, \dots, y_r) = (y_1 + x, \dots, y_r + x)$$

for $y_1, \dots, y_r \in \mathbb{R}^d$.

Consider the space $\mathcal{Y} = \mathbb{R}^{d(r-1)} \times \mathcal{G}$. Using an essentially identical argument to that in Lemma 12.1.IV of Daley and Vere-Jones (2007), we consider the function from $\mathbb{R}^{d(r-1)} \times \mathcal{G}$ given by $((y_1, \dots, y_{r-1}, x)) \mapsto (x + y_1, \dots, x + y_{r-1}, x)$. This is a bijection from \mathcal{Y} to itself, and continuous, so measurable. This means we can use Lemma A2.7.II of Daley and Vere-Jones (2003), so that we have for any bounded measurable function $g : \mathbb{R}^{d(r-1)} \times \mathcal{G} \rightarrow \mathbb{C}$,

$$\begin{aligned} & \int_{\mathbb{R}^{d(r-1)} \times \mathcal{G}} g(y_1, \dots, y_r) C_{p_1, \dots, p_r}^{(\zeta)}(dy_1 \times \dots \times dy_r) \\ &= \int_{\mathcal{G}} \int_{\mathbb{R}^{d(r-1)}} g(x + u_1, \dots, x + u_{r-1}, x) \check{C}_{p_1, \dots, p_r}^{(\zeta)}(du_1 \times \dots \times du_{r-1}) \ell_{\mathcal{G}}(dx), \end{aligned}$$

where $\ell_{\mathcal{G}}$ is the counting measure on the grid \mathcal{G} . Now because the last process is sampled on the grid, we only have mass at the points in the grid in the last coordinate of $C_{p_1, \dots, p_r}^{(\zeta)}$, and similarly with $\ell_{\mathcal{G}}$, and so

$$\begin{aligned} & \int_{\mathbb{R}^d} g(y_1, \dots, y_r) C_{p_1, \dots, p_r}^{(\zeta)}(dy_1 \times \dots \times dy_r) \\ &= \int_{\mathbb{R}^{d(r-1)} \times \mathcal{G}} g(y_1, \dots, y_r) C_{p_1, \dots, p_r}^{(\zeta)}(dy_1 \times \dots \times dy_r) \\ &= \int_{\mathcal{G}} \int_{\mathbb{R}^{d(r-1)}} g(x + u_1, \dots, x + u_{r-1}, x) \check{C}_{p_1, \dots, p_r}^{(\zeta)}(du_1 \times \dots \times du_{r-1}) \ell_{\mathcal{G}}(dx) \\ &= \int_{\mathbb{R}^d} \int_{\mathbb{R}^{d(r-1)}} g(x + u_1, \dots, x + u_{r-1}, x) \check{C}_{p_1, \dots, p_r}^{(\zeta)}(du_1 \times \dots \times du_{r-1}) \ell_{\mathcal{G}}(dx). \end{aligned}$$

This establishes the required result. \square

S2.4 Theorem 2

Proof of Theorem 2. Begin with the bias result. Noting that we assume λ_p is known, we have

$$\begin{aligned} \left| \hat{f}_{p,q;n}(k) - \tilde{f}_{p,q}(k) \right| &= \left| \frac{1}{M_n} \sum_{m=1}^{M_n} I_{p,q;m,n}(k) - \tilde{f}_{p,q}(k) \right| \\ &\leq \max_{m \in [M_n]} \left| I_{p,q;m,n}(k) - \tilde{f}_{p,q}(k) \right| \\ &= \max_{m \in [M_n]} \left| \text{cov}(J_{p;m,n}(k), J_{q;m,n}(k)) - \tilde{f}_{p,q}(k) \right| \\ &\rightarrow 0 \end{aligned}$$

as $n \rightarrow \infty$ by Proposition S4 with $k_1 = k_2 = k$.

Now for the variance, firstly, for any $p, q \in [P]$ and $k \in \mathbb{R}^d$,

$$\text{var}(\hat{f}_{p,q;n}(k)) = \frac{1}{M_n^2} \sum_{m=1}^{M_n} \sum_{m'=1}^{M_n} \text{cov}(I_{p,q;m,n}(k), I_{p,q;m',n}(k)).$$

Now using the relations between moments and cumulants for mean-zero random variables

$$\begin{aligned}
\text{cov}(I_{p,q;m,n}(k), I_{p,q;m',n}(k')) &= \mathbb{E} \left[I_{p,q;m,n}(k) \overline{I_{p,q;m',n}(k')} \right] - \mathbb{E} [I_{p,q;m,n}(k)] \mathbb{E} \left[\overline{I_{p,q;m',n}(k')} \right] \\
&= \mathbb{E} \left[J_{p;m,n}(k) \overline{J_{q;m,n}(k)} \overline{J_{p;m',n}(k')} J_{q;m',n}(k') \right] \\
&\quad - \mathbb{E} [I_{p,q;m,n}(k)] \mathbb{E} \left[\overline{I_{p,q;m',n}(k')} \right] \\
&= \mathcal{C} \left[J_{p;m,n}(k), \overline{J_{q;m,n}(k)}, \overline{J_{p;m',n}(k')}, J_{q;m',n}(k') \right] \\
&\quad + \mathbb{E} \left[J_{p;m,n}(k) \overline{J_{p;m',n}(k')} \right] \mathbb{E} \left[\overline{J_{q;m,n}(k)} J_{q;m',n}(k') \right] \\
&\quad + \mathbb{E} [J_{p;m,n}(k) J_{q;m',n}(k')] \mathbb{E} \left[\overline{J_{q;m,n}(k)} \overline{J_{p;m',n}(k')} \right],
\end{aligned}$$

where $\mathcal{C}[\cdot]$ is the joint cumulant. Therefore we can split the variance into multiple parts, in particular

$$\begin{aligned}
\text{var}(\hat{f}_{p,q;n}(k)) &= \frac{1}{M_n^2} \sum_{m=1}^{M_n} \sum_{m'=1}^{M_n} \mathcal{C} \left[J_{p;m,n}(k), \overline{J_{q;m,n}(k)}, \overline{J_{p;m',n}(k)}, J_{q;m',n}(k) \right] \\
&\quad + \frac{1}{M_n^2} \sum_{m=1}^{M_n} \sum_{m'=1}^{M_n} \mathbb{E} \left[J_{p;m,n}(k) \overline{J_{p;m',n}(k)} \right] \mathbb{E} \left[\overline{J_{q;m,n}(k)} J_{q;m',n}(k) \right] \\
&\quad + \frac{1}{M_n^2} \sum_{m=1}^{M_n} \sum_{m'=1}^{M_n} \mathbb{E} [J_{p;m,n}(k) J_{q;m',n}(k)] \mathbb{E} \left[\overline{J_{q;m,n}(k)} \overline{J_{p;m',n}(k)} \right].
\end{aligned}$$

Again we name each term

$$\begin{aligned}
S_n^{(1)} &= \frac{1}{M_n^2} \sum_{m=1}^{M_n} \sum_{m'=1}^{M_n} \mathcal{C} \left[J_{p;m,n}(k), \overline{J_{q;m,n}(k)}, \overline{J_{p;m',n}(k)}, J_{q;m',n}(k) \right] \\
S_n^{(2)} &= \frac{1}{M_n^2} \sum_{m=1}^{M_n} \sum_{m'=1}^{M_n} \mathbb{E} \left[J_{p;m,n}(k) \overline{J_{p;m',n}(k)} \right] \mathbb{E} \left[\overline{J_{q;m,n}(k)} J_{q;m',n}(k) \right] \\
S_n^{(3)} &= \frac{1}{M_n^2} \sum_{m=1}^{M_n} \sum_{m'=1}^{M_n} \mathbb{E} [J_{p;m,n}(k) J_{q;m',n}(k)] \mathbb{E} \left[\overline{J_{q;m,n}(k)} \overline{J_{p;m',n}(k)} \right].
\end{aligned}$$

Firstly then

$$\begin{aligned}
S_n^{(2)} &= \frac{1}{M_n^2} \sum_{m=1}^{M_n} \sum_{m'=1}^{M_n} \mathbb{E} \left[J_{p;m,n}(k) \overline{J_{p;m',n}(k)} \right] \mathbb{E} \left[\overline{J_{q;m,n}(k)} J_{q;m',n}(k) \right] \\
&= \frac{1}{M_n^2} \sum_{m=1}^{M_n} \sum_{m'=1}^{M_n} |\text{cov}(J_{p;m,n}(k), J_{p;m',n}(k))|^2.
\end{aligned}$$

For notational convenience, write the following

$$\begin{aligned}
C_n(m, m') &= \text{cov}(J_{p;m,n}(k), J_{p;m',n}(k)), \\
Q(m, m') &= \tilde{f}_{p,q}(k) \delta_{m,m'}.
\end{aligned}$$

then note that

$$|C_n(m, m') - Q(m, m')|^2 = |C_n(m, m')|^2 - 2 \text{Re}\{C_n(m, m')Q(m, m')\} + |Q(m, m')|^2$$

so rearranging

$$\begin{aligned}
|C_n(m, m')|^2 &= |C_n(m, m') - Q(m, m')|^2 + 2 \text{Re}\{C_n(m, m')Q(m, m')\} - |Q(m, m')|^2 \\
&\leq |C_n(m, m') - Q(m, m')|^2 + 2|C_n(m, m')||Q(m, m')| + |Q(m, m')|^2 \\
&\leq |C_n(m, m') - Q(m, m')|^2 + 2|C_n(m, m') - Q(m, m')||Q(m, m')| + 2|Q(m, m')|^2.
\end{aligned}$$

Therefore,

$$\begin{aligned}
S_n^{(2)} &= \frac{1}{M_n^2} \sum_{m=1}^{M_n} \sum_{m'=1}^{M_n} |C_n(m, m')|^2 \\
&\leq \frac{1}{M_n^2} \sum_{m=1}^{M_n} \sum_{m'=1}^{M_n} |C_n(m, m') - Q(m, m')|^2 \\
&\quad + 2 \frac{1}{M_n^2} \sum_{m=1}^{M_n} \sum_{m'=1}^{M_n} |C_n(m, m') - Q(m, m')| |Q(m, m')| \\
&\quad + 2 \frac{1}{M_n^2} \sum_{m=1}^{M_n} \sum_{m'=1}^{M_n} |Q(m, m')|^2 \\
&\leq \max_{m, m' \in [M_n]} |C_n(m, m') - Q(m, m')|^2 \\
&\quad + \max_{m, m' \in [M_n]} |C_n(m, m') - Q(m, m')| \|\tilde{f}_{p,q}\|_\infty \\
&\quad + \frac{\|\tilde{f}_{p,q}\|_\infty}{M_n} \\
&\rightarrow 0
\end{aligned}$$

as $n \rightarrow \infty$ by Proposition S4 with $k_1 = k_2 = k$ and the assumption that $M_n \rightarrow \infty$.

Now

$$\begin{aligned}
S_n^{(3)} &= \frac{1}{M_n^2} \sum_{m=1}^{M_n} \sum_{m'=1}^{M_n} \mathbb{E} [J_{p;m,n}(k) J_{q;m',n}(k)] \mathbb{E} [\overline{J_{q;m,n}(k)} \overline{J_{p;m',n}(k)}] \\
&= \frac{1}{M_n^2} \sum_{m=1}^{M_n} \sum_{m'=1}^{M_n} \text{cov}(J_{p;m,n}(k), J_{q;m',n}(-k)) \text{cov}(J_{q;m,n}(-k), J_{p;m',n}(k))
\end{aligned}$$

by the same argument we used for $S_n^{(2)}$ setting $Q(m, m') = \tilde{f}_{p,q}(k) \delta_{m,m'}$ if $2k \in \Psi_p \cup \Psi_q$ and zero otherwise, we get

$$S_n^{(3)} \rightarrow 0$$

as $n \rightarrow \infty$.

Finally then we need to deal with the last term.

$$S_n^{(1)} = \frac{1}{M_n^2} \sum_{m=1}^{M_n} \sum_{m'=1}^{M_n} \mathcal{C} [J_{p;m,n}(k), \overline{J_{q;m,n}(k)}, \overline{J_{p;m',n}(k)}, J_{q;m',n}(k)].$$

In particular, let us study the term

$$\mathcal{C} [J_{p;m,n}(k), \overline{J_{q;m,n}(k)}, \overline{J_{p;m',n}(k)}, J_{q;m',n}(k)].$$

Recall that we defined the grid \mathcal{G} to be the grid which contains all of the other grids of interest. Therefore, when the p th process is sampled on a grid, we can write $g_{p;m,n} = \prod (\Delta_p) h_{m,n} \mathbb{1}_{\mathcal{G}_p}$, and think about the grid sampled transforms as sums of $g_{p;m,n}$ over the grid \mathcal{G} . For convenience, when the p th process is sampled continuously, we can set $g_{p;m,n} = h_{m,n}$, which is just the continuous transform.

For further notational convenience, define

$$\begin{aligned}
\phi_{1,n}(x) &= g_{p;m,n}(x) e^{-2\pi i k \cdot x}, \\
\phi_{2,n}(x) &= g_{q;m,n}(x) e^{2\pi i k \cdot x}, \\
\phi_{3,n}(x) &= g_{p;m',n}(x) e^{2\pi i k \cdot x}, \\
\phi_{4,n}(x) &= g_{q;m',n}(x) e^{-2\pi i k \cdot x}.
\end{aligned}$$

Again assume without loss of generality that if at least one process is sampled on a grid, then the q th process is sampled on a grid. Since the functions $h_{m,n}$ are bounded and have bounded support, from Lemma 1 we have that

$$\begin{aligned}
& \mathcal{C} \left[J_{p;m,n}(k), \overline{J_{q;m,n}(k)}, \overline{J_{p;m',n}(k)}, J_{q;m',n}(k) \right] \\
&= \mathcal{C} \left[\int_{\mathbb{R}^d} \phi_{1,n}(x) \xi_p^0(dx), \int_{\mathbb{R}^d} \phi_{2,n}(x) \xi_q^0(dx), \int_{\mathbb{R}^d} \phi_{3,n}(x) \xi_p^0(dx), \int_{\mathbb{R}^d} \phi_{4,n}(x) \xi_q^0(dx) \right] \\
&= \int_{\mathbb{R}^{4d}} \phi_{1,n}(x_1) \phi_{2,n}(x_2) \phi_{3,n}(x_3) \phi_{4,n}(x_4) C_{p,q,p,q}^{(\zeta)}(dx_1 \times dx_2 \times dx_3 \times dx_4) \\
&= \int_{\mathbb{R}^d} \int_{\mathbb{R}^{3d}} \phi_{1,n}(u_1 + x) \phi_{2,n}(u_2 + x) \phi_{3,n}(u_3 + x) \phi_{4,n}(x) \check{C}_{p,q,p,q}^{(\zeta)}(du_1 \times du_2 \times du_3) \ell_q(dx).
\end{aligned}$$

Now notice that the functions $\phi_{1,n}, \dots, \phi_{4,n}$ are all bounded with bounded support, and therefore the integral is well-defined. Furthermore, they are continuous functions, with continuous and L^1 Fourier transforms, meaning that we can write them as their Fourier inverse transforms. In particular, we have

$$\begin{aligned}
& \mathcal{C} \left[J_{p;m,n}(k), \overline{J_{q;m,n}(k)}, \overline{J_{p;m',n}(k)}, J_{q;m',n}(k) \right] \\
&= \int_{\mathbb{R}^d} \phi_{4,n}(x) \int_{\mathbb{R}^{3d}} \prod_{j=1}^3 \int_{\mathbb{R}^d} \Phi_{j,n}(k_j) e^{2\pi i k_j \cdot (u_1 + x)} dk_j \check{C}_{p,q,p,q}^{(\zeta)}(du_1 \times du_2 \times du_3) \ell_q(dx).
\end{aligned}$$

We will need to interchange the order of intergration, for which we will need to use Fubini's theorem. To check this is legitimate, we see

$$\begin{aligned}
& \int_{\mathbb{R}^d} |\phi_{4,n}(x)| \int_{\mathbb{R}^{3d}} \prod_{j=1}^3 \int_{\mathbb{R}^d} |\Phi_{j,n}(k_j)| dk_j \left| \check{C}_{p,q,p,q}^{(\zeta)} \right| (du_1 \times du_2 \times du_3) \ell_q(dx) \\
&= \prod_{j=1}^3 \|\Phi_{j,n}\|_1 \sum_{x \in \mathcal{G}} |\phi_{4,n}(x)| \left| \check{C}_{p,q,p,q}^{(\zeta)} \right| (\mathbb{R}^{3d}) \\
&< \infty
\end{aligned}$$

where $\left| \check{C}_{p,q,p,q}^{(\zeta)} \right|$ is the absolute value measure defined from the reduce cumulant measure using the Jordan-Hahn decomposition, and the integral is finite because the functions $\Phi_{j,n}$ are L^1 functions, $\phi_{1,n}$ is bounded and has bounded support, so that sum/integral (depending on wether the q th process is grid-sampled) is finite, and $\check{C}_{p,q,p,q}^{(\zeta)}$ is a totally finite measure.

Therefore, we can interchange the order of integration and write

$$\begin{aligned}
& \mathcal{C} \left[J_{p;m,n}(k), \overline{J_{q;m,n}(k)}, \overline{J_{p;m',n}(k)}, J_{q;m',n}(k) \right] \\
&= \int_{\mathbb{R}^d} \int_{\mathbb{R}^d} \int_{\mathbb{R}^d} \Phi_{1,n}(k_1) \Phi_{2,n}(k_2) \Phi_{3,n}(k_3) \int_{\mathbb{R}^d} \phi_{4,n}(x) e^{2\pi i k_1 + k_2 + k_3 \cdot x} dx \\
&\quad \cdot e^{2\pi i (k_1 \cdot u_1 + k_2 \cdot u_2 + k_3 \cdot u_3)} \check{C}_{p,q,p,q}^{(\zeta)}(du_1 \times du_2 \times du_3) dk_1 dk_2 dk_3 \\
&= \int_{\mathbb{R}^d} \int_{\mathbb{R}^d} \int_{\mathbb{R}^d} \Phi_{1,n}(k_1) \Phi_{2,n}(k_2) \Phi_{3,n}(k_3) \Phi_{4,n}(-k_1 - k_2 - k_3) \\
&\quad \cdot e^{2\pi i (k_1 \cdot u_1 + k_2 \cdot u_2 + k_3 \cdot u_3)} \check{C}_{p,q,p,q}^{(\zeta)}(du_1 \times du_2 \times du_3) dk_1 dk_2 dk_3 \\
&\leq \int_{\mathbb{R}^d} \int_{\mathbb{R}^d} \int_{\mathbb{R}^d} |\Phi_{1,n}(k_1) \Phi_{2,n}(k_2) \Phi_{3,n}(k_3) \Phi_{4,n}(-k_1 - k_2 - k_3)| dk_1 dk_2 dk_3 \left| \check{C}_{p,q,p,q}^{(\zeta)} \right| (\mathbb{R}^{3d}).
\end{aligned}$$

Now we consider two cases. Firstly, if the p th process is sampled continuously, then $\Phi_{4,n}(k') = H_{m',n}(k' - k)$ which is in L^1 . Therefore from Lemma S3 we have

$$\begin{aligned} & \mathcal{C} \left[J_{p;m,n}(k), \overline{J_{q;m,n}(k)}, \overline{J_{p;m',n}(k)}, J_{q;m',n}(k) \right] \\ & \leq \prod_{j=1}^4 \|\Phi_j\|_2^{\frac{1}{2}} \|\Phi_j\|_1^{\frac{1}{2}} \left| \check{C}_{p,q,p,q}^{(\zeta)} \right| (\mathbb{R}^{3d}) \\ & = \|H_{m,n}\|_2^{\frac{1}{4}} \|H_{m,n}\|_1^{\frac{1}{2}} \|H_{m',n}\|_2^{\frac{1}{4}} \|H_{m',n}\|_1^{\frac{1}{2}} \left| \check{C}_{p,q,p,q}^{(\zeta)} \right| (\mathbb{R}^{3d}) \\ & = \|H_{m,n}\|_2^{\frac{1}{4}} \|H_{m,n}\|_1^{\frac{1}{2}} \|H_{m',n}\|_2^{\frac{1}{4}} \|H_{m',n}\|_1^{\frac{1}{2}} \left| \check{C}_{p,q,p,q}^{(\zeta)} \right| (\mathbb{R}^{3d}). \end{aligned}$$

Therefore,

$$\begin{aligned} S_n^{(1)} &= \frac{1}{M_n^2} \sum_{m=1}^{M_n} \sum_{m'=1}^{M_n} \mathcal{C} \left[J_{p;m,n}(k), \overline{J_{q;m,n}(k)}, \overline{J_{p;m',n}(k)}, J_{q;m',n}(k) \right] \\ &\leq \left| \check{C}_{p,q,p,q}^{(\zeta)} \right| (\mathbb{R}^{3d}) \max_{m \in [M_n]} \|H_{m,n}\|_2^{\frac{1}{4}} \|H_{m,n}\|_1 \max_{m \in [M_n]} \|H_{m',n}\|_2^{\frac{1}{4}} \|H_{m',n}\|_1 \\ &= \left| \check{C}_{p,q,p,q}^{(\zeta)} \right| (\mathbb{R}^{3d}) \max_{m \in [M_n]} \|H_{m,n}\|_1 \max_{m \in [M_n]} \|H_{m',n}\|_1 \\ &\rightarrow 0 \end{aligned}$$

as $n \rightarrow \infty$.

Now if the p th process is sampled on a grid, then we have $\Phi_{4,n}(k') = H_{q;m',n}(k' - k)$, which repeats, so needs different treatment. In particular, we have that for $\psi \in \Psi_q$, $|\Phi_{4,n}(k' + \psi)| = |\Phi_{4,n}(k')|$.

Now

$$\begin{aligned} & \int_{\mathbb{R}^d} \int_{\mathbb{R}^d} \int_{\mathbb{R}^d} |\Phi_{1,n}(k_1) \Phi_{2,n}(k_2) \Phi_{3,n}(k_3) \Phi_{4,n}(-k_1 - k_2 - k_3)| dk_1 dk_2 dk_3 \\ &= \sum_{\psi_1, \psi_2, \psi_3 \in \Psi_q} \int_{K_p + \psi_1} \int_{K_q + \psi_2} \int_{K_q + \psi_3} |\Phi_{1,n}(k_1) \Phi_{2,n}(k_2) \Phi_{3,n}(k_3) \Phi_{4,n}(-k_1 - k_2 - k_3)| dk_1 dk_2 dk_3 \\ &= \sum_{\psi_1, \psi_2, \psi_3 \in \Psi_q} \int_{K_q} \int_{K_q} \int_{K_q} |\Phi_{1,n}(k_1 + \psi_1) \Phi_{2,n}(k_2 + \psi_2) \Phi_{3,n}(k_3 + \psi_3) \Phi_{4,n}(-k_1 - k_2 - k_3)| dk_1 dk_2 dk_3 \\ &\leq \left(\int_{K_q} |\Phi_{4,n}(k)|^{\frac{4}{3}} dk \right)^{3/4} \prod_{j=1}^3 \sum_{\psi_j \in \Psi_q} \int_{K_q} \left(|\Phi_{j,n}(k_j + \psi_j)|^{\frac{4}{3}} dk_j \right)^{3/4} \\ &\leq \left(\int_{K_q} |\Phi_{4,n}(k)|^2 dk \right)^{1/4} \left(\int_{K_q} |\Phi_{4,n}(k)| dk \right)^{1/2} \prod_{j=1}^3 \sum_{\psi_j \in \Psi_q} \int_{K_q} \left(|\Phi_{j,n}(k_j + \psi_j)|^2 dk_j \right)^{\frac{1}{2}} \ell(K_q)^{\frac{1}{4}} \\ &\leq \left(\int_{K_q} |\Phi_{4,n}(k)|^2 dk \right)^{1/4} \left(\int_{K_q} |\Phi_{4,n}(k)| dk \right)^{1/2} \ell(K_q)^{1/4} \prod_{j=1}^3 \sum_{\psi_j \in \Psi_q} \left(\int_{K_q + \psi_j} |\Phi_{j,n}(k_j)|^2 dk_j \right)^{1/2}, \end{aligned}$$

where we used Lemma S4. Therefore,

$$\begin{aligned} S_n^{(1)} &= \frac{1}{M_n^2} \sum_{m=1}^{M_n} \sum_{m'=1}^{M_n} \mathcal{C} \left[J_{p;m,n}(k), \overline{J_{q;m,n}(k)}, \overline{J_{p;m',n}(k)}, J_{q;m',n}(k) \right] \\ &\leq \left| \check{C}_{p,q,p,q}^{(\zeta)} \right| (\mathbb{R}^{3d}) \ell(K_q)^{1/4} \max_{m \in [M_n]} \left(\int_{K_q} |H_{q;m,n}(k)|^2 dk \right)^{1/4} \left(\int_{K_q} |H_{q;m,n}(k)| dk \right)^{1/2} \\ &\quad \times \left\{ \max_{m \in [M_n]} \sum_{\psi \in \Psi_q} \left(\int_{K_q + \psi} |H_{m,n}(k)|^2 dk \right)^{1/2} \right\}^3 \\ &\rightarrow 0 \end{aligned}$$

as $n \rightarrow \infty$ by assumptions 3 and 5. This completes the proof of the variance result. \square

Lemma S3. For $r \geq 3$, consider some functions $A_j : \mathbb{R}^d \rightarrow \mathbb{C}$ for $1 \leq j \leq r$ and $n \in \mathbb{N}$ such that $\|A_j\|_1 < \infty$ and $\|A_j\|_2 < \infty$, then

$$\int_{\mathbb{R}^d} \cdots \int_{\mathbb{R}^d} \left| \left\{ \prod_{j=1}^{r-1} A_j(k_j) \right\} A_r \left(- \sum_{j=1}^{r-1} k_j \right) \right| dk_1 \cdots dk_{r-1} \leq \prod_{j=1}^r \left(\int_{\mathbb{R}^d} |A_j(k)|^{\frac{r}{r-1}} dk \right)^{\frac{r-1}{r}}$$

Proof. Firstly we have

$$\begin{aligned} \|A_j\|_{\frac{r}{r-1}} &\leq \left(\int_{\mathbb{R}^d} |A_j(k)|^{\frac{r}{r-1}} dk \right)^{\frac{r-1}{r}} \\ &= \left(\left\| A_j^{\frac{2}{r-1}} A_j^{\frac{r-2}{r-1}} \right\|_1 \right)^{\frac{r-1}{r}} \\ &\leq \left(\left\| A_j^{\frac{2}{r-1}} \right\|_{r-1} \left\| A_j^{\frac{r-2}{r-1}} \right\|_{\frac{r-1}{r-2}} \right)^{\frac{r-1}{r}} \\ &= \left(\int_{\mathbb{R}^d} |A_j(k)|^2 dk \right)^{\frac{1}{r}} \left(\int_{\mathbb{R}^d} |A_j(k)| dk \right)^{\frac{r-2}{r}} \\ &= \|A_j\|_2^{\frac{1}{r}} \|A_j\|_1^{\frac{r-2}{r}} \\ &< \infty \end{aligned}$$

from Hölder's inequality and by the assumption of finiteness of $\|A_j\|_1$ and $\|A_j\|_2$.

Following the approach of Brillinger (1982), we begin by making the substitution

$$\begin{aligned} k'_1 &= k_1 \\ k'_j &= k_j + k'_{j-1} \quad \text{for } 2 \leq j \leq r-1, \end{aligned}$$

then we get

$$\begin{aligned} &\int_{\mathbb{R}^d} \cdots \int_{\mathbb{R}^d} \left| A_1(k'_1) \left\{ \prod_{j=2}^{r-1} A_j(k'_j - k'_{j-1}) \right\} A_r(-k'_{r-1}) \right| dk'_1 \cdots dk'_{r-1} \\ &= \int_{\mathbb{R}^d} |\phi_{r-1}(k) A_r(-k)| dk \\ &= \|\phi_{r-1} A_r\|_1, \end{aligned}$$

where

$$\begin{aligned} \phi_1(k) &= A_1(k), \\ \phi_j(k) &= \int_{\mathbb{R}^d} |A_j(k - k') \phi_{j-1}(k')| dk, \end{aligned}$$

for $2 \leq j \leq r-1$.

Now we have by Hölder's inequality

$$\|\phi_{r-1} A_r\|_1 \leq \|A_r\|_{\frac{r}{r-1}} \|\phi_{r-1}\|_r$$

and by definition and Young's inequality

$$\begin{aligned} \|\phi_1\|_{\frac{r}{r-1}} &= \|A_1\|_{\frac{r}{r-1}} \\ \|\phi_j\|_{\frac{r}{r-j}} &= \|A_j * \phi_{j-1}\|_{\frac{r}{r-1}} \\ &\leq \|A_j\|_{\frac{r}{r-1}} \|\phi_{j-1}\|_{\frac{r}{r-(j-1)}} \end{aligned}$$

for $2 \leq j \leq r-1$. Here Young's inequality applies because, $\|A_j\|_{\frac{r}{r-1}}$ is finite, and $\|\phi_{j-1}\|_{\frac{r}{r-(j-1)}}$ is therefore finite by induction. Applying this recursively we obtain

$$\|\phi_{r-1} A_r\|_1 \leq \prod_{j=1}^r \|A_j\|_{\frac{r}{r-1}}$$

giving the result. \square

Lemma S4. For any $r > 0$, if $h : \mathbb{R}^d \rightarrow \mathbb{C}$ for $1 \leq j \leq r$ is such that $\|h\|_1 < \infty$ and $\|h\|_2 < \infty$, then

$$\|h \mathbb{1}_K\|_{\frac{r}{r-1}} \leq \|h \mathbb{1}_K\|_2 \ell(K)^{\frac{r-2}{2r}}.$$

Proof. We have

$$\begin{aligned} \|h \mathbb{1}_K\|_{\frac{r}{r-1}} &= \|(h \mathbb{1}_K)^{\frac{r}{r-1}} \mathbb{1}_K\|_1^{\frac{r-1}{r}} \\ &\leq \left(\|(h \mathbb{1}_K)^{\frac{r}{r-1}}\|_{\frac{2(r-1)}{r}} \|\mathbb{1}_K\|_{\frac{2(r-1)}{r-2}} \right)^{\frac{r-1}{r}} \\ &= \left(\left(\int_K |h(x)|^2 dx \right)^{\frac{r}{2(r-1)}} \ell(K)^{\frac{r-2}{2(r-1)}} \right)^{\frac{r-1}{r}} \\ &= \|h \mathbb{1}_K\|_2 \ell(K)^{\frac{r-2}{2r}} \end{aligned}$$

where in the second line we used Hölder's inequality with $p = \frac{2(r-1)}{r}$ and $q = \frac{2(r-1)}{r-2}$. \square

S2.5 Theorem 3

Proof of Theorem 3. To establish this result, we use a similar argument to Brillinger (1982). In particular, we need to show that the mean is asymptotically zero, the variance and relation converges to a finite value, and that the cumulants of order greater than two converge to zero. The mean is asymptotically zero by construction. Recall we have restricted ourselves to the case where k_1, \dots, k_r are such that $k_i \pm k_j \notin \cup_{p \in [P]} \Psi_p$. Now from Proposition S4, for $j \in [r]$

$$\begin{aligned} \text{cov}(J_{p;m,n}(k_j), J_{q;m,n}(k_j)) &\rightarrow \tilde{f}_{p,q}(k_j) \overline{w_q(0)} \\ &= \tilde{f}_{p,q}(k_j) \end{aligned}$$

as $n \rightarrow \infty$ and have relation

$$\begin{aligned} \text{Rel}(J_{p;m,n}(k_j), J_{q;m,n}(k_j)) &= \text{cov}(J_{p;m,n}(k_j), \overline{J_{q;m,n}(k_j)}) \\ &= \text{cov}(J_{p;m,n}(k_j), J_{q;m,n}(-k_j)) \\ &\rightarrow 0 \end{aligned}$$

as $n \rightarrow \infty$ by conjugate symmetry of $J_{q;m,n}$ and because by assumption $k_j - (-k_j) = 2k_j \notin \Psi_p \cup \Psi_q$.

Finally for two different frequencies where $i \neq j$,

$$\text{cov}(J_{p;m,n}(k_i), J_{q;m,n}(k_j)) \rightarrow 0$$

as $n \rightarrow \infty$ and

$$\begin{aligned} \text{Rel}(J_{p;m,n}(k_i), J_{q;m,n}(k_j)) &= \text{cov}(J_{p;m,n}(k_i), J_{q;m,n}(-k_j)) \\ &\rightarrow 0 \end{aligned}$$

as $n \rightarrow \infty$ again from the assumption that $k_i \pm k_j \notin \Psi_p \cup \Psi_q$. The higher-order cumulants tending to zero follows the same argument used for the proof of consistency in Appendix S2.4, modified to the arbitrary order cumulants.

This means we have asymptotic normality and uncorrelatedness across k_i and k_j , and therefore we have asymptotic independence across k_i and k_j . \square

S2.6 Proposition 2

Proof of Proposition 2. The restriction to the set $\tilde{\mathcal{R}} = \{s \in \mathcal{R} \mid s + \Delta \circ [-1, 1]^d \subseteq \mathcal{R}\}$ ensures that when we linearly interpolate the tapers, we do not leave the region \mathcal{R} . This holds because the contribution to the linear interpolation from the discrete tapers we make at a point $s \in \mathcal{G}$ only impacts the values of the taper at points within $s + \Delta \circ [-1, 1]^d$, so if we only include such boxes contained in \mathcal{R} , the resultant tapers are supported on a subset of \mathcal{R} .

Now, by construction the tapers are bounded and continuous. Using Proposition S7, we can standardise the tapers to have unit L^2 norm. Finally, from Proposition S8 we have

$$H_m(k) = G_m^{(\mathcal{G})}(k) \prod_{j=1}^d \text{sinc}^2(\pi \Delta_j k_j)$$

where $G_m^{(\mathcal{G})}$ is the Fourier transform of the taper $g_m^{(\mathcal{G})}$. The Fourier transform $G_m^{(\mathcal{G})}$ is a finite sum because the region \mathcal{R} is bounded, and therefore it is bounded. As a result, $\|H_m\|_1 < \infty$ since sinc^2 is integrable. \square

S3 Proofs of additional results

S3.1 Proof of Theorem S1

Proof of Theorem S1. We utilise the central limit theorem result from Biscio and Waagepetersen (2019). There are four assumptions which must be verified to use this result, which they name $(\mathcal{H}1) - (\mathcal{H}4)$. For their full statement, see Biscio and Waagepetersen (2019). We will address each of these in turn. Note that the result in Biscio and Waagepetersen (2019) is for real valued statistics, and ours are complex valued. We handle this with the standard isomorphism between \mathbb{C} and \mathbb{R}^2 , so that we can treat the real and imaginary parts separately. In particular, write

$$\phi : \mathbb{C} \rightarrow \mathbb{R}^2, \quad \phi(x) = (\text{Re}(x), \text{Im}(x))^\top.$$

The statistic in question whose asymptotic normality we wish to establish is the vector given by

$$T_n = \ell(\mathcal{R}_n)^{1/2} \text{vec} [\phi(J_{p;m,n}(k_j))]_{p \in [P], m \in [M], j \in [r]},$$

which is a vector in \mathbb{R}^{2PMr} , recalling P is the number of processes, M then number of tapers and r the number of wavenumbers.

Firstly, starting with $(\mathcal{H}1)$. We require that $\mathcal{R}_1 \subset \mathcal{R}_2 \subset \dots$ and $\ell(\bigcup_{n=1}^{\infty} \mathcal{R}_n) = \infty$, which we satisfy by assumption. Furthermore, we need to be able to decompose the statistic T_n into an additive form,

$$T_n = \sum_{l \in \mathbb{Z}^d \cap \mathcal{R}_n} Z_n(l)$$

where $Z_n(l)$ is some function of the general process U , that only depends on U in the region $C(l) = l + (-1/2, 1/2]^d$. In Biscio and Waagepetersen (2019), they consider more generality than this, but we do not require such generality. In particular, we can consider a fixed grid and need only consider the boxes of the form $l + (-1/2, 1/2]^d$. So in the notation of Biscio and Waagepetersen (2019), we set $\eta = 0$ and $R = 0$ (see Biscio and Waagepetersen (2019) for their definition). Our tapered Fourier transforms certainly can be written in this form, as we can simply set

$$J_{p;m,n}(k, l) = \int_{C(l)} h_{p;m,n}(x) e^{-2\pi i k \cdot x} \xi_p^0(dx).$$

and then

$$Z_n(l) = \ell(\mathcal{R}_n)^{1/2} \text{vec} [\phi(J_{p;m,n}(k_j, l))]_{p \in [P], m \in [M], j \in [r]}.$$

Now to satisfy $(\mathcal{H}2)$, since we set $\eta = 0$, we just require that the process is α -mixing. In other words, the first part of Assumption S2.

Now to satisfy $(\mathcal{H}3)$, we need to show a moment condition. In particular, we require that the exists some $\tau > 2d/\epsilon$ such that

$$\sup_{n \in \mathbb{N}} \sup_{l \in \mathbb{Z}^d \cap \mathcal{R}_n} \mathbb{E} [|Z_n(l) - \mathbb{E}[Z_n(l)]|^{2+\tau}] < \infty,$$

where $|\cdot|$ here is the Frobenius norm. Note that $\mathbb{E}[Z_n(l)] = 0$, because we assumed λ_p is known. Furthermore, we have

$$\begin{aligned} \mathbb{E} [|Z_n(l) - \mathbb{E}[Z_n(l)]|^{2+\tau}] &= \mathbb{E} [|Z_n(l)|^{2+\tau}] \\ &= \ell(\mathcal{R}_n)^{1+\tau/2} \mathbb{E} \left[\left(\sum_{p=1}^P \sum_{m=1}^M \sum_{j=1}^r \text{Re}\{J_{p;m,n}(k_j, l)\}^2 + \text{Im}\{J_{p;m,n}(k_j, l)\}^2 \right)^{1+\tau/2} \right] \\ &= \ell(\mathcal{R}_n)^{1+\tau/2} \mathbb{E} \left[\left(\sum_{p=1}^P \sum_{m=1}^M \sum_{j=1}^r |J_{p;m,n}(k_j, l)|^2 \right)^{1+\tau/2} \right]. \end{aligned}$$

Now define

$$Z_p = \begin{cases} \xi_p^0([0, 1]^d) & \text{if } \xi_p \text{ corresponds to a point process,} \\ Y_p(\Delta_p) & \text{if } \xi_p \text{ corresponds to a random field.} \end{cases}$$

In the case of a point process we have

$$\begin{aligned}
|J_{p;m,n}(k_j, l)| &= \left| \int_{C(l)} h_{p;m,n}(x) e^{-2\pi i k \cdot x} \xi_p^0(dx) \right| \\
&= \left| \int_{C(l)} h_{m,n}(x) e^{-2\pi i k \cdot x} \xi_p^0(dx) \right| \\
&= \left| \int_{C(l)} h_{m,n}(x) e^{-2\pi i k \cdot x} \xi_p(dx) - \lambda_p \int_{C(l)} h_{m,n}(x) e^{-2\pi i k \cdot x} dx \right| \\
&\leq \|h_{m,n}\|_\infty \{ \xi_p(C(l)) + \lambda_p \}.
\end{aligned}$$

because both $\xi_p(C(l))$ and λ_p are non-negative and $\ell(C(l)) = 1$. In the case of a random field we have

$$\begin{aligned}
|J_{p;m,n}(k_j, l)| &= \left| \int_{C(l)} h_{p;m,n}(x) e^{-2\pi i k \cdot x} \xi_p^0(dx) \right| \\
&= \left(\prod_{j=1}^d \Delta_{p;j} \right) \sum_{u \in \mathcal{G}_p \cap C(l)} h_{m,n}(u) e^{-2\pi i k \cdot u} [Y_p(u) - \lambda_p] \\
&\leq \left(\prod_{j=1}^d \Delta_{p;j} \right) \|h_{m,n}\|_\infty \sum_{u \in \mathcal{G}_p \cap C(l)} |Y_p(u) - \lambda_p|.
\end{aligned}$$

W.l.o.g we can consider the case when at most one such point is present in $\mathcal{G}_p \cap C(l)$, as one could always just rescale the grid \mathbb{Z}^d by a constant (or rescale space). Clearly then the moments in question will be larger when there is a point (else $|Z_n(l)|$ is zero). Therefore, by stationarity we can choose to consider the variables around zero, so

$$\mathbb{E} [|Z_n(l) - \mathbb{E}[Z_n(l)]|^{2+\tau}] \leq C \ell(\mathcal{R}_n)^{1+\tau/2} \max_{m \in [M]} \|h_{m,n}\|_\infty^{2+\tau} \mathbb{E} \left[\left(\sum_{p=1}^P \sum_{m=1}^M \sum_{j=1}^r |Z_p - \mathbb{E}[Z_p]|^2 \right)^{1+\tau/2} \right]$$

where the constant C encodes nuisance constants like the products of Δ_p , and

$$Z_p = \begin{cases} \xi_p([0, 1]^d) & \text{if } \xi_p \text{ corresponds to a point process,} \\ Y_p(0) & \text{if } \xi_p \text{ corresponds to a random field.} \end{cases}$$

Therefore,

$$\begin{aligned}
&\sup_{n \in \mathbb{N}} \sup_{l \in \mathbb{Z}^d \cap \mathcal{R}_n} \mathbb{E} [|Z_n(l) - \mathbb{E}[Z_n(l)]|^{2+\tau}] \\
&\leq C \cdot \left(\sum_{p=1}^P \sum_{m=1}^M \sum_{j=1}^r |Z_p - \mathbb{E}[Z_p]|^2 \right)^{1+\tau/2} \left[\max_{m \in [M]} \sup_{n \in \mathbb{N}} \ell(\mathcal{R}_n) \|h_{m,n}\|_\infty^2 \right]^{1+\tau/2}
\end{aligned}$$

which is finite by assumptions S1 and S2.

Finally, need to show that (H4) holds. In particular, that

$$\liminf_{n \rightarrow \infty} \lambda_{\min} \left(\frac{\Sigma_n}{|D_n|} \right) > 0$$

where $\Sigma_n = \text{var}(T_n)$ and λ_{\min} is the smallest eigenvalue of a matrix. Now we have that

$$\Sigma_n = \ell(\mathcal{R}_n) S_n$$

where S_n is a matrix formed by appropriate combinations of $\mathbb{E}[I_{p,q;m,n}(k_j)]$ and zero. We have that for any $n \in \mathbb{N}$

$$\lambda_{\min} \left(\frac{\Sigma_n}{|D_n|} \right) = \frac{\ell(\mathcal{R}_n)}{|D_n|} \lambda_{\min}(S_n).$$

Now $\frac{\ell(\mathcal{R}_n)}{|D_n|}$ is bounded by 1, and $\lambda_{\min}(S_n)$ converges, therefore

$$\liminf_{n \rightarrow \infty} \lambda_{\min} \left(\frac{\Sigma_n}{|D_n|} \right) = \left(\lim_{n \rightarrow \infty} \lambda_{\min}(S_n) \right) \left(\liminf_{n \rightarrow \infty} \frac{\ell(\mathcal{R}_n)}{|D_n|} \right).$$

By Assumption S2 the second part is strictly positive. For the other part we see

$$\lim_{n \rightarrow \infty} \lambda_{\min}(S_n) = \lambda_{\min} \left(\lim_{n \rightarrow \infty} S_n \right).$$

Now $\lim_{n \rightarrow \infty} S_n$ is a block-diagonal matrix comprised of $\tilde{f}(k_j)$ by Lemma S2.

Finally, if $f(k)$ is positive definite for all k , then $\tilde{f}(k)$ is also positive definite by Lemma S10. Therefore, $\lambda_{\min}(\lim_{n \rightarrow \infty} S_n) > 0$ since block diagonal matrices have eigenvalues given by the union of the eigenvalues of their blocks. Therefore, from Biscio and Waagepetersen (2019)

$$\ell(\mathcal{R}_n)^{-1/2} T_n \xrightarrow{d} \mathcal{N}(0, I_{2PMr})$$

as $n \rightarrow \infty$. Meaning that

$$S_n^{-1/2} \text{vec} [\phi(J_{p;m,n}(k_j))]_{p \in [P], m \in [M], j \in [r]} \xrightarrow{d} \mathcal{N}(0, I_{2PMr}).$$

Writing S to be the limit of S_n (which is a block diagonal matrix with blocks $\tilde{f}(k_j)$), we have that

$$\text{vec} [\phi(J_{p;m,n}(k_j))]_{p \in [P], m \in [M], j \in [r]} \xrightarrow{d} \mathcal{N}(0, S)$$

as $n \rightarrow \infty$. This can then be appropriately converted back to complex notation and unpacked to give the desired result. \square

S3.2 Proposition S1

Proof of Proposition S1. Recall that the region is of the form

$$\mathcal{R}_n = \mathcal{R} \circ l_n$$

for some template region \mathcal{R} and we have set for $x \in \mathbb{R}^d$ and all $m, n \in \mathbb{N}$

$$h_{m,n}(x) = \prod (l_n)^{-1/2} h_m(x \otimes l_n),$$

where $\{h_m\}_{m \in \mathbb{N}}$ is an orthonormal family of tapers on \mathcal{R} that are continuous, orthonormal, and the bandwidth b_n so that $b_n \rightarrow 0$ and

$$\min_{m \in [M_n]} \int_{B_{b_n} \circ l_n} |H_m(k)|^2 dk \rightarrow 1,$$

Beginning with checking Assumption 2, by construction h_m is bounded and continuous, and therefore $h_{m,n}$ is also bounded and continuous for any $n \in \mathbb{N}$, since we scale by a decreasing sequence. Furthermore, if $x \notin \mathcal{R}_n$ then $x \otimes l_n \notin \mathcal{R}$, and so $h_{m,n}(x) = 0$.

Next we have

$$\begin{aligned} \langle h_{m,n}, h_{m',n} \rangle &= \int_{\mathbb{R}^d} h_{m,n}(x) \overline{h_{m',n}(x)} dx \\ &= \frac{1}{\prod (l_n)} \int_{\mathbb{R}^d} h_m(x \otimes l_n) \overline{h_{m'}(x \otimes l_n)} dx \\ &= \frac{\prod (l_n)}{\prod (l_n)} \int_{\mathbb{R}^d} h_m(u) \overline{h_{m'}(u)} du \\ &= \langle h_m, h_{m'} \rangle. \end{aligned}$$

Since h_m is orthonormal, we have that $\langle h_{m,n}, h_{m',n} \rangle = \delta_{m,m'}$.

We also have that for all $n \in \mathbb{N}$

$$\begin{aligned}
\int_{\mathbb{R}^d} |H_{m,n}(k)| dk &= \prod (l_n)^{1/2} \int_{\mathbb{R}^d} |H_m(k \circ l_n)| dk \\
&= \prod (l_n)^{-1/2} \int_{\mathbb{R}^d} |H_m(k')| dk' \\
&\leq C_m \prod (l_n)^{-1/2} \int_{\mathbb{R}^d} (1 + \|x\|_2)^{-d-\delta} dk' \\
&< \infty.
\end{aligned}$$

As for Assumption 3, we need to prove that

$$\begin{aligned}
\max_{m \in [M_n]} \left| \int_{B_{b_n}} H_{p;m,n}(k) \overline{H_{q;m,n}(k)} dk - 1 \right| &\rightarrow 0, \\
\max_{m \in [M_n]} \left| \int_{K_p \setminus B_{b_n}} |H_{p;m,n}(k)|^2 dk \right| &\rightarrow 0,
\end{aligned}$$

as $n \rightarrow \infty$.

Now we will need to utilise the aliasing relationship. In particular, we have that

$$H_{p;m,n}(k) = \sum_{\psi \in \Psi_p} H_{m,n}(k + \psi) w_p(\psi)$$

which holds given the conditions by Lemma S5.

Therefore, we have

$$\begin{aligned}
&\int_{B_{b_n}} H_{p;m,n}(k) \overline{H_{q;m,n}(k)} dk \\
&= \sum_{\psi_p \in \Psi_p} \sum_{\psi_q \in \Psi_q} w_p(\psi_p) \overline{w_q(\psi_q)} \int_{B_{b_n}} H_{m,n}(k + \psi_p) \overline{H_{m,n}(k + \psi_q)} dk \\
&= \sum_{\psi_p \in \Psi_p \setminus \{0\}} \sum_{\psi_q \in \Psi_q \setminus \{0\}} w_p(\psi_p) \overline{w_q(\psi_q)} \int_{B_{b_n}} H_{m,n}(k + \psi_p) \overline{H_{m,n}(k + \psi_q)} dk \\
&\quad + \sum_{\psi_p \in \Psi_p \setminus \{0\}} w_p(\psi_p) \int_{B_{b_n}} H_{m,n}(k + \psi_p) \overline{H_{m,n}(k)} dk \\
&\quad + \sum_{\psi_q \in \Psi_q \setminus \{0\}} \overline{w_q(\psi_q)} \int_{B_{b_n}} H_{m,n}(k) \overline{H_{m,n}(k + \psi_q)} dk \\
&\quad + \int_{B_{b_n}} |H_{m,n}(k)|^2 dk.
\end{aligned}$$

Therefore

$$\begin{aligned}
& \max_{m \in [M_n]} \left| \int_{B_{b_n}} H_{p;m,n}(k) \overline{H_{q;m,n}(k)} dk - 1 \right| \\
& \leq \max_{m \in [M_n]} \left| \sum_{\psi_p \in \Psi_p \setminus \{0\}} \sum_{\psi_q \in \Psi_q \setminus \{0\}} w_p(\psi_p) \overline{w_q(\psi_q)} \int_{B_{b_n}} H_{m,n}(k + \psi_p) \overline{H_{m,n}(k + \psi_q)} dk \right| \\
& \quad + \max_{m \in [M_n]} \left| \sum_{\psi_p \in \Psi_p \setminus \{0\}} w_p(\psi_p) \int_{B_{b_n}} H_{m,n}(k + \psi_p) \overline{H_{m,n}(k)} dk \right| \\
& \quad + \max_{m \in [M_n]} \left| \sum_{\psi_q \in \Psi_q \setminus \{0\}} \overline{w_q(\psi_q)} \int_{B_{b_n}} H_{m,n}(k) \overline{H_{m,n}(k + \psi_q)} dk \right| \\
& \quad + \max_{m \in [M_n]} \left| \int_{B_{b_n}} |H_{m,n}(k)|^2 dk - 1 \right|.
\end{aligned}$$

Note that

$$0 \leq \int_{B_{b_n}} |H_{m,n}(k)|^2 dk \leq \int_{\mathbb{R}^d} |H_{m,n}(k)|^2 dk = 1$$

and therefore

$$\begin{aligned}
\max_{m \in [M_n]} \left| \int_{B_{b_n}} |H_{m,n}(k)|^2 dk - 1 \right| &= 1 - \min_{m \in [M_n]} \int_{B_{b_n}} |H_{m,n}(k)|^2 dk \\
&= 1 - \min_{m \in [M_n]} \prod(l_n) \int_{B_{b_n}} |H_m(k \circ l_n)|^2 dk \\
&= 1 - \min_{m \in [M_n]} \frac{\prod(l_n)}{\prod(l_n)} \int_{B_{b_n} \circ l_n} |H_m(k')|^2 dk' \\
&= 1 - \min_{m \in [M_n]} \int_{B_{b_n} \circ l_n} |H_m(k)|^2 dk \\
&\rightarrow 0
\end{aligned}$$

because by assumption, we have that $\min_{m \in [M_n]} \int_{B_{b_n} \circ l_n} |H_m(k)|^2 dk \rightarrow 1$ as $n \rightarrow \infty$.

Now recall that

$$|H_m(k)| \leq \frac{C_m}{(1 + \min_{x \in B_{b_n}} \|k\|_2)^{d+\delta}}$$

and therefore

$$|H_{m,n}(k)| \leq \frac{C_m \prod(l_n)^{1/2}}{(1 + \min_{x \in B_{b_n}} \|k \circ l_n\|_2)^{d+\delta}}.$$

Now consider the first term. In particular, we have

$$\begin{aligned}
& \left| \int_{B_{b_n}} H_{m,n}(k + \psi_p) \overline{H_{m,n}(k + \psi_q)} dk \right| \\
& \leq \int_{B_{b_n}} \left| H_{m,n}(k + \psi_p) \overline{H_{m,n}(k + \psi_q)} \right| dk \\
& \leq \ell(B_{b_n}) \frac{C_m^2 \prod(l_n)}{(1 + \min_{x \in B_{b_n}} \|(\psi_q + x) \circ l_n\|_2)^{d+\delta} (1 + \min_{x \in B_{b_n}} \|(\psi_q + x) \circ l_n\|_2)^{d+\delta}} \\
& \leq \frac{\ell(B_{b_n}) \prod(l_n)}{\min l_n^{2(d+\delta)}} \frac{C_m^2}{(1/\min l_n + \min_{x \in B_{b_n}} \|\psi_p + x\|_2)^{d+\delta} (1/\min l_n + \min_{x \in B_{b_n}} \|\psi_q + x\|_2)^{d+\delta}}
\end{aligned}$$

therefore

$$\begin{aligned}
& \max_{m \in [M_n]} \left| \sum_{\psi_p \in \Psi_p \setminus \{0\}} \sum_{\psi_q \in \Psi_q \setminus \{0\}} w_p(\psi_p) \overline{w_q(\psi_q)} \int_{B_{b_n}} H_{m,n}(k + \psi_p) \overline{H_{m,n}(k + \psi_q)} dk \right| \\
& \leq \sum_{\psi_p \in \Psi_p \setminus \{0\}} \sum_{\psi_q \in \Psi_q \setminus \{0\}} \max_{m \in [M_n]} \left| \int_{B_{b_n}} H_{m,n}(k + \psi_p) \overline{H_{m,n}(k + \psi_q)} dk \right| \\
& \leq \sum_{\psi_p \in \Psi_p \setminus \{0\}} \sum_{\psi_q \in \Psi_q \setminus \{0\}} \max_{m \in [M_n]} \frac{\ell(B_{b_n})}{\min l_n^2} \frac{C_m^2}{(1/\min l_n + \min_{x \in B_{b_n}} \|\psi_p + x\|_2)^{d+\delta}} \frac{C_m^2}{(1/\min l_n + \min_{x \in B_{b_n}} \|\psi_q + x\|_2)^{d+\delta}} \\
& \leq \max_{m \in [M_n]} C_m^2 \frac{\ell(B_{b_n}) \prod (l_n)}{\min l_n^{2(d+\delta)}} \sum_{\psi_p \in \Psi_p \setminus \{0\}} \frac{1}{(\min_{x \in B_{b_n}} \|\psi_p + x\|_2)^{d+\delta}} \sum_{\psi_q \in \Psi_q \setminus \{0\}} \frac{1}{(\min_{x \in B_{b_n}} \|\psi_q + x\|_2)^{d+\delta}} \\
& \rightarrow 0
\end{aligned}$$

as $n \rightarrow \infty$ because by assumption $\ell(B_{b_n}) \rightarrow 0$ and $\max_{m \in [M_n]} C_m \prod (l_n)^{1/2} (\min l_n)^{-d-\delta} \rightarrow 0$ as $n \rightarrow \infty$. The second and third terms are symmetric, so we treat only one of them. In particular, note that

$$\begin{aligned}
\int_{B_{b_n}} H_{m,n}(k) \overline{H_{m,n}(k + \psi_q)} dk & \leq \left(\int_{B_{b_n}} |H_{m,n}(k)|^2 dk \right)^{1/2} \left(\int_{B_{b_n}} |H_{m,n}(k + \psi_q)|^2 dk \right)^{1/2} \\
& \leq \left(\int_{B_{b_n}} |H_{m,n}(k + \psi_q)|^2 dk \right)^{1/2} \\
& \leq \frac{\ell(B_{b_n})^{1/2} \prod (l_n)^{1/2}}{\min l_n^{d+\delta}} \frac{C_m}{(1/\min l_n + \min_{x \in B_{b_n}} \|\psi_q + x\|_2)^{d+\delta}}
\end{aligned}$$

by similar arguments as above. Therefore

$$\begin{aligned}
& \max_{m \in [M_n]} \left| \sum_{\psi_p \in \Psi_p \setminus \{0\}} w_p(\psi_p) \int_{B_{b_n}} H_{m,n}(k + \psi_p) \overline{H_{m,n}(k)} dk \right| \\
& \leq \sum_{\psi_p \in \Psi_p \setminus \{0\}} \max_{m \in [M_n]} \left| \int_{B_{b_n}} H_{m,n}(k + \psi_p) \overline{H_{m,n}(k)} dk \right| \\
& \leq \max_{m \in [M_n]} C_m \frac{\ell(B_{b_n})^{1/2} \prod (l_n)^{1/2}}{\min l_n^{d+\delta}} \sum_{\psi_p \in \Psi_p \setminus \{0\}} \frac{1}{(\min_{x \in B_{b_n}} \|\psi_p + x\|_2)^{d+\delta}} \\
& \rightarrow 0
\end{aligned}$$

as $n \rightarrow \infty$ by the same arguments as above. This completes the proof.

The second condition, namely

$$\max_{m \in [M_n]} \left| \int_{K_p \setminus B_{b_n}} |H_{p;m,n}(k)|^2 dk \right| \rightarrow 0$$

as $n \rightarrow \infty$ follows the exact same argument as above (as we do not use the fact that $\ell(B_{b_n}) \rightarrow 0$) with the only difference being the term where there is no aliasing. In particular, we have

$$\begin{aligned}
\max_{m \in [M_n]} \left| \int_{K_p \setminus B_{b_n}} |H_{p;m,n}(k)|^2 dk \right| & \leq \max_{m \in [M_n]} \left| \sum_{\psi \in \Psi_p \setminus \{0\}} \sum_{\psi' \in \Psi_p \setminus \{0\}} w_p(\psi) \overline{w_p(\psi')} \int_{K_p \setminus B_{b_n}} H_{m,n}(k + \psi) \overline{H_{m,n}(k + \psi')} dk \right| \\
& + 2 \max_{m \in [M_n]} \left| \sum_{\psi_p \in \Psi_p \setminus \{0\}} w_p(\psi_p) \int_{K_p \setminus B_{b_n}} H_{m,n}(k + \psi_p) \overline{H_{m,n}(k)} dk \right| \\
& + \max_{m \in [M_n]} \left| \int_{K_p \setminus B_{b_n}} |H_{m,n}(k)|^2 dk \right|.
\end{aligned}$$

The first two terms are handled in the same way as above. The last term

$$\begin{aligned}
\max_{m \in [M_n]} \left| \int_{K_p \setminus B_{b_n}} |H_{m,n}(k)|^2 dk \right| &\leq \max_{m \in [M_n]} \left| \int_{K_p} |H_{m,n}(k)|^2 dk - 1 \right| + \max_{m \in [M_n]} \left| 1 - \int_{B_{b_n}} |H_{m,n}(k)|^2 dk \right| \\
&\leq \max_{m \in [M_n]} \left| \int_{K_p \circ l_n} |H_m(k)|^2 dk - 1 \right| + \max_{m \in [M_n]} \left| 1 - \int_{B_{b_n} \circ l_n} |H_m(k)|^2 dk \right| \\
&\leq 2 \left(1 - \min_{m \in [M_n]} \int_{B_{b_n} \circ l_n} |H_m(k)|^2 dk \right) \\
&\rightarrow 0
\end{aligned}$$

as $n \rightarrow \infty$ by assumption.

Moving on to Assumption 4, we firstly have $\langle h_{m,n}, h_{m',n} \rangle = 0$ for any $m \neq m'$ by assumption. Then by a similar argument to the above, again have

$$\begin{aligned}
&\max_{m \in [M_n]} \max_{m' \in [M_n] \setminus \{m\}} \left| \int_{B_{b_n}} H_{p;m,n}(k) \overline{H_{q;m',n}(k)} dk \right| \\
&\leq \max_{m \in [M_n]} \max_{m' \in [M_n] \setminus \{m\}} \left| \sum_{\psi_p \in \Psi_p} \sum_{\psi_q \in \Psi_q} w_p(\psi_p) \overline{w_q(\psi_q)} \int_{B_{b_n}} H_{m,n}(k + \psi_p) \overline{H_{m',n}(k + \psi_q)} dk \right| \\
&\quad + \max_{m \in [M_n]} \max_{m' \in [M_n] \setminus \{m\}} \left| \sum_{\psi_p \in \Psi_p} w_p(\psi_p) \int_{B_{b_n}} H_{m,n}(k + \psi_p) \overline{H_{m',n}(k)} dk \right| \\
&\quad + \max_{m \in [M_n]} \max_{m' \in [M_n] \setminus \{m\}} \left| \sum_{\psi_q \in \Psi_q} \overline{w_q(\psi_q)} \int_{B_{b_n}} H_{m,n}(k) \overline{H_{m',n}(k + \psi_q)} dk \right| \\
&\quad + \max_{m \in [M_n]} \max_{m' \in [M_n] \setminus \{m\}} \left| \int_{B_{b_n}} H_{m,n}(k) \overline{H_{m',n}(k)} dk \right|.
\end{aligned}$$

By the same arguments used above we need only consider the last term. In particular, we have (because $H_m, H_{m'}$ is orthogonal when $m \neq m'$)

$$\begin{aligned}
&\max_{m \in [M_n]} \max_{m' \in [M_n] \setminus \{m\}} \left| \int_{B_{b_n}} H_{m,n}(k) \overline{H_{m',n}(k)} dk \right| \\
&= \max_{m \in [M_n]} \max_{m' \in [M_n] \setminus \{m\}} \left| \int_{B_{b_n} \circ l_n} H_m(k) \overline{H_{m'}(k)} dk \right| \\
&= \max_{m \in [M_n]} \max_{m' \in [M_n] \setminus \{m\}} \left| \int_{\mathbb{R}^d \setminus B_{b_n} \circ l_n} H_m(k) \overline{H_{m'}(k)} dk - \int_{\mathbb{R}^d} H_m(k) \overline{H_{m'}(k)} dk \right| \\
&\leq \max_{m \in [M_n]} \max_{m' \in [M_n] \setminus \{m\}} \left(\int_{\mathbb{R}^d \setminus B_{b_n} \circ l_n} |H_m(k)|^2 \int_{\mathbb{R}^d \setminus B_{b_n} \circ l_n} |H_{m'}(k)|^2 dk \right)^{1/2} \\
&\leq \max_{m \in [M_n]} \int_{\mathbb{R}^d \setminus B_{b_n} \circ l_n} |H_m(k)|^2 \\
&\rightarrow 0
\end{aligned}$$

as $n \rightarrow \infty$ as already established.

Now for Assumption 5. In particular, we need to show that

$$\begin{aligned} \max_{m \in [M_n]} \int_{K_p} |H_{p;m,n}(k)| dk &\rightarrow 0, \\ \max_{m \in [M_n]} \sum_{\psi \in \Psi_p} \left(\int_{K_p + \psi} |H_{m,n}(k)|^2 dk \right)^{1/2} &\rightarrow C, \end{aligned}$$

as $n \rightarrow \infty$.

Starting with the first condition, we have

$$\begin{aligned} \int_{K_p} |H_{p;m,n}(k)| dk &= \int_{K_p} \left| \sum_{\psi \in \Psi_p} H_{m,n}(k) w_p(\psi) \right| dk \\ &\leq \sum_{\psi \in \Psi_p} \int_{K_p} |H_{m,n}(k + \psi)| dk \\ &= \int_{\mathbb{R}^d} |H_{m,n}(k)| dk \\ &= \prod (l_n)^{1/2} \int_{\mathbb{R}^d} |H_m(k \circ l_n)| dk \\ &= \prod (l_n)^{-1/2} \int_{\mathbb{R}^d} |H_m(k')| dk' \\ &= \prod (l_n)^{-1/2} \|H_m\|_1 \\ &\leq \prod (l_n)^{-1/2} C_m C \end{aligned}$$

where $C = \int_{\mathbb{R}^d} (1 + \|x\|_2)^{-d-\delta} dx < \infty$. Therefore the result holds because by assumption

$$\max_{m \in [M_n]} C_m \prod (l_n)^{-1/2} \rightarrow 0$$

as $n \rightarrow \infty$. For the second condition, we have

$$\begin{aligned} \max_{m \in [M_n]} \sum_{\psi \in \Psi_p} \left(\int_{K_p + \psi} |H_{m,n}(k)|^2 dk \right)^{1/2} &= \max_{m \in [M_n]} \left(\int_{K_p} |H_{m,n}(k)|^2 dk \right)^{1/2} + \sum_{\psi \in \Psi_p \setminus \{0\}} \left(\int_{K_p + \psi} |H_{m,n}(k)|^2 dk \right)^{1/2} \\ &= 1 + \max_{m \in [M_n]} \sum_{\psi \in \Psi_p \setminus \{0\}} \left(\int_{K_p + \psi} |H_{m,n}(k)|^2 dk \right)^{1/2} \\ &\leq 1 + \max_{m \in [M_n]} C_m \prod (l_n)^{1/2} \ell(K_p)^{1/2} \sum_{\psi \in \Psi_p \setminus \{0\}} \max_{k \in K_p + \psi} (1 + \|k \circ l_n\|)^{-d-\delta} \\ &\leq 1 + \max_{m \in [M_n]} C_m \prod (l_n)^{1/2} \ell(K_p)^{1/2} \min(l_n)^{-d-\delta} \sum_{\psi \in \Psi_p \setminus \{0\}} \max_{k \in K_p + \psi} (\|\psi\|)^{-d-\delta} \\ &\rightarrow 1 \end{aligned}$$

as $n \rightarrow \infty$, by similar arguments as above around pulling out $\min(l_n)$.

Finally to establish Assumption S1. For any fixed m , for any $n \in \mathbb{N}$ such that $m \in [M_n]$,

$$\ell(\mathcal{R}_n) \|h_{m,n}\|_\infty^2 = \ell(\mathcal{R}) \prod (l_n) \frac{1}{\prod (l_n)} \|h_m\|_\infty^2 = \ell(\mathcal{R}) \|h_m\|_\infty^2 < \infty.$$

Finally consider $\ell(\mathcal{R}_n) |D_n|^{-1}$. Note that the region \mathcal{R} is bounded, and therefore contained in a bounding box $\mathcal{R} \subseteq B = \prod_{j=1}^d [a_j, b_j]$. Therefore,

$$\begin{aligned} D_n &\subseteq \{x \in \mathbb{Z}^d : B \circ l_n \cap x + [-1/2, 1/2]^d \neq \emptyset\} \\ &\subseteq \{x \in \mathbb{Z}^d : l_{n;j} a_j - 1 < x_j < l_{n;j} b_j + 1\} \end{aligned}$$

where $l_{n;j}$ denotes the j th element of l_n . Therefore we have that $|D_n| \leq \prod_{j=1}^d (l_{n;j}(b_j - a_j) + 2)$. So

$$\begin{aligned} \frac{\ell(\mathcal{R}_n)}{|D_n|} &\geq \frac{\ell(\mathcal{R})}{\prod_{j=1}^d (l_{n;j}(b_j - a_j) + 2)} \prod (l_n) \\ &= \frac{\ell(\mathcal{R})}{\prod_{j=1}^d ((b_j - a_j) + 2/l_{n;j})} \\ &\geq \frac{\ell(\mathcal{R})}{\prod_{j=1}^d ((b_j - a_j) + 2/l_{1;j})} \\ &> 0, \end{aligned}$$

and so $\liminf_{n \rightarrow \infty} \ell(\mathcal{R}_n) |D_n|^{-1} > 0$, completing the proof. \square

S3.3 Proposition S2

Proof of Proposition S2. In order to verify the assumptions, we will reuse the results from Proposition S1, with appropriate modifications. Note that the assumptions on the decay of the tapers in Proposition S1 are no longer satisfied by these tapers, so parts of the proof requiring these need modification.

Recall that we are interested in the case $\mathcal{R} = \prod_{j=1}^d [a_j, b_j]$, where

$$h_m(x) = \prod_{j=1}^d \frac{1}{\sqrt{b_j - a_j}} g_{\gamma(m)_j} \left(\frac{x_j - a_j}{b_j - a_j} \right).$$

Starting with Assumption 2, clearly the tapers h_m are bounded and continuous. Now if $x \notin \mathcal{R}$, then $(x - a) \otimes (b - a) \notin [0, 1]^d$. Therefore by the assumption that $g_m(y)$ is zero when $y \notin [0, 1]$, we have $h_m(x) = 0$. Next we have that for $m, m' \in \mathbb{N}$

$$\begin{aligned} \langle h_m, h_{m'} \rangle &= \prod_{j=1}^d \frac{1}{b_j - a_j} \int_{\mathbb{R}} g_{\gamma(m)_j} \left(\frac{x_j - a_j}{b_j - a_j} \right) g_{\gamma(m')_j} \left(\frac{x_j - a_j}{b_j - a_j} \right) dx_j \\ &= \prod_{j=1}^d \int_{\mathbb{R}} g_{\gamma(m)_j}(y) g_{\gamma(m')_j}(y) dy \\ &= \prod_{j=1}^d \langle g_{\gamma(m)_j}, g_{\gamma(m')_j} \rangle. \end{aligned}$$

This is equal to 1 if $\gamma(m) = \gamma(m')$, and zero otherwise. Since $\gamma(m) = \gamma(m')$ if and only if $m = m'$, this completes the proof of orthonormality. Next we have

$$\begin{aligned} H_m(k) &= \prod_{j=1}^d \frac{1}{\sqrt{b_j - a_j}} \int_{\mathbb{R}} g_{\gamma(m)_j} \left(\frac{x_j - a_j}{b_j - a_j} \right) e^{-2\pi i k_j x_j} dx_j \\ &= \prod_{j=1}^d \sqrt{b_j - a_j} \int_{\mathbb{R}} g_{\gamma(m)_j}(y) e^{-2\pi i k_j (y(b_j - a_j) + a_j)} dy \\ &= \prod_{j=1}^d \sqrt{b_j - a_j} G_{\gamma(m)_j}(k_j [b_j - a_j]) e^{-2\pi i k_j a_j} \end{aligned}$$

and so

$$\begin{aligned}
\|H_m\|_1 &= \int_{\mathbb{R}^d} |H_m(k)| dk \\
&= \prod_{j=1}^d \sqrt{b_j - a_j} \int_{\mathbb{R}} |G_{\gamma(m)_j}(k_j[b_j - a_j])| dk_j \\
&= \prod_{j=1}^d \frac{1}{\sqrt{b_j - a_j}} \int_{\mathbb{R}} |G_{\gamma(m)_j}(k_j)| dk_j \\
&\leq \left(\int_{\mathbb{R}} (1 + |x|)^{-1-\delta} dx \right)^d \prod_{j=1}^d C_{\gamma(m)_j} \frac{1}{\sqrt{b_j - a_j}} \\
&< \infty.
\end{aligned}$$

Now we need to verify the asymptotic assumptions (assumptions 3 to 5). In particular, for any $p \in [P]$, and any n, m we can always write

$$H_{p;m,n}(k) = \prod_{j=1}^d \tilde{G}_{p;m,j,n}(k_j)$$

where k_j is the j th element of k , and $\tilde{G}_{p;m,j,n}(k_j)$ is Fourier transform of the taper $\tilde{g}_{p;m,j,n}(k_j)$, which is either grid sampled on or not depending on p , from

$$\tilde{g}_{m,j,n}(u) = g_{\gamma(m)_j}(u/l_{n,j})/l_{n,j}^{1/2}$$

where $l_{n,j}$ is the j th element of l_n .

We need the second condition of Assumption 3, in order to prove the first, and so we start with that. For the second condition of Assumption 3, the nuance is that the integral is over the non-separable set $K_p \setminus B_{b_n}$, even though the function is separable. However, noting that $[-b_n/\sqrt{d}, b_n/\sqrt{d}]^d \subset B_{b_n}$, we can bound the desired integral as

$$\begin{aligned}
\int_{K_p \setminus B_{b_n}} |H_{p;m,n}(k)|^2 dk &\leq \int_{K_p \setminus [-b_n/\sqrt{d}, b_n/\sqrt{d}]^d} |H_{p;m,n}(k)|^2 dk \\
&= \prod_{j=1}^d \int_{-b_n/\sqrt{d}}^{b_n/\sqrt{d}} |\tilde{G}_{p;m,j,n}(k_j)|^2 dk_j
\end{aligned}$$

and therefore

$$\max_{m \in [M_n]} \left| \int_{K_p \setminus B_{b_n}} |H_{p;m,n}(k)|^2 dk \right| \leq \prod_{j=1}^d \max_{m \in [M_{n,j}]} \int_{-b_n/\sqrt{d}}^{b_n/\sqrt{d}} |G_{p;m,n}(k_j)|^2 dk_j$$

where we recall $M_{n,j} = \max_{m \in [M_n]} \gamma(m)_j$.⁸ This upper bound holds because $M_{n,j}$ is such that we include all utilised one-dimensional tapers in the j th dimension (plus potentially some extras, meaning we have an upper bound).

Now we can apply the results of Proposition S1, with one-dimensional tapers. In particular, we apply Proposition S1 to the tapers $\{g_m\}_{m \in \mathbb{N}}$ with $M'_n = M_{n,j}$ and $l'_n = l_{n,j}$ and $b'_n = b_n/\sqrt{d}$. Note because this is one dimensional, the condition $\max_{m \in [M'_n]} C_m \prod (l'_n)^{1/2} (\min l'_n)^{-d-\delta} \rightarrow 0$ reduces to $\max_{m \in [M_{n,j}]} C_m l_{n,j}^{-1/2-\delta} \rightarrow 0$ which is already satisfied by assumption as $l_{n,j}^{-1/2-\delta} \leq l_{n,j}^{-1/2}$ and we assume $\max_{m \in [M_{n,j}]} C_m l_{n,j}^{-1/2} \rightarrow 0$ as $n \rightarrow \infty$. Therefore, we have

$$\max_{m \in [M_{n,j}]} \int_{-b_n/\sqrt{d}}^{b_n/\sqrt{d}} |G_{p;m,n}(k_j)|^2 dk_j \rightarrow 0$$

as $n \rightarrow \infty$ for each $j \in [d]$.

⁸Note here we use $G_{p;m,n}$, which is the Fourier transform of the taper made on the n th region with the p th grid, but specifically using the m th taper (not the $\gamma(m)_j$ th taper).

For this first condition of Assumption 3, we need to show that

$$\max_{m \in [M_n]} \left| \int_{B_{b_n}} H_{p;m,n}(k) \overline{H_{q;m,n}} dk - 1 \right| \rightarrow 0.$$

Firstly, to make this separable

$$\begin{aligned} \max_{m \in [M_n]} \left| \int_{B_{b_n}} H_{p;m,n}(k) \overline{H_{q;m,n}} dk - 1 \right| &\leq \max_{m \in [M_n]} \left| \int_{[-b_n/\sqrt{d}, b_n/\sqrt{d}]^d} H_{p;m,n}(k) \overline{H_{q;m,n}} dk - 1 \right| \\ &\quad + \max_{m \in [M_n]} \left| \int_{B_{b_n} \setminus [-b_n/\sqrt{d}, b_n/\sqrt{d}]^d} H_{p;m,n}(k) \overline{H_{q;m,n}} dk \right|. \end{aligned}$$

Considering the second of these terms

$$\begin{aligned} &\max_{m \in [M_n]} \left| \int_{B_{b_n} \setminus [-b_n/\sqrt{d}, b_n/\sqrt{d}]^d} H_{p;m,n}(k) \overline{H_{q;m,n}} dk \right| \\ &\leq \max_{m \in [M_n]} \left(\int_{B_{b_n} \setminus [-b_n/\sqrt{d}, b_n/\sqrt{d}]^d} |H_{p;m,n}(k)|^2 dk \int_{B_{b_n} \setminus [-b_n/\sqrt{d}, b_n/\sqrt{d}]^d} |H_{q;m,n}(k)|^2 dk \right)^{1/2} \\ &\leq \max_{m \in [M_n]} \left(\int_{K_p \setminus [-b_n/\sqrt{d}, b_n/\sqrt{d}]^d} |H_{p;m,n}(k)|^2 dk \int_{K_q \setminus [-b_n/\sqrt{d}, b_n/\sqrt{d}]^d} |H_{q;m,n}(k)|^2 dk \right)^{1/2} \\ &\rightarrow 0 \end{aligned}$$

as we just established.

Finally then, note that for any $a_1, \dots, a_d \in \mathbb{C}$, and writing for convenience $a_0 = 1$

$$\left| \prod_{j=1}^d a_j - 1 \right| \leq \sum_{j=1}^d |a_j - 1| \prod_{j'=0}^{j-1} a_{j'}$$

which follows from induction and the relation

$$|ab - 1| \leq |a - 1||b| + |b - 1|$$

which itself follows from the triangle inequality.

Setting $a_{m,j} = \int_{-b_n/\sqrt{d}}^{b_n/\sqrt{d}} \tilde{G}_{p;m,j,n}(k_j) \overline{\tilde{G}_{q;m,j,n}(k_j)} dk_j$, and $a_{m,0} = 1$ we see that

$$\begin{aligned} \max_{m \in [M_n]} \left| \int_{[-b_n/\sqrt{d}, b_n/\sqrt{d}]^d} H_{p;m,n}(k) \overline{H_{q;m,n}} dk - 1 \right| &\leq \max_{m \in [M_n]} \sum_{j=1}^d |a_{m,j} - 1| \prod_{j'=0}^{j-1} a_{m,j'} \\ &\leq \sum_{j=1}^d \max_{m \in [M_n]} |a_{m,j} - 1| \prod_{j'=0}^{j-1} \max_{m \in [M_n]} |a_{m,j'}| \end{aligned}$$

so provided

$$\max_{m \in [M_n]} |a_{m,j} - 1| \rightarrow 0 \tag{3}$$

as $n \rightarrow \infty$ the result follows, because Eq. (3) implies

$$\max_{m \in [M_n]} |a_{m,j}| \leq \max_{m \in [M_n]} |a_{m,j} - 1| + 1 \rightarrow 1$$

as $n \rightarrow \infty$, meaning we can use algebra of limits. Equation (3) holds because

$$\max_{m \in [M_n]} |a_{m,j} - 1| \leq \max_{m \in [M_{n,j}]} \left| \int_{-b_n/\sqrt{d}}^{b_n/\sqrt{d}} G_{p;m,n}(k_j) \overline{G_{q;m,n}(k_j)} dk_j - 1 \right| \rightarrow 0$$

where we apply Proposition S1 in one dimension to obtain the result as above.

Now for Assumption 4, we have again

$$\begin{aligned} & \max_{m \in [M_n]} \max_{m' \in [M_n] \setminus \{m\}} \left| \int_{B_{b_n}} H_{p;m,n}(k) \overline{H_{q;m',n}} dk \right| \\ & \leq \max_{m \in [M_n]} \max_{m' \in [M_n] \setminus \{m\}} \left| \int_{[-b_n/\sqrt{d}, b_n/\sqrt{d}]^d} H_{p;m,n}(k) \overline{H_{q;m',n}} dk \right| \\ & + \max_{m \in [M_n]} \max_{m' \in [M_n] \setminus \{m\}} \left| \int_{B_{b_n} \setminus [-b_n/\sqrt{d}, b_n/\sqrt{d}]^d} H_{p;m,n}(k) \overline{H_{q;m',n}} dk \right|. \end{aligned}$$

The second term converges to zero as we have already established. The first term is now separable, and so we again apply Proposition S1 in one dimension.

Finally for assumption Assumption 5, we note for the first part we have separability because

$$\begin{aligned} \max_{m \in [M_n]} \int_{K_p} |H_{p;m,n}(k)| dk &= \max_{m \in [M_n]} \prod_{j=1}^d \int_{-b_n/\sqrt{d}}^{b_n/\sqrt{d}} |\tilde{G}_{p;m,j,n}(k_j)| dk_j \\ &\leq \prod_{j=1}^d \max_{m \in [M_{n,j}]} \int_{-b_n/\sqrt{d}}^{b_n/\sqrt{d}} |\tilde{G}_{p;m,j,n}(k_j)| dk_j, \end{aligned}$$

so again we apply Proposition S1 in one dimension. Then for the last condition, writing $\Psi_p = \prod_{j=1}^d \Psi_{p;j}$ and $K_p = \prod_{j=1}^d K_{p;j}$, we have

$$\begin{aligned} \max_{m \in [M_n]} \sum_{\psi \in \Psi_p} \left(\int_{K_p + \psi} |H_{p;m,n}(k)|^2 dk \right)^{1/2} &= \max_{m \in [M_n]} \sum_{\psi_1 \in \Psi_{p;1}} \dots \sum_{\psi_d \in \Psi_{p;d}} \prod_{j=1}^d \left(\int_{K_{p;j} + \psi_j} |\tilde{G}_{p;m,j,n}(k_j)|^2 dk_j \right)^{1/2} \\ &= \max_{m \in [M_n]} \prod_{j=1}^d \sum_{\psi_j \in \Psi_{p;j}} \left(\int_{K_{p;j} + \psi_j} |\tilde{G}_{p;m,j,n}(k_j)|^2 dk_j \right)^{1/2} \\ &\leq \prod_{j=1}^d \sum_{\psi_j \in \Psi_{p;j}} \max_{m \in [M_{n,j}]} \left(\int_{K_{p;j} + \psi_j} |G_{p;m,n}(k_j)|^2 dk_j \right)^{1/2} \end{aligned}$$

which converges to 1 by again applying Proposition S1 in one dimension.

Assumption S1 is then satisfied by an identical argument to that in Proposition S1. \square

S3.4 Proposition S3

Proof of Proposition S3. Recall that

$$g_m(x) = \sqrt{2} \sin(\pi mx) \mathbb{1}_{[0,1]}(x),$$

and we assume that for all $n \in \mathbb{N}$, $b_n l_{n,j} \geq M_{n,j} \sqrt{d}$ and there exists some $\delta > 0$ such that $M_{n,j}^{1+\delta} l_{n,j}^{-1/2} \rightarrow 0$ as $n \rightarrow \infty$.

Firstly, we aim to prove that $\{g_m\}_{m \in \mathbb{N}}$ is an orthonormal family tapers supported on a subset of $[0,1]$ that are bounded and continuous. Secondly that

$$\min_{m \in [M_n]} \int_{-b_n l_{n,j} / \sqrt{d}}^{b_n l_{n,j} / \sqrt{d}} |g_m(x)|^2 dx \rightarrow 1.$$

And finally, that for all $m \in \mathbb{N}$ there exists $\delta > 0$ and $C_m > 0$ such that for all $x \in \mathbb{R}^d$, $|g_m(x)| + |G_m(x)| \leq C_m (1 + |x|)^{-1-\delta}$, where $\max_{m \in [M_n]} C_m l_{n,j}^{-1/2} \rightarrow 0$ as $n \rightarrow \infty$.

The minimum bias tapers are an orthonormal family of functions (Riedel and Sidorenko, 1995). Clearly g_m are continuous and $\|g_m\|_\infty = \sqrt{2} < \infty$ so they are bounded. This establishes the first part.

For the second part, note⁹

$$G_m(k) = \frac{1}{\sqrt{2}} e^{-\pi i(k - \frac{m-1}{2})} \frac{m \operatorname{sinc}(\pi[k - m/2])}{k + m/2}.$$

Note, $|G_m(k)|$ is an even function of frequency. Now, we have for all $m \in [M_n]$

$$\begin{aligned} \int_{M_n}^R |G_m(k)|^2 dk &= \frac{m^2}{2} \int_{M_n}^R \frac{\operatorname{sinc}^2(\pi[k - m/2])}{(k + m/2)^2} dk \\ &\leq \frac{m^2}{2\pi} \int_{M_n}^R \frac{1}{(k + m/2)^2 (k - m/2)^2} dk \\ &= \frac{m^2}{2\pi} \int_{M_n - m/2}^R \frac{1}{(k + m)^2 k^2} dk \\ &= \frac{1}{2\pi m} \left[\frac{m}{M_n + m/2} + \frac{m}{M_n - m/2} - 2 \log \left(\frac{M_n - m/2}{M_n + m/2} \right) \right. \\ &\quad \left. - \left(\frac{M_n}{R + m} + \frac{m}{R} \right) + 2 \log \left(\frac{R + m}{R} \right) \right] \\ &\rightarrow \frac{1}{2\pi m} \left[\frac{m}{M_n + m/2} + \frac{m}{M_n - m/2} - 2 \log \left(\frac{M_n - m/2}{M_n + m/2} \right) \right] \end{aligned}$$

as $R \rightarrow \infty$. So we have for any $m \in [M_n]$

$$\begin{aligned} \int_{M_n}^{\infty} |G_m(k)|^2 dk &\leq \frac{1}{2\pi} \left[\frac{4M_n}{4M_n^2 + m^2} + \frac{2}{m} \log \left(\frac{M_n + m/2}{M_n - m/2} \right) \right] \\ &= \frac{1}{2\pi} \left[\frac{4M_n}{4M_n^2 + m^2} + \frac{2}{m} \log \left(1 + \frac{2}{2M_n/m - 1} \right) \right] \\ &\leq \frac{1}{2\pi} \left[\frac{1}{4M_n} + \frac{2}{2M_n - m} \right] \\ &\leq \frac{1}{2\pi} \left[\frac{1}{4M_n} + \frac{2}{M_n} \right] \\ &= \frac{9}{8\pi M_n}. \end{aligned}$$

So we have

$$\max_{m \in [M_n]} \int_{M_n}^{\infty} |G_m(k)|^2 dk \leq \frac{9}{8\pi M_n}.$$

As a result, we have that

$$\max_{m \in [M_n]} \int_{M_n}^{\infty} |G_m(k)|^2 dk \rightarrow 0$$

as $M_n \rightarrow \infty$. Thus

$$\begin{aligned} \min_{m \in [M_n]} \int_{-M_n}^{M_n} |G_m(k)|^2 dk &= \min_{m \in [M_n]} 1 - 2 \int_{M_n}^{\infty} |G_m(k)|^2 dk \\ &= 1 - 2 \max_{m \in [M_n]} \int_{M_n}^{\infty} |G_m(k)|^2 dk \\ &\rightarrow 1 \end{aligned}$$

⁹Note there is a slight typo in Riedel and Sidorenko (1995) in the statement of the Fourier transform of g_m . We have corrected it here.

as $M_n \rightarrow \infty$. Now by assumption $M_{n,j} \leq b_n l_{n,j} / \sqrt{d}$ and so with some relabelling

$$\begin{aligned} \min_{m \in [M_{n,j}]} \int_{-b_n l_{n,j} / \sqrt{d}}^{b_n l_{n,j} / \sqrt{d}} |G_m(k)|^2 dk &\leq \min_{m \in [M_{n,j}]} \int_{-M_{n,j}}^{M_{n,j}} |G_m(k)|^2 dk \\ &\rightarrow 1 \end{aligned}$$

as $n \rightarrow \infty$.

The final condition is to check the tail decay, more specifically for all $m \in \mathbb{N}$ there exists $\delta > 0$ and $C_m > 0$ such that for all $x \in \mathbb{R}^d$, $|g_m(x)| + |G_m(x)| \leq C_m(1 + |x|)^{-1-\delta}$, where $\max_{m \in [M_{n,j}]} C_m l_{n,j}^{-1/2} \rightarrow 0$ as $n \rightarrow \infty$. Since the tapers decay like x^{-2} in wavenumber, for some $0 < \delta' < 1$ we just need to find appropriate choices for C_m . Recall

$$\begin{aligned} |g_m(x)| &= \sqrt{2} |\sin(\pi mx)| \mathbb{1}_{[0,1]}(x) \\ &\leq \sqrt{2}. \end{aligned}$$

So since our bounding function $C_m(1 + |x|)^{-1-\delta'}$ is decreasing, we have

$$|g_m(x)| \leq C_m(1 + |x|)^{-1-\delta'}$$

if

$$\sqrt{2} \leq C_m 2^{-1-\delta'} \Leftrightarrow C_m \geq 2^{1+\delta'+1/2},$$

as we must cover the corner of the box at least. Now we need to also consider the Fourier transform. Recall that

$$|G_m(k)| = \frac{1}{\sqrt{2}} \left| \frac{m \operatorname{sinc}(\pi[k - m/2])}{k + m/2} \right|.$$

Since this is symmetric, we can consider the case $k \geq 0$. We further decompose this into two cases, $k \in [0, m]$ and $k \in [m, \infty)$. If we can find a lower bound for C_m in each case, then taking C_m to be the maximum of these two bounds and the previous bound will suffice. Firstly, when $k \in [0, m]$, we have

$$\begin{aligned} |G_m(k)| &\leq \frac{m}{\sqrt{2}} \left| \frac{1}{k + m/2} \right| \\ &\leq \sqrt{2}. \end{aligned}$$

In particular, again we have a constant bound we need to cover with $C_m(1 + |k|)^{-1-\delta'}$. So we have for $k \in [0, m]$

$$|G_m(k)| \leq C_m(1 + |k|)^{-1-\delta'}$$

if

$$\sqrt{2} \leq C_m(1 + m)^{-1-\delta'} \Leftrightarrow C_m \geq \sqrt{2}(1 + m)^{1+\delta'}.$$

Since $m \in \mathbb{N}$, we have

$$\sqrt{2}(1 + m)^{1+\delta'} \geq 2^{1+\delta'+1/2}$$

meaning we subsume the previous bound. Now consider the case $k \in [m, \infty)$. In this case, we have

$$\begin{aligned} |G_m(k)| &= \frac{1}{\sqrt{2}} \left| \frac{m \operatorname{sinc}(\pi[k - m/2])}{k + m/2} \right| \\ &\leq \frac{1}{\sqrt{2}} \frac{m}{k^2 - m^2/4}. \end{aligned}$$

So, we now need to find a C_m such that

$$\frac{1}{\sqrt{2}} \frac{m}{k^2 - m^2/4} \leq C_m(1 + |k|)^{-1-\delta'} \Leftrightarrow C_m \geq \frac{m}{\sqrt{2}} \frac{(1 + |k|)^{1+\delta'}}{k^2 - m^2/4}.$$

So we need only find an upper bound on the last fraction. In particular, because $k \geq m$ and $m \geq 1$,

$$\begin{aligned}
\frac{m}{\sqrt{2}} \frac{(1+|k|)^{1+\delta'}}{k^2 - m^2/4} &\leq \frac{m}{\sqrt{2}} \frac{(1+|k|)^2}{k^2 - m^2/4} \\
&= \frac{1}{\sqrt{2}} \left(m + \frac{1+2x+m^2/4}{x^2 - m^2/4} \right) \\
&= \frac{1}{\sqrt{2}} \left(m + \frac{1}{x+m/2} \left(2 + \frac{m^2/4+m+1}{x-m/2} \right) \right) \\
&\leq \frac{1}{\sqrt{2}} \left(m + \frac{1}{3m/2} \left(2 + \frac{m^2/4+m+1}{m/2} \right) \right) \\
&= \frac{1}{\sqrt{2}} \left(m + \frac{4}{3m} + \frac{1}{3} + \frac{4}{3m} + \frac{4}{3m^2} \right) \\
&\leq \frac{1}{\sqrt{2}} \left(m + 4 + \frac{1}{3} \right) \\
&\leq \frac{1}{\sqrt{2}} (5+m).
\end{aligned}$$

Therefore, we set

$$C_m = \max \left\{ \frac{1}{\sqrt{2}} (5+m), \sqrt{2}(1+m)^{1+\delta'} \right\}.$$

Importantly, this means

$$\max_{m \in [M_{n,j}]} C_m l_{n,j}^{-1/2} = \max \left\{ \frac{1}{\sqrt{2}} (5+M_{n,j}) l_{n,j}^{-1/2}, \sqrt{2}(1+M_{n,j})^{1+\delta'} l_{n,j}^{-1/2} \right\} \rightarrow 0$$

as $n \rightarrow \infty$ because the second case dominates asymptotically and by assumption for some $\delta > 0$, $M_{n,j}^{1+\delta} l_{n,j}^{-1/2} \rightarrow 0$ as $n \rightarrow \infty$. Therefore, choosing $0 < \delta < 1$ such that $\delta' < \delta$ we have $\max_{m \in [M_n]} C_m l_{n,j}^{-1/2}$ is dominated by

$$M_{n,j}^{1+\delta'} l_{n,j}^{-1/2} = M_{n,j}^{1+\delta} l_{n,j}^{-1/2} \rightarrow 0$$

as $n \rightarrow \infty$. \square

S4 Lemmas for main theorems

S4.1 Aliasing of tapers

Lemma S5. Consider a function $g : \mathbb{R}^d \rightarrow \mathbb{C}$ and a grid \mathcal{G} on which it will be sampled. Say that g is continuous and bounded, with an L^1 Fourier transform G . Furthermore, assume that there are some constants $C > 0$ and $\delta > 0$ such that for all $x \in \mathbb{R}^d$

$$|g(x)| + |G(x)| \leq C (1 + \|x\|_2)^{-d-\delta}.$$

Then for all $k \in \mathbb{R}^d$

$$\begin{aligned}
G_m^{(\mathcal{G})}(k) &= \prod(\Delta) \sum_{u \in \mathcal{G}} g(u) e^{-2\pi i k \cdot u} \\
&= \sum_{z \in \mathbb{Z}^d} G_m(k + z \oslash \Delta) e^{-2\pi i v \cdot (z \oslash \Delta)}.
\end{aligned}$$

Proof. We will need the Poisson summation formula (Stein and Weiss, 1971). There are a variety of conditions for this, but the most convenient here is the conditions given in Lemma 4 of Gröchenig (1996), namely that for a function $\phi : \mathbb{R}^d \rightarrow \mathbb{C}$ with Fourier transform Φ , both ϕ and Φ are continuous and satisfy

$$\sum_{x \in \mathbb{Z}^d} \max_{u \in [0,1]^d} |\phi(x+u)| < \infty, \quad \sum_{x \in \mathbb{Z}^d} \max_{u \in [0,1]^d} |\Phi(x+u)| < \infty$$

then

$$\sum_{u \in \mathbb{Z}^d} \phi(u) e^{-2\pi i k \cdot u} = \sum_{z \in \mathbb{Z}^d} \Phi(k + z).$$

Therefore, we just need to apply this to certain transformations of g . In particular, given our grid \mathcal{G} , we set

$$\phi(x) = \prod(\Delta) g(x \circ \Delta + v), \quad x \in \mathbb{R}^d.$$

Then the Fourier transform is given by

$$\begin{aligned} \Phi(k) &= \int_{\mathbb{R}^d} \phi(x) e^{-2\pi i k \cdot x} dx \\ &= \prod(\Delta) \int_{\mathbb{R}^d} g(x \circ \Delta + v) e^{-2\pi i k \cdot x} dx \\ &= \frac{\prod(\Delta)}{\prod(\Delta)} \int_{\mathbb{R}^d} g(u) e^{-2\pi i k \cdot (u-v) \circ \Delta} du \\ &= G(k \circ \Delta) e^{2\pi i k \circ \Delta \cdot v}. \end{aligned}$$

Given the conditions on g and G , we see that the condition for the Poisson summation holds for ϕ and Φ . Firstly we have

$$\begin{aligned} |\phi(x)| &= |\prod(\Delta) g(x \circ \Delta + v)| \\ &\leq \prod(\Delta) C (1 + \|x \circ \Delta + v\|_2)^{-d-\delta}, \end{aligned}$$

and

$$\begin{aligned} |\Phi(x)| &= |G(x \circ \Delta)| \\ &\leq C (1 + \|x \circ \Delta\|_2)^{-d-\delta}, \end{aligned}$$

both of which decay sufficiently fast to satisfy the required condition for Poisson summation. Therefore we have for all $k \in \mathbb{R}^d$

$$\begin{aligned} H_m^{(\mathcal{G})}(k) &= \prod(\Delta) \sum_{u \in \mathcal{G}} h(u) e^{-2\pi i k \cdot u} \\ &= \sum_{z \in \mathbb{Z}^d} \phi(z) e^{-2\pi i k \cdot (z \circ \Delta + v)} \\ &= e^{-2\pi i k \cdot v} \sum_{z \in \mathbb{Z}^d} \phi(z) e^{-2\pi i (k \circ \Delta) \cdot z} \\ &= e^{-2\pi i k \cdot v} \sum_{z \in \mathbb{Z}^d} \Phi(k \circ \Delta + z) \\ &= e^{-2\pi i k \cdot v} \sum_{z \in \mathbb{Z}^d} G((k \circ \Delta + z) \circ \Delta) e^{2\pi i ((k+z) \circ \Delta) \cdot v} \\ &= \sum_{z \in \mathbb{Z}^d} G(k + z \circ \Delta) e^{2\pi i (z \circ \Delta) \cdot v} \end{aligned}$$

which yields the result. \square

S4.2 Covariance of spatial processes

The following Lemma enables us to work with weighted integrals and sums of the spatial processes.

Lemma S6. *Given Assumption 1 hold. Without loss of generality, let ξ_1, ξ_2 be either marked point processes or integrated random fields, and ξ_3, ξ_4 be integrated random fields. Let $\phi_1, \phi_2, \phi_3, \phi_4$ be integrable functions with bounded support and integrable Fourier transforms, and let $\mathcal{G}_3, \mathcal{G}_4$ be a regular grids with sampling intervals Δ_3, Δ_4 and offset v_3, v_4 . Then*

$$\begin{aligned} \text{cov} \left(\int_{\mathbb{R}^d} \phi_1(s) \xi_1(ds), \int_{\mathbb{R}^d} \phi_2(s) \xi_2(ds) \right) &= \int_{\mathbb{R}^d} \Phi_1(-k) \overline{\Phi_2(-k)} f_{1,2}(k) dk, \\ \text{cov} \left(\int_{\mathbb{R}^d} \phi_1(s) \xi_1(ds), \int_{\mathbb{R}^d} \phi_3^{(\mathcal{G}_3)}(s) \xi_3(ds) \right) &= \int_{\mathbb{R}^d} \Phi_1(-k) \overline{\Phi_3^{(\mathcal{G}_3)}(-k)} f_{1,3}(k) dk, \\ \text{cov} \left(\int_{\mathbb{R}^d} \phi_3^{(\mathcal{G}_3)}(s) \xi_3(ds), \int_{\mathbb{R}^d} \phi_4^{(\mathcal{G}_4)}(s) \xi_4(ds) \right) &= \int_{\mathbb{R}^d} \Phi_3^{(\mathcal{G}_3)}(-k) \overline{\Phi_4^{(\mathcal{G}_4)}(-k)} f_{1,4}(k) dk. \end{aligned}$$

where Φ_j is the Fourier transform of ϕ_j , i.e. $\Phi_j(k) = \int_{\mathbb{R}^d} \phi_j(u) e^{-2\pi i u \cdot k} du$, $k \in \mathbb{R}^d$.

Therefore if ξ_p, ξ_q are either marked point processes or integrated random fields and ϕ_p, ϕ_q are integrable functions with bounded support and integrable Fourier transforms, or sampled versions of such functions if the corresponding process is an integrated random field, then from the previous cases

$$\text{cov} \left(\int_{\mathbb{R}^d} \phi_p(s) \xi_p(ds), \int_{\mathbb{R}^d} \phi_q(s') \xi_q(ds') \right) = \int_{\mathbb{R}^d} \Phi_p(-k) \overline{\Phi_q(-k)} f_{p,q}(k) dk.$$

Proof. We have that for $j \in \{1, \dots, 4\}$, $\phi_j(u) = \int_{\mathbb{R}^d} \Phi_j(k) e^{2\pi i k \cdot s} dk$. Begin with the first case,

$$\begin{aligned} LHS &= \text{cov} \left(\int_{\mathbb{R}^d} \phi_1(s) \xi_1(ds), \int_{\mathbb{R}^d} \phi_2(s) \xi_2(ds) \right) \\ &= \int_{\mathbb{R}^d} \int_{\mathbb{R}^d} \phi_1(s+u) \overline{\phi_2(s)} \ell(ds) \check{C}_{1,2}(du) \\ &= \int_{\mathbb{R}^d} \int_{\mathbb{R}^d} \int_{\mathbb{R}^d} \Phi_1(-k) e^{-2\pi i k \cdot (s+u)} dk \overline{\phi_2(s)} \ell(ds) \check{C}_{1,2}(du) \\ &= \int_{\mathbb{R}^d} \Phi_1(-k) \int_{\mathbb{R}^d} \overline{\phi_2(s)} e^{-2\pi i k \cdot s} \ell(ds) \int_{\mathbb{R}^d} \check{c}_{1,2}(u) e^{-2\pi i k \cdot u} \check{C}_{1,2}(du) dk \\ &= \int_{\mathbb{R}^d} \Phi_1(-k) \overline{\Phi_2(-k)} f_{1,2}(k) dk \end{aligned}$$

where the interchange of limits is justified because Φ_1, ϕ_2 are assumed to be integrable; and $\check{C}_{1,2}$ is totally finite from Assumption 1.

Now in the second case, $\check{C}_{1,3}$ has a density $\check{c}_{1,3}$ because one of the processes is an integrated random field, so

$$\begin{aligned} \text{cov} \left(\int_{\mathbb{R}^d} \phi_1(u) \xi_1(du), Y_3(s) \right) &= \int_{\mathbb{R}^d} \phi_1(u) \check{c}_{1,3}(u-s) du \\ &= \int_{\mathbb{R}^d} \int_{\mathbb{R}^d} \Phi_1(-k) e^{-2\pi i k \cdot u} dk \check{c}_{1,3}(u-s) du \\ &= \int_{\mathbb{R}^d} \Phi_1(-k) \int_{\mathbb{R}^d} \check{c}_{1,3}(u-s) e^{-2\pi i k \cdot u-s} du e^{-2\pi i k \cdot s} dk \\ &= \int_{\mathbb{R}^d} \Phi_1(-k) f_{1,3}(k) e^{-2\pi i s \cdot k} dk, \end{aligned}$$

where the interchange is justified as both Φ_1 and $\check{c}_{1,3}$ are integrable. Therefore

$$\begin{aligned} LHS &= \text{cov} \left(\int_{\mathbb{R}^d} \phi_1(u) \xi_1(du), \int_{\mathbb{R}^d} \overline{\phi_3^{(\mathcal{G}_3)}(u)} \xi_3(du) \right) \\ &= \prod (\Delta_3) \sum_{s \in \mathcal{G}} \overline{\phi_3^{(\mathcal{G}_3)}(u)} \int_{\mathbb{R}^d} \Phi_1(-k) f_{1,3}(k) e^{-2\pi i s \cdot k} dk \\ &= \int_{\mathbb{R}^d} \Phi_1(-k) f_{1,3}(k) \prod (\Delta_3) \sum_{s \in \mathcal{G}} \overline{\phi_3^{(\mathcal{G}_3)}(u)} e^{-2\pi i s \cdot k} dk \\ &= \int_{\mathbb{R}^d} \Phi_1(-k) \overline{\Phi_3^{(\mathcal{G})}(-k)} f_{p,q}(k) dk, \end{aligned}$$

where the interchange is justified because the summands are only non-zero for a finite subset of \mathcal{G}_3 (as ϕ_3 has bounded support).

For the final case, $\check{c}_{3,4}$ is continuous by assumption, so we have the inverse relation

$$\check{c}_{3,4}(u) = \int_{\mathbb{R}^d} f_{3,4}(k) e^{2\pi i u \cdot k} dk.$$

Therefore,

$$\begin{aligned}
LHS &= \text{cov} \left(\int_{\mathbb{R}^d} \phi_3^{(\mathcal{G}_3)}(u) \xi_3(du), \int_{\mathbb{R}^d} \phi_4^{(\mathcal{G}_4)}(u) \xi_4(du) \right) \\
&= \prod (\Delta_3) \prod (\Delta_4) \sum_{u \in \mathcal{G}_3} \sum_{s \in \mathcal{G}_4} \phi_3(u) \overline{\phi_4(s)} \check{c}_{3,4}(u - s) \\
&= \prod (\Delta_3) \prod (\Delta_4) \sum_{u \in \mathcal{G}_3} \sum_{s \in \mathcal{G}_4} \phi_3(u) \overline{\phi_4(s)} \int_{\mathbb{R}^d} f_{3,4}(k) e^{2\pi i (u-s) \cdot k} dk \\
&= \int_{\mathbb{R}^d} \Phi_3^{(\mathcal{G}_3)}(-k) \overline{\Phi_4^{(\mathcal{G}_4)}(-k)} f_{3,4}(k) dk,
\end{aligned}$$

where the final equality holds because they are both finite sums. The general statement is covered by these three cases. \square

S4.3 Properties of the sampled taper

Lemma S7. *The following properties hold*

$$\begin{aligned}
\forall k \in \mathbb{R}^d, \quad w_p(k) &= \overline{w_p(-k)}, \\
\forall k, k' \in \mathbb{R}^d, \quad w_p(k+k') &= w_p(k)w_p(k'), \\
\psi_1, \psi_2 \in \Psi_p \Rightarrow \psi_1 \pm \psi_2 &\in \Psi_p.
\end{aligned}$$

Proof. This is immediate from the Definition. \square

S4.4 Properties of the aliased spectra

Lemma S8. *Consider two different grids \mathcal{G} and \mathcal{G}' , with sampling intervals $\Delta, \Delta' \in \mathbb{Q}_{>0}^d$. Write Ψ and Ψ' to be the sets of aliasing frequencies for the first and second grid respectively, i.e.*

$$\Psi = \mathbb{Z}^d \oslash \Delta, \quad \Psi' = \mathbb{Z}^d \oslash \Delta'$$

then we can write

$$\Psi \cap \Psi' = a \circ \mathbb{Z}^d \oslash \Delta$$

where $a = (a_1, \dots, a_d)^\top$ is a vector such that $a_j/a'_j = \Delta_j/\Delta'_j$ and a_j, a'_j are coprime.

Proof. Firstly, note that if $\Psi_j = \mathbb{Z}/\Delta_j$, then $\Psi = \prod_{j=1}^d \Psi_j$, and similarly for Ψ' . Therefore, we may prove the result for each dimension separately.

In particular, we wish to show that

$$\Psi_j \cap \Psi'_j = a_j \circ \mathbb{Z}/\Delta_j$$

We begin by showing that if $\psi \in \mathbb{Z}/\Delta_j$, then $\psi \in \Psi_j \cap \Psi'$. In particular, for any $z \in \mathbb{Z}$, set $\psi = a_j z / \Delta_j$ with $a_j \in \mathbb{Z}$ as defined in the Lemma. Then $a_j z \in \mathbb{Z}$, so $\psi \in \Psi_j$. Now, $\psi = a_j z / \Delta_j = a'_j z / \Delta'_j \in \Psi'$.

Now for the other direction, let $\psi \in \Psi_j \cap \Psi'_j$, then there exists $z, z' \in \mathbb{Z}$ such that

$$z/\Delta_j = \psi = z'/\Delta'_j.$$

This is always satisfied by $\psi = 0$. If $\psi \neq 0$, then

$$z/z' = \Delta_j/\Delta'_j = a_j/a'_j$$

can only be satisfied if $\Delta_j/\Delta'_j \in \mathbb{Q}$. Finally therefore $z' = z a'_j / a_j$, and so since the a s are coprime, $z = z'' a_j$. Thus $\phi = z'' a_j / \Delta_j$ for some $z'' \in \mathbb{Z}$, as required. \square

From Lemma S8 we see that the joint aliasing effect also lies on a regular grid.

Lemma S9. *Given Assumption 1, the aliased spectra $\tilde{f}_{p,q}$ is bounded and continuous for all $p, q \in [P]$. Furthermore, we have*

$$\sum_{\psi \in \Psi_p \cap \Psi_q} |f_{p,q}(k + \psi)| < \infty, \quad \forall k \in \mathbb{R}^d.$$

Proof. In the case where one of the two processes is not sampled on a grid, then $\tilde{f}_{p,q} = f_{p,q}$ which is bounded and continuous by the assumption that $\check{C}_{p,q}$ is totally finite (Daley and Vere-Jones, 2003). Let $\check{C}_{p,q}^+$ and $\check{C}_{p,q}^-$ be the positive and negative parts of the Jordan-Hahn decomposition for $\check{C}_{p,q}$ (see Daley and Vere-Jones (2003) for example). Then from the assumption that $\check{C}_{p,q}$ is totally finite, $\check{C}_{p,q}^+(\mathbb{R}^d) + \check{C}_{p,q}^-(\mathbb{R}^d) < \infty$, and by construction $\check{C}_{p,q} = \check{C}_{p,q}^+ - \check{C}_{p,q}^-$. In this case we have for any $k \in \mathbb{R}^d$, since $|e^{-2\pi i k \cdot u}| \leq 1$ for all $u \in \mathbb{R}^d$, we can use the dominated convergence theorem to establish continuity. Furthermore, we also have for all $k \in \mathbb{R}^d$

$$\begin{aligned} |f_{p,q}(k)| &= \left| \int_{\mathbb{R}^d} e^{-2\pi i k \cdot u} \check{C}_{p,q}(du) \right| \\ &= \left| \int_{\mathbb{R}^d} e^{-2\pi i k \cdot u} \check{C}_{p,q}^+(du) - \int_{\mathbb{R}^d} e^{-2\pi i k \cdot u} \check{C}_{p,q}^-(du) \right| \\ &\leq \check{C}_{p,q}^+(\mathbb{R}^d) + \check{C}_{p,q}^-(\mathbb{R}^d) \\ &< \infty. \end{aligned}$$

The final statement then holds trivially, as $\Psi_p \cap \Psi_q = \{0\}$, and so

$$\sum_{\psi \in \Psi_p \cap \Psi_q} |f_{p,q}(k + \psi)| = |f_{p,q}(k)| < \infty.$$

We need only check the cases where there is aliasing, in other words, when we have two random fields. In this case, we have

$$\begin{aligned} \tilde{f}_{p,q}(k) &= \sum_{\psi \in \Psi_p \cap \Psi_q} f_{p,q}(k + \psi) w_p(\psi) \overline{w_q(\psi)} \\ &= \sum_{\psi \in \Psi_p \cap \Psi_q} f_{p,q}(k + \psi) e^{-2\pi i (v_p - v_q) \cdot k}. \end{aligned}$$

Now by Lemma S8, the intersection is a grid. In addition, by Assumption 1

$$|f_{p,q}(k)| < \frac{C}{(1 + \|k\|)^{d+\delta}}$$

for some $C > 0$ and $\delta > 0$. Therefore, we can write

$$\begin{aligned} |\tilde{f}_{p,q}(k)| &\leq \sum_{\psi \in \Psi_p \cap \Psi_q} |f_{p,q}(k + \psi)| \\ &\leq C \sum_{\psi \in \Psi_p \cap \Psi_q} \frac{1}{(1 + \|k + \psi\|)^{d+\delta}} \\ &< \infty. \end{aligned}$$

This established both boundedness and finiteness of the sum. Since $f_{p,q}(k)$ is continuous by the previous argument applied to $\check{C}_{p,q}$, this also establishes continuity of $\tilde{f}_{p,q}(k)$. \square

Lemma S10. *If the spectral density matrix $f(k)$ is positive definite for all $k \in \mathbb{R}^d$, then the aliased spectral density matrix $\tilde{f}(k)$ is positive definite for all $k \in \mathbb{R}^d$.*

Proof. Begin by recalling that \tilde{f} is the matrix with elements

$$\tilde{f}_{p,q}(k) = \sum_{\psi \in \Psi_p \cap \Psi_q} f_{p,q}(k + \psi) w_p(\psi) \overline{w_q(\psi)}, \quad k \in \mathbb{R}^d.$$

So we could rewrite the matrix as

$$\tilde{f}(k) = \sum_{\psi \in \Psi} \{w(\psi)w(\psi)^H\} \circ f(k + \psi)$$

where $\Psi = \bigcup_{p=1}^P \Psi_p$ and

$$w(\psi) = [w_p(\psi) \mathbb{1}_{\Psi_p}(\psi)]_{p \in [P]}.$$

We need to show that for any $x \in \mathbb{C}^P \setminus \{0\}$,

$$x^H \tilde{f}(k) x > 0.$$

Now by linearity

$$x^H \tilde{f}(k) x = \sum_{\psi \in \Psi} x^H \{w(\psi)w(\psi)^H\} \circ f(k + \psi) x.$$

Firstly $0 \in \Psi$, and in this case $w(0) = 1$. Therefore for one term, the summand is positive. All that remains is to show that all of the remaining summands are non-negative.

Take some $\psi \in \Psi \setminus \{0\}$. Let $S = \{w(\psi)w(\psi)^H\} \circ f(k + \psi)$. By the Schur product theorem (Schur, 1911), the Hadamard product of two positive semi-definite matrices is positive semi-definite. Now $w(\psi)w(\psi)^H$ is positive semi-definite because for any $x \in \mathbb{C}^P$, we have $x^H (w(\psi)w(\psi)^H) x = |w(\psi)^H x|^2 \geq 0$. Therefore S is positive semi-definite, and so the summands $x^H S x$ are non-negative. As a result, $\tilde{f}(k)$ is positive definite as

$$x^H \tilde{f}(k) x \geq x^H f(k) x > 0.$$

and by assumption $f(k)$ is positive definite for all $k \in \mathbb{R}^d$. \square

S5 The non-oracle case

Typically when developing the theory of spectral analysis, it is assumed that the process is either mean zero, or that the mean is easily estimated and removed, and so we may act as though the mean is known. We also make this assumption in the theory developed prior to this point, however, it is important to justify this decision. In our case, the mean is often not zero (a simple point process for instance), and so this should be explicitly addressed. Doing no mean removal results in substantial bias, as was noted in the original paper introducing spectra of point processes (Bartlett, 1963). Doing mean removal greatly reduces this bias, as shown by Rajala et al. (2023). However, for finite samples this bias is not completely removed by subtracting the sample mean, though it is greatly reduced in most scenarios. The most extreme case of this is when no taper is applied, and the sample mean used. In this case the tapered Fourier transform is always zero at zero wavenumber. As we will see from the results in this section, in general, the error introduced by not knowing the true intensity/mean can only be large for wavenumbers where $H(k)$ is large (in particular, when doing multitaper estimation, for wavenumbers whose norm is less than the bandwidth).

Say that the intensity (mean) of the process is estimated with a weighted mean, i.e.

$$\hat{\lambda}_p = \int_{\mathbb{R}^d} g_p(u) \xi_p(u)$$

for some function g_p supported on \mathcal{R} satisfying the assumptions of Lemma S6. Studying the mean of the periodogram in this case, we see that the mean is the same as the oracle case, plus some extra error terms.

Proposition S5 (Expectation of the periodogram with unknown mean). *Say that the processes in question satisfy the assumptions of Proposition 1 (the expectation of the periodogram), but that the mean is estimated by a weighted mean as just described. Then*

$$\begin{aligned} \mathbb{E} [I_{p,q;m}(k)] &= \int_{\mathbb{R}^d} H_{p;m}(k - k') \overline{H_{q;m}(k - k')} f_{p,q}(k') dk' \\ &\quad + H_{p;m}(k) \overline{H_{q;m}(k)} (G_p(0) - 1)(G_q(0) - 1) \lambda_p \lambda_q \\ &\quad + H_{p;m}(k) \overline{H_{q;m}(k)} \int_{\mathbb{R}^d} G_p(-k') \overline{G_q(-k')} f_{p,q}(k') dk' \\ &\quad - \overline{H_{q;m}(k)} \int_{\mathbb{R}^d} H_{p;m}(k - k') \overline{G_q(-k')} f_{p,q}(k') dk' \\ &\quad - \overline{H_{q;m}(k)} \int_{\mathbb{R}^d} G_p(-k') \overline{H_{q;m}(k - k')} f_{p,q}(k') dk' \end{aligned}$$

for $k \in \mathbb{R}^d$.

Proof. Write $\xi_p^0(du) = \xi_p(du) - \lambda_p du$. Begin by noting that

$$\hat{\lambda}_p = \int_{\mathbb{R}^d} g_p(u) \xi_p^0(u) + \lambda_p G_p(0).$$

Therefore we can write

$$J_{p;m}(k) = \int_{\mathbb{R}^d} H_{p;m}(u) e^{-2\pi i u \cdot k} \xi_{p0}(du) + H_{p;m}(k) \lambda_p \{1 - G_p(0)\} - H_{p;m}(k) \int_{\mathbb{R}^d} g_p(u) \xi_p^0(du).$$

Terms involving products of the middle term with one of the other in the periodogram will have zero expectation, and so

$$\begin{aligned} \mathbb{E}[I_{p,q;m}(k)] &= \mathbb{E} \left[\int_{\mathbb{R}^d} H_{p;m}(u) e^{-2\pi i u \cdot k} \xi_{0,p}(du) \overline{\int_{\mathbb{R}^d} H_{q;m}(u) e^{-2\pi i u \cdot k} \xi_q^0(du)} \right] \\ &\quad + H_{p;m}(k) \lambda_p (1 - G_p(0)) \overline{H_{q;m}(k) \lambda_q (1 - G_q(0))} \\ &\quad + H_{p;m}(k) \overline{H_{q;m}(k)} \mathbb{E} \left[\int_{\mathbb{R}^d} g_p(u) \xi_p^0(du) \overline{\int_{\mathbb{R}^d} g_q(u) \xi_q^0(du)} \right] \\ &\quad - \overline{H_{q;m}(k)} \mathbb{E} \left[\int_{\mathbb{R}^d} H_{p;m}(u) e^{-2\pi i u \cdot k} \xi_p^0(du) \overline{\int_{\mathbb{R}^d} g_q(u) \xi_q^0(du)} \right] \\ &\quad - H_{p;m}(k) \mathbb{E} \left[\int_{\mathbb{R}^d} g_p(u) \xi_p^0(du) \overline{\int_{\mathbb{R}^d} H_{q;m}(u) e^{-2\pi i u \cdot k} \xi_q^0(du)} \right] \end{aligned}$$

with the remaining terms having zero expectation. All that remains is applying Lemma S6. \square

This is the usual bias, plus terms that scale like the size of the Fourier transform of the taper. Outside of the bandwidth of the taper, this is negligible. If an unbiased estimator of λ is used (for either process), then the second term is zero. The remaining terms are nowhere near the magnitude of bias observed if no mean correction is performed; however, for small samples they may still generate noticeable bias. One approach to address this may be to down weight certain tapers in the multitaper estimator, to remove tapers whose Fourier transform is large at the wavenumber being investigated. Even if this wavenumber is in the bandwidth of the tapers, some of the Fourier transforms will still have little magnitude at this wavenumber (just not all of them). In any case, this issue impacts few wavenumbers, often by negligible amounts in practice.

S6 Linear interpolation

S6.1 Definitions and basic properties

We use multilinear interpolation to interpolate functions defined on a grid $\mathcal{G} \subset \mathbb{R}^d$ to a function defined on \mathbb{R}^d . This form of interpolation is the common form of multivariate “linear” interpolation, generalising bilinear and trilinear interpolation to d dimensions. The interpolation works by applying linear interpolation in each dimension recursively, and so is defined by the following definition.

Definition S1. Let \mathcal{I} be the multilinear interpolation operator, that maps a function of a grid $f : \mathcal{G} \rightarrow \mathbb{R}$ to a function of \mathbb{R}^d so that $\mathcal{I}[f] : \mathbb{R}^d \rightarrow \mathbb{R}$ with

$$\mathcal{I}[f](u) = \frac{1}{\prod(\Delta)} \sum_{z \in \mathcal{G}} \mathbb{1}_{[0,\Delta)}(u - z) \sum_{v \in \{0,1\}^d} f(z + v \circ \Delta) \prod_{j=1}^d (u_j - z_j)^{v_j} (\Delta_j - u_j + z_j)^{1-v_j}$$

for any $u \in \mathbb{R}^d$, where $[0, \Delta) = \prod_{j=1}^d [0, \Delta_j)$ and z_j, v_j denote the j th elements of z and v respectively.

Definition S2. Let the interpolation weight for a given z and v be the function $\mathcal{I}_{v,z} : \mathbb{R}^d \rightarrow \mathbb{R}$ defined by

$$\mathcal{I}_{v,z}(u) = \prod_{j=1}^d (u_j - z_j)^{v_j} (\Delta_j - (u_j - z_j))^{1-v_j} \mathbb{1}_{[0,\Delta_j)}(u_j - z_j).$$

Consider two functions f, g with domain \mathbb{R}^d and codomain \mathbb{R} . Let

$$\langle f, g \rangle_2 = \int_{\mathbb{R}^d} f(u) g(u) du$$

denote the L^2 inner product.

Proposition S6. *The inner product between a multilinear interpolation of $g : \mathcal{G} \rightarrow \mathbb{R}^d$ and some other function $h : \mathbb{R}^d \rightarrow \mathbb{R}$ is given by*

$$\langle \mathcal{I}[g], h \rangle_2 = \frac{1}{\prod(\Delta)} \sum_{z \in \mathcal{G}} \sum_{v \in \{0,1\}^d} g(z + v \circ \Delta) \langle h, \mathcal{I}_{v,z} \rangle_2.$$

Proof. Follows from rearranging the definition and linearity of inner products. \square

Now, many quantities of interest can be derived by considering $\langle h, \mathcal{I}_{v,z} \rangle_2$ for appropriate choices of h . In particular, in the next two sections, we consider h to be an interpolated function, and then the Fourier basis, so that we can explore the effect on orthogonality and wavenumber domain concentration.

S6.2 Linear interpolation with linear interpolation

Lemma S11. *If $v_j, v'_j \in \{0, 1\}$ then*

$$\int_0^{\Delta_j} x_j^{v_j+v'_j} (\Delta_j - x_j)^{2-v_j-v'_j} dx_j = \frac{\Delta_j^3}{6} [1 + \delta_{v_j, v'_j}].$$

Proof. We have the four cases $v_j, v'_j \in \{0, 1\}$. When $v_j = v'_j = 0$

$$\begin{aligned} \int_0^{\Delta_j} x_j^{v_j+v'_j} (\Delta_j - x_j)^{2-v_j-v'_j} dx_j &= \int_0^{\Delta_j} (\Delta_j - x_j)^2 dx_j \\ &= \int_0^{\Delta_j} y_j^2 dy_j \\ &= \frac{1}{3} \Delta_j^3. \end{aligned}$$

which is equivalent to the case $v_j = 1, v'_j = 1$. Finally, by symmetry we need only consider $v_j = 0, v'_j = 1$

$$\begin{aligned} \int_0^{\Delta_j} x_j (\Delta_j - x_j) dx_j &= \Delta_j \int_0^{\Delta_j} x_j dx_j - \int_0^{\Delta_j} x_j^2 dx_j \\ &= \frac{1}{2} \Delta_j^3 - \frac{1}{3} \Delta_j^3 \\ &= \frac{1}{6} \Delta_j^3. \end{aligned}$$

Therefore, we have

$$\int_0^{\Delta_j} x_j^{v_j+v'_j} (\Delta_j - x_j)^{2-v_j-v'_j} dx_j = \begin{cases} \frac{1}{3} \Delta_j^3 & \text{if } v_j \neq v'_j \\ \frac{1}{6} \Delta_j^3 & \text{if } v_j = v'_j. \end{cases}$$

\square

Lemma S12. *For any $z, z' \in \mathcal{G}$ and $v, v' \in \{0, 1\}^d$ we have*

$$\begin{aligned} z \neq z' &\implies \forall u \in \mathbb{R}^d, \mathcal{I}_{v,z}(u) \mathcal{I}_{v',z'}(u) = 0, \\ z = z' &\implies \forall u \in \mathbb{R}^d \text{ s.t. } u - z \notin [0, \Delta), \mathcal{I}_{v,z}(u) \mathcal{I}_{v',z'}(u) = 0. \end{aligned}$$

Proof. This follows from the presence of the indicator functions in the definition of $\mathcal{I}_{v,z}$. In particular, because we have something multiplied by

$$\mathbb{1}_{[0, \Delta)}(u - z) \mathbb{1}_{[0, \Delta)}(u - z')$$

which is zero in the cases indicated in this Lemma. \square

Lemma S13. *We have that for any $z, z' \in \mathcal{G}$ and $v, v' \in \{0, 1\}^d$*

$$\langle \mathcal{I}_{v',z'}, \mathcal{I}_{v,z} \rangle_2 = \delta_{z,z'} \prod_{j=1}^d \frac{\Delta_j^3}{6} [1 + \delta_{v_j, v'_j}].$$

Proof. From we see

$$\begin{aligned}
\langle \mathcal{I}_{v',z'}, \mathcal{I}_{v,z} \rangle_2 &= \int_{\mathbb{R}^d} \mathcal{I}_{v',z'}(u) \mathcal{I}_{v,z}(u) du \\
&= \delta_{z,z'} \prod_{j=1}^d \int_0^{\Delta_j} x_j^{v_j+v'_j} (\Delta_j - x_j)^{2-v_j-v'_j} dx_j \quad (\text{by Lemma S12}) \\
&= \delta_{z,z'} \prod_{j=1}^d \frac{\Delta_j^3}{6} \left[1 + \delta_{v_j, v'_j} \right]. \quad (\text{by Lemma S11})
\end{aligned}$$

□

Proposition S7. *We have that*

$$\langle \mathcal{I}[g], \mathcal{I}[h] \rangle_2 = \prod(\Delta) \sum_{z \in \mathcal{G}} \sum_{v, v' \in \{0,1\}^d} g(z + v \circ \Delta) h(z + v' \circ \Delta) \prod_{j=1}^d \frac{1}{6} \left[1 + \delta_{v_j, v'_j} \right].$$

Proof. Using Lemma S13 and Proposition S6

$$\begin{aligned}
\langle \mathcal{I}[g], \mathcal{I}[h] \rangle_2 &= \frac{1}{\prod(\Delta)} \sum_{z \in \mathcal{G}} \sum_{v \in \{0,1\}^d} g(z + v \circ \Delta) \langle \mathcal{I}[h], \mathcal{I}_{v,z} \rangle_2 \\
&= \frac{1}{\prod(\Delta)^2} \sum_{z \in \mathcal{G}} \sum_{v, v' \in \{0,1\}^d} g(z + v \circ \Delta) h(z + v' \circ \Delta) \prod_{j=1}^d \frac{\Delta_j^3}{6} \left[1 + \delta_{v_j, v'_j} \right]
\end{aligned}$$

□

Now we can rescale the interpolated tapers to have an L^2 norm of one, and use this to check the cross inner products are still close to zero. If they are not, we can fix this by increasing the grid resolution. The best way to see why is by considering the Fourier transform of the interpolated sequence.

S6.3 Linear interpolation with Fourier basis

The following proposition tells us how to calculate the Fourier transform of a multilinearly interpolated taper, which we will require for mean removal of the point patterns, and for examining the quality of our tapers.

Proposition S8. *Let $\phi_k(u) = e^{-2\pi i u \cdot k}$ and $g : \mathcal{G} \rightarrow \mathbb{R}$ then*

$$\langle \mathcal{I}[g], \phi_k \rangle_2 = G^{(\mathcal{G})}(k) \prod_{j=1}^d \text{sinc}^2(\pi \Delta_j k_j)$$

where k_j is the j th element of k .

Proof. Firstly, notice that

$$\begin{aligned}
\langle \phi_k, \mathcal{I}_{v,z} \rangle_2 e^{2\pi i (z + v \circ \Delta) \cdot k} &= e^{2\pi i (z + v \circ \Delta) \cdot k} \prod_{j=1}^d \int_0^{\Delta_j} x_j^{v_j} (\Delta_j - x_j)^{1-v_j} e^{-2\pi i k_j (x_j + z_j)} dx_j \\
&= \prod_{j=1}^d \int_0^{\Delta_j} x_j^{v_j} (\Delta_j - x_j)^{1-v_j} e^{-2\pi i k_j (x_j - v_j \Delta_j)} dx_j,
\end{aligned}$$

is invariant to z . Therefore

$$\begin{aligned}
\langle \mathcal{I}[g], \phi_k \rangle_2 &= \frac{1}{\prod(\Delta)} \sum_{z \in \mathcal{G}} \sum_{v \in \{0,1\}^d} g(z + v \circ \Delta) \langle \phi_k, \mathcal{I}_{v,z} \rangle_2 \\
&= \frac{1}{\Delta} \sum_{v \in \{0,1\}^d} \left(\sum_{z \in \mathcal{G}} g(z + v \circ \Delta) e^{-2\pi i (z + v \circ \Delta) \cdot k} \right) \langle \phi_k, \mathcal{I}_{v,z} \rangle_2 e^{2\pi i (z + v \circ \Delta) \cdot k} \\
&= \frac{1}{\Delta^2} G^{(\mathcal{G})}(k) \sum_{v \in \{0,1\}^d} \langle \phi_k, \mathcal{I}_{v,z} \rangle_2 e^{2\pi i (z + v \circ \Delta) \cdot k}.
\end{aligned}$$

Now we have

$$\begin{aligned}
\sum_{v \in \{0,1\}^d} \langle \phi_k, \mathcal{I}_{v,z} \rangle_2 e^{2\pi i (z + v \circ \Delta) \cdot k} &= \sum_{v \in \{0,1\}^d} \prod_{j=1}^d \int_0^{\Delta_j} x^{v_j} (\Delta_j - x_j)^{1-v_j} e^{-2\pi i k_j (x_j - v_j \Delta_j)} dx_j \\
&= \prod_{j=1}^d \sum_{v=0}^1 \int_0^{\Delta_j} x^{v_j} (\Delta_j - x_j)^{1-v_j} e^{-2\pi i k_j (x_j - v_j \Delta_j)} dx_j \\
&= \prod_{j=1}^d \int_0^{\Delta_j} (\Delta_j - x_j) e^{-2\pi i k_j x_j} + x_j e^{-2\pi i k_j (x_j - \Delta_j)} dx_j \\
&= \prod_{j=1}^d \text{sinc}^2(\pi \Delta_j k_j) \Delta_j^2,
\end{aligned}$$

because if $k_j \neq 0$

$$\begin{aligned}
&\int_0^{\Delta_j} (\Delta_j - x_j) e^{-2\pi i k_j x_j} + x_j e^{-2\pi i k_j (x_j + \Delta_j)} dx_j \\
&= \int_0^{\Delta_j} (\Delta_j - x_j) e^{-2\pi i k_j x_j} dx_j + \int_0^{\Delta_j} (\Delta_j - x_j) e^{2\pi i k_j x_j} dx_j \\
&= 2 \operatorname{Re} \left\{ \int_0^{\Delta_j} (\Delta_j - x_j) e^{2\pi i k_j x_j} dx_j \right\} \\
&= 2 \operatorname{Re} \left\{ \frac{2\pi i \Delta_j k_j - e^{2\pi i \Delta_j k_j} + 1}{2\pi^2 k_j^2} \right\} \\
&= \frac{\sin^2(\pi \Delta_j k_j)}{\pi^2 k_j^2},
\end{aligned}$$

otherwise if $k_j = 0$,

$$\int_0^{\Delta_j} (\Delta_j - x_j) e^{-2\pi i k_j x_j} + x_j e^{-2\pi i k_j (x_j + \Delta_j)} dx_j = \int_0^{\Delta_j} \Delta_j dx_j = \Delta_j^2.$$

The stated result follows. \square

In practice, we scale g such that $\|\mathcal{I}[g]\|_2 = 1$.

S7 Bias in marked point processes

S7.1 The expectation of the biased periodogram

Periodograms have been proposed for marked point processes, both in the univariate (Renshaw, 2002) and multivariate (Eckardt and Mateu, 2019a) cases, however, these estimators are unfortunately systematically biased. Without loss of generality, consider the univariate case, where X is the point locations and W_x is the mark at that location. We call this process the marked process, and the point process without the marks the ground process (Daley and Vere-Jones, 2003).

Breaking slightly from our previous notation, write λ_g for the intensity of the ground process, λ_m for the intensity of the marked process, and μ for the mean of the marks. (Renshaw, 2002) write an alternate discrete Fourier transform for the marked case as

$$\mathfrak{F}(k) = \frac{1}{\sqrt{\ell(\mathcal{R})}} \sum_{x \in X \cap \mathcal{R}} (W_x - \mu) e^{-2\pi i x k}.$$

Renshaw (2002) only define this for rectangular regions but for convenience we study the general case here. The proposed periodogram is then $|\mathfrak{F}(k)|^2$.

Denote the discrete Fourier transform of the ground process (using only the points) and marked process by

$$\begin{aligned} J_g(k) &= \frac{1}{\sqrt{\ell(\mathcal{R})}} \sum_{x \in X \cap \mathcal{R}} e^{-2\pi i x k} - \lambda_g \int_{\mathcal{R}} e^{-2\pi i x k} dx, \\ J_m(k) &= \frac{1}{\sqrt{\ell(\mathcal{R})}} \sum_{x \in X \cap \mathcal{R}} W_x e^{-2\pi i x k} - \lambda_m \int_{\mathcal{R}} e^{-2\pi i x k} dx, \end{aligned}$$

respectively. The mean correction we propose is different to that of Renshaw (2002) in that we subtract λ_m not μ , and we do this everywhere, not just at the atoms of the mark sum measure. In any case, $\lambda_m = \mu \lambda_g$ (Illian et al., 2008, equation 5.1.19), and so

$$\begin{aligned} \mathfrak{F}(k) &= \frac{1}{\sqrt{\ell(\mathcal{R})}} \sum_{x \in X \cap \mathcal{R}} (W_x - \mu) e^{-2\pi i x k} \\ &= \frac{1}{\sqrt{\ell(\mathcal{R})}} \sum_{x \in X \cap \mathcal{R}} W_x e^{-2\pi i x k} - \lambda_m H(k) - \mu \left[\frac{1}{\sqrt{\ell(\mathcal{R})}} \sum_{x \in X \cap \mathcal{R}} e^{-2\pi i x k} - \lambda_g H(k) \right] \\ &= J_m(k) - \mu J_g(k), \end{aligned}$$

where for convenience we define

$$H(k) = \int_{\mathcal{R}} \frac{1}{\sqrt{\ell(\mathcal{R})}} e^{-2\pi i x k} dk.$$

Therefore

$$\begin{aligned} |\mathfrak{F}(k)|^2 &= I_{mm}(k) + \mu^2 I_{gg}(k) - 2\mu \operatorname{Re}\{I_{mg}(k)\} \\ &\rightarrow f_{mm}(k) + \mu^2 f_{gg}(k) - 2\mu \operatorname{Re}\{f_{mg}(k)\}, \end{aligned}$$

as the region grows. This does not equal $f_{mm}(k)$, our desired estimand.

S7.2 The definition of spectra for marked processes

In fact, the definition of the spectral density function given in Renshaw (2002) and Eckardt and Mateu (2019a) is not the same as the definition we use in this paper. However, it is not equal to $f_{mm}(k) + \mu^2 f_{gg}(k) - 2\mu \operatorname{Re}\{f_{mg}(k)\}$. In particular, Renshaw (2002) define the spectral density function as the Fourier transform of the reduced factorial moment measure of the mark sum measure (though it is written differently in the paper, it is equivalent). In contrast, we Fourier transform the reduced cumulant measure, matching the definition for point processes, random fields and general random measures (Daley and Vere-Jones, 2003). In particular, define

- λ_g : the intensity of the ground process
- μ : the mean of the mark (conditional on a point existing)
- $\lambda_m = \lambda_g \mu$: the mark intensity
- μ_2 : the second moment of the mark (conditional on a point)
- ρ_{gg}, ρ_{mm} : the second-order product density of the ground process and mark sum measure respectively (factorial moment density)
- \check{C}_m : the covariance measure of the mark sum measure
- $k_{mm}(x) = \rho_{mm}(x)/\rho_{gg}(x)\mu^2$: the mark correlation, note this definition is from Eckardt and Mateu (2019b) and Illian et al. (2008), who divide by μ^2 . Eckardt and Mateu (2019a) only divide by μ , though this doesn't impact the point of what follows.

Define the mean product of marks as

$$\begin{aligned} U(x) &= \rho_{gg}(x)k_{mm}(x) \\ &= \rho_{mm}(x)\frac{1}{\mu^2} \end{aligned}$$

Then Renshaw (2002) define the spectra to be

$$S(k) = \int_{\mathbb{R}^d} U(x)e^{2\pi i k \cdot x} dx.$$

In contrast, the spectral density function of the mark sum measure is given by

$$f_m(k) = \int_{\mathbb{R}^d} e^{2\pi i k \cdot x} \check{C}_m(dx).$$

Now we have for $B \in \mathcal{B}(\mathbb{R}^d)$

$$\check{C}_m(B) = \int_B \rho_{mm}(x) - \lambda_m^2 dx + a_m \delta(B)$$

where the value of the atom a_m can be found from Proposition 8.1.IV of Daley and Vere-Jones (2003). One can therefore see that the difference between the two definitions is that Renshaw (2002) use the reduced factorial moment measure (up to some scaling), which is not the same as the reduced covariance measure. Typically it is not totally finite, and omitting the atom at zero means the spectral density function can be negative, which removes the interpretation as a variance of a wavenumber domain process.

More specifically, we have

$$\begin{aligned} f_m(k) &= \int_{\mathbb{R}^d} e^{2\pi i k \cdot x} \check{C}_m(dx) \\ &= \int_{\mathbb{R}^d} e^{2\pi i k \cdot x} (\rho_{mm}(x) - \lambda_m^2) dx + a_m \\ &= \int_{\mathbb{R}^d} e^{2\pi i k \cdot x} \mu^2 U(x) dx - \lambda_m^2 \delta(k) + a_m \end{aligned}$$

and therefore

$$S(k) = \frac{1}{\mu^2} (f_m(k) + \lambda_m^2 \delta(k) - a_m).$$

Notice that one of the two spectra will not be a function in the usual sense. Consider the case when the ground point process has a spectral density f_g , and the marks are independent of the ground process and are IID, then the ground and mark spectra are related by

$$f_m(k) = \mu_1^2 f_g(k) + \lambda_g(\mu_2 - \mu^2)$$

(Daley and Vere-Jones, 2003). So in this case, our definition of spectral density function is a density, whilst the Renshaw spectra is not. Furthermore, if we set the marks to have a point mass at 1, we obtain $\mu_2 = \mu = 1$, and so

$$f_m(k) = f_g(k)$$

as one would expect. Again this is not true of Renshaw spectra.

Whilst this is a choice, it is sensible to choose the cumulant measure to Fourier transform, a choice which is made in the point process case, even in Renshaw (2002). Consider a basic null model where we have multiple independent Poisson processes with IID marks. Under the definition of Renshaw (2002) and Eckardt and Mateu (2019a), the spectral density matrix function would be zero (except for a point mass at zero). This means that the spectral density matrix is not invertible at most frequencies, and thus partial coherence would not be well define even in the most simple case, in contrast to our definition. Furthermore, our definition is an exact generalisation of the unmarked case, as setting the marks to a point mass at one recovers the unmarked case, both in the spectral density function and our proposed estimators.

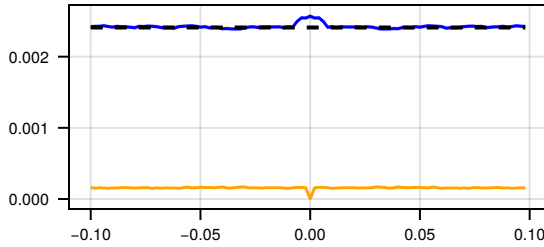


Figure 6: The true spectral density function of the IID marked Poisson process (dashed), the average of the multitaper estimates (blue) and the average of the alternate periodogram (orange). Taken at the slice $k_2 = 0$.

S7.3 Small simulation study

To verify the bias in the alternate periodogram, we performed a small simulation study. We simulate Poisson processes with intensity $\lambda = 0.001$, with marks drawn from an IID Normal(1.5,0.4) distribution. We generate 1000 replications and at each estimate the spectra with multitapering and the alternate periodogram. We show a comparison of the true spectra to two estimates in Fig. 6. To ease comparison, we take a slice at $k_2 = 0$. We can see that indeed the existing methodology is significantly biased, but the multitaper estimator is not.

S8 Irregular sampling

Recall that we assume we have a mean-zero random field Y and point process X , the locations where we will sample Y . Then we can regard this sampled process as a marked point process, say ξ , with marks $Y(x)$ for $x \in X$. Then, if the marks are independent of the locations, from Daley and Vere-Jones (2003), page 338, we have

$$f_{\xi\xi}(k) = \int_{\mathbb{R}^d} f_{YY}(k - k') f_{XX}(k') dk' + \lambda_X f_{YY}(k), \quad k \in \mathbb{R}^d$$

where $f_{\xi\xi}$ is the spectral density function of the marked process, f_{YY} is the spectral density function of the random field, f_{XX} is the spectral density function of the point process, and λ_X is the intensity of the point process. If the point process used for sampling is Poisson, then

$$f_{\xi\xi}(k) = \lambda_X \text{var}(Y(0)) + \lambda_X^2 f_{YY}(k), \quad k \in \mathbb{R}^d.$$

In fact, this corresponds to the approach proposed in Matsuda and Yajima (2009). To see this, note that Matsuda and Yajima (2009) also assume that the random field is mean zero. They assume that you sample the process with some random points with pdf given by g supported on some subset of $[0, 1]^d$ say $\tilde{\mathcal{R}}$. They then assume that we observe the process at random locations $x_i = A \circ u_i$ where u_i is a realisation of a random variable with pdf g , and the non-negative vector A defines the region scaling. They then scale the periodogram (which corresponds to our periodogram in the marked case with mean-zero marks) by a factor. In particular, let $G = \|g\|_2^2$ and $S = \prod_{j=1}^d [0, A_j]$, the box the region is rescaled too. Then write the rescaled region as \mathcal{R} . For simplicity we consider the untapered Fourier transform here. The untapered Fourier transform from Matsuda and Yajima (2009) is

$$\begin{aligned} \tilde{J}(k) &= G^{-1/2} \ell(S)^{1/2} n^{-1} \sum_{j=1}^n Y(x_j) e^{-2\pi i k \cdot x_j} \\ &= G^{-1/2} \ell(S)^{1/2} n^{-1} \ell(\mathcal{R})^{1/2} \frac{1}{\ell(\mathcal{R})^{1/2}} \sum_{j=1}^n Y(x_j) e^{-2\pi i k \cdot x_j} \\ &= G^{-1/2} \ell(S)^{1/2} n^{-1} \ell(\mathcal{R})^{1/2} J(k) \\ &= C J(k). \end{aligned}$$

where $J(k)$ is taken to be our marked tapered Fourier transform with taper $\ell(\mathcal{R})^{-1/2} \mathbb{1}_{\mathcal{R}}$ (if we were to view the collection of points as a point process), and $C = G^{-1/2} \ell(S)^{1/2} n^{-1} \ell(\mathcal{R})^{1/2}$. Of course, this will not satisfy all of the assumptions of our method (we would always use tapers) but we do not need the results that require the L^1 assumption here and this simplifies the point (it is about scaling).

In particular, assume that the sampling is uniform over the region, then

$$G = \int_{\tilde{\mathcal{R}}} \frac{1}{\ell(\tilde{\mathcal{R}})^2} dx = \frac{1}{\ell(\tilde{\mathcal{R}})}.$$

Now we see that

$$\begin{aligned} C &= G^{-1/2} \ell(S)^{1/2} n^{-1} \ell(\mathcal{R})^{1/2} \\ &= \ell(S)^{1/2} n^{-1} \ell(\mathcal{R})^{1/2} \ell(\tilde{\mathcal{R}})^{1/2} \\ &= \frac{\ell(\mathcal{R})}{n}. \end{aligned}$$

Now Matsuda and Yajima (2009) point out that there will be an additional bias term which should be removed, which is

$$\begin{aligned} B &= \frac{\ell(S)}{Gn} \text{var}(Y) \\ &= \frac{\ell(S)\ell(\tilde{\mathcal{R}})}{n} \text{var}(Y) \\ &= \frac{\ell(\mathcal{R})}{n} \text{var}(Y). \end{aligned}$$

Putting all this together then, the periodogram version of the estimator proposed by Matsuda and Yajima (2009) is

$$\tilde{I}(k) = \frac{I(k)}{\hat{\lambda}_X^2} - \frac{\text{var}(Y)}{\hat{\lambda}_X}$$

where $\hat{\lambda}_X = n/\ell(\mathcal{R})$. Contrasting this with the equation from Daley and Vere-Jones (2003)

$$\begin{aligned} f_{\xi\xi}(k) &= \lambda_X \text{var}(Y) + \lambda_X^2 f_{YY}(k) \\ \Rightarrow f_{YY}(k) &= \frac{f_{\xi\xi}(k) - \lambda_X \text{var}(Y)}{\lambda_X^2} \\ &= \frac{f_{\xi\xi}(k)}{\lambda_X^2} - \frac{\text{var}(Y)}{\lambda_X}. \end{aligned}$$

Therefore, the estimator one would construct from our marked process methodology using the relation given by Daley and Vere-Jones (2003) coincides precisely with that proposed by Matsuda and Yajima (2009) in this case (we are just saying that n is random).

Of course, this does not tell us about the case when the sampling is not uniform (which in the framework of Matsuda and Yajima (2009) would correspond to inhomogeneity which we could not deal with). However, the approach of Matsuda and Yajima (2009) does not resolve the other, probably larger, issue of preferential sampling. By this we mean, when the point locations at which we sample the field are not independent of the field. The methodology proposed by Matsuda and Yajima (2009) also does not address dependence within the sampling locations, independent of the field.

S9 Additional details from the main simulation study

Say that the p th process is a log-Gaussian random field, and the q th and r th processes are point processes which are conditionally inhomogeneous Poisson processes with rate function $Y_p(s)$, but which are conditionally independent of each other. Let c be the covariance function of the Gaussian random field, from Møller et al. (1998) we have

$$\begin{aligned} \lambda_q &= e^{\lambda_p + c(0)/2} \\ \check{c}_{q,q}(u) &= (\lambda_q)^2 [e^{c(u)} - 1] + \lambda_q \delta(u). \end{aligned}$$

By similar arguments one also has

$$\begin{aligned} \check{c}_{q,p}(u) &= (\lambda_q)^2 [e^{c(u)} - 1] \\ \check{c}_{q,r}(u) &= (\lambda_q)^2 [e^{c(u)} - 1] \end{aligned}$$

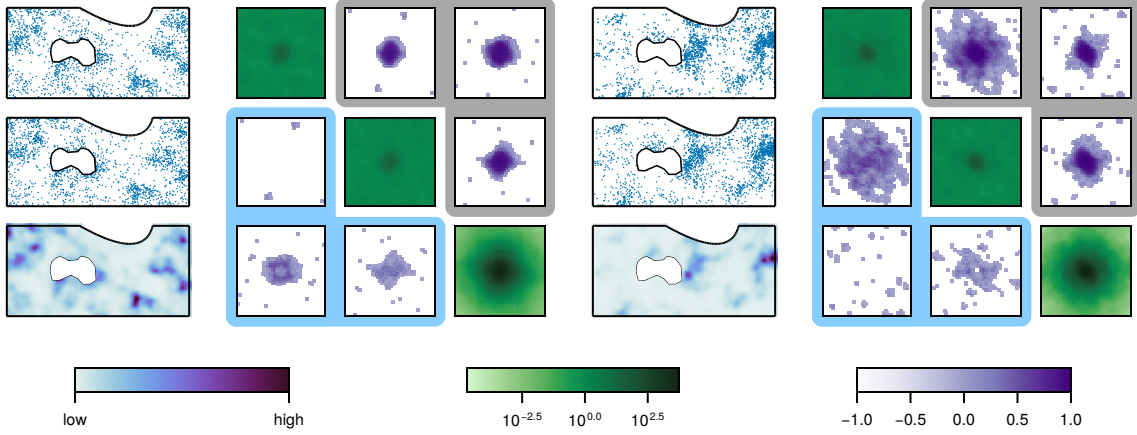


Figure 7: A realization of models 2 (left) and 3 (right). The spatial data has axes 0 to 1000 and 0 to 500, and the wavenumber domain plots show both k_1 and k_2 ranging from -0.05 to 0.05. Colorbars indicate from left to right, the value of the field from low to high, the value of the log standardized marginal spectra and the value of the signed coherence and signed partial coherence. In both cases, the swamp is excluded.

In the wavenumber domain, the spectral density functions are therefore

$$\begin{aligned} f_{q,q}(k) &= (\lambda_q)^2 \int_{\mathbb{R}^d} (e^{c(u)} - 1) e^{-2\pi i u \cdot k} du + \lambda_q, \\ f_{p,q}(k) &= (\lambda_q)^2 \int_{\mathbb{R}^d} (e^{c(u)} - 1) e^{-2\pi i u \cdot k} du, \\ f_{p,r}(k) &= (\lambda_q)^2 \int_{\mathbb{R}^d} (e^{c(u)} - 1) e^{-2\pi i u \cdot k} du. \end{aligned}$$

For the final model, we approximate the true spectral density function through simulations. In particular, we simulate 1000 realizations on the full 1000m by 500m square, and then estimate the spectral density matrix function using a small bandwidth. We then average the results to get a good approximation of the true spectral density matrix function. From this, we then compute coherence and partial coherence for the comparisons.

Example realizations and corresponding spectral estimates for models 2 and 3 are shown in Fig. 7. We can see that the estimated spectra do a good job of reflecting the underlying structure of the model from which the data was simulated.

S10 Additional simulation models and results

S10.1 Colocation model

Consider a multivariate random field model, in particular, a colocation model, see Waagepetersen et al. (2016) for a description. In our case, we consider one shared latent field, and two individual fields, so that the output fields are given by

$$\begin{aligned} Y_1(s) &= U_1(s) + \alpha_1 X(s), \\ Y_2(s) &= U_2(s) + \alpha_2 X(s), \end{aligned}$$

for some $\alpha_1, \alpha_2 \in \mathbb{R}$. In our case, the random fields U_1, U_2, X are all assumed to be independent of each other. In this case, we have that for $1 \leq p, q \leq 2$,

$$f_{p,q}^{(Y)}(k) = f_{p,q}^{(U)}(k) \delta_{p,q} + \alpha_p \alpha_q f^{(X)}(k),$$

where subscripts indicate the spectrum corresponds to that kind of process.

Furthermore, we assume the processes U_1, U_2, X are Gaussian with the same marginal covariance structure, but we choose different grids for the sampling two processes Y_1 and Y_2 . Recall the grid for the j th process is specified by its spatial offset v_j , and sampling interval Δ_j , which in this case are both in \mathbb{R}^2 . In particular,

The grids are defined by

$$\begin{aligned} v_1 &= (0, 0), & \Delta_1 &= (5, 5), \\ v_2 &= (0, 3), & \Delta_2 &= (10, 15). \end{aligned}$$

And the covariance function is Matérn, with length scale $\ell = 20$ and smoothness parameter $\nu = 3$ (and variance $\sigma = 1.0$). We take $\alpha_1 = 0.8$ and $\alpha_2 = 0.5$.

We run the simulation 1000 times. We show the average of the log spectrum, and the coherence and phase in Fig. 8. The average estimate is close to the true value, and the estimate from a single realization is also close to the true value. However, as expected we can see the effect of aliasing in the second process, as that grid is courser.

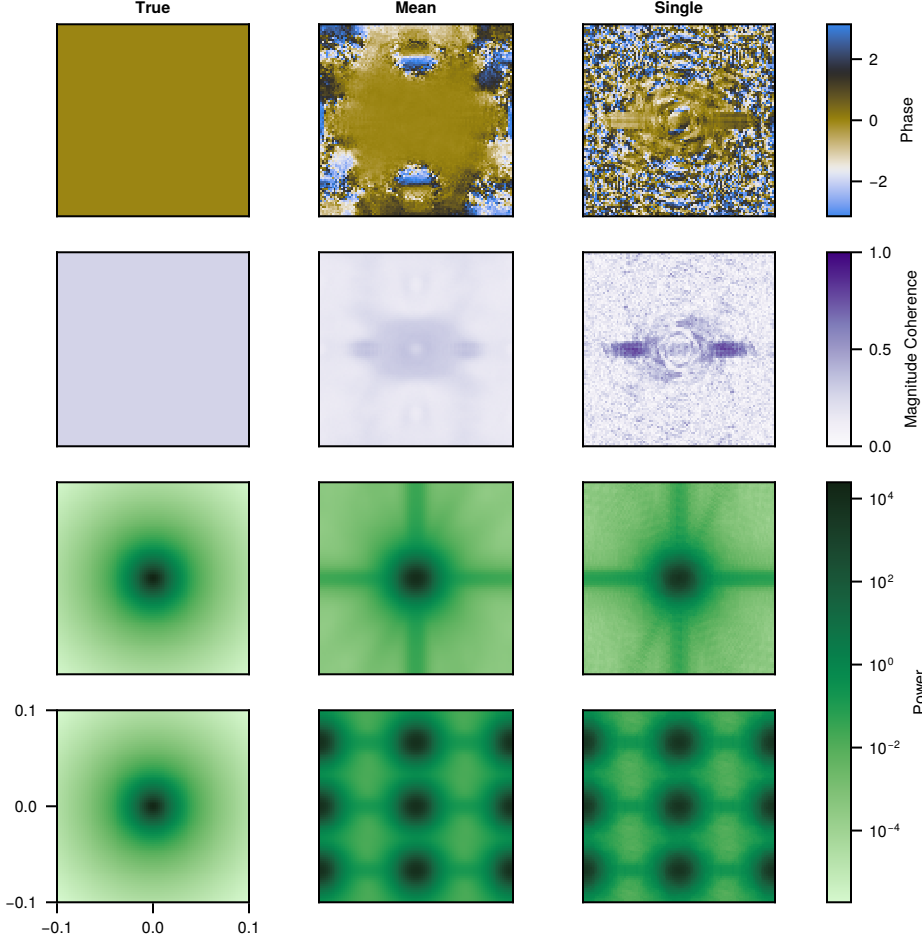


Figure 8: The log marginal spectra, coherence and phase for the colocation model. In each case, we show and the ground truth (left), the average over 1000 replications (middle) and the estimate from a single realization (right). In the case of phase, the average estimate uses a circular average.

S10.2 Shifted point pattern

Say that we have some initial point pattern ξ_p , whose covariance has no atoms other than at zero. Construct ξ_q by shifting every point in the original pattern by some fixed $\tau \in \mathbb{R}^d \setminus \{0\}$, i.e. so that $\xi_q(B) = \xi_p(B - \tau)$. Then there is an atom present in the cross-covariance (though it is not at zero), in particular

$$\check{c}_{p,q}(u) = \lambda_p \delta(u + \tau) + \check{c}_{[p,p]}(u + \tau) = \check{c}_{p,p}(u + \tau), \quad u \in \mathbb{R}^d,$$

where $\check{c}_{[p,p]}$ is the factorial covariance density of the point process ξ_p . Thus the cross-spectral density function is given by

$$\begin{aligned} f_{p,q}(k) &= \int_{\mathbb{R}^d} \check{c}_{p,p}(u + \tau) e^{-2\pi i u \cdot k} du \\ &= f_{p,p}(k) e^{2\pi i \tau \cdot k}, \end{aligned}$$

for $k \in \mathbb{R}^d$.

Though not a realistic process, this shifted example is still important as these simple cases are helpful for developing intuition about the cross-spectral density function and related quantities. In particular, the two processes in question have perfect coherence, but with some fixed phase. In the time series case, taking a process and its deterministic shift, we also have perfect coherence and some phase determined by the shift. As in the time series case, such examples allow us to build intuition about phase in terms of spatial shifts.

Consider a Poisson process with intensity $\lambda = 0.001$, and then make a second by shifting the first by $(10.5, 15)$, again performing 1000 replications. The average vs true log marginal spectra, coherence and phase are shown in Fig. 9. We see that as in the theory, the estimate obtains a constant coherence with a phase which is linear, though it is plotted modulus 2π on the interval $(-\pi, \pi]$.

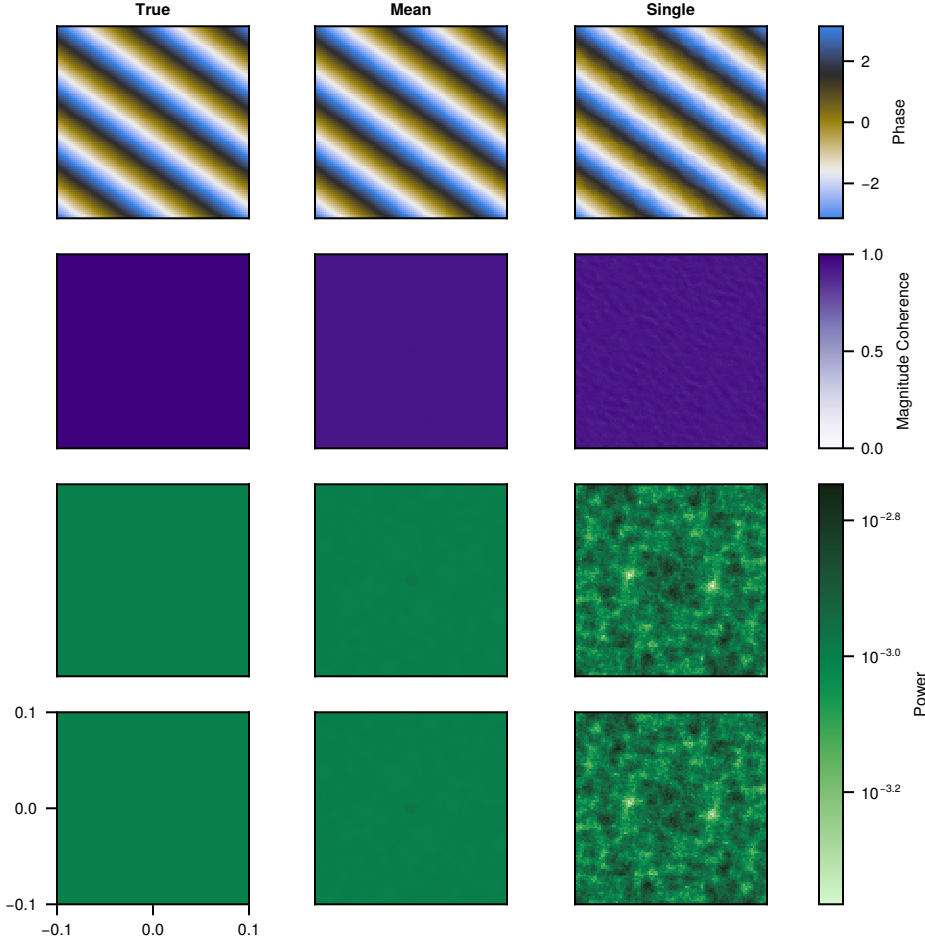


Figure 9: The log marginal spectra, coherence and phase for the shifted model. In each case, we show the ground truth (left), the average over 1000 replications (middle) and the estimate from a single realization (right). In the case of phase, the average estimate uses a circular average.

S10.3 Partial correlation of normal random variables

We use the distribution of magnitude correlation for magnitude partial correlation of normal random variables in the paper. To examine this, we consider a simple simulation experiment. In particular, define

$$\begin{aligned} z &\sim \mathcal{CN}(0, 1, 0) \\ \epsilon &\sim \mathcal{CN}(0, 1, 0) \\ \nu &\sim \mathcal{CN}(0, 1, 0) \\ \eta &= \rho\epsilon + (1 - \rho^2)^{1/2}\nu \\ x &= z + \epsilon\sigma \\ y &= z + \eta\sigma \end{aligned}$$

and consider the correlation of x and y , and the partial correlation of x and y given z . Assume that we obtain n replications of x, y, z . We compute the sample magnitude correlation and partial magnitude correlation for a range of ρ in simulations (assuming the mean is known to be zero and fixing $\sigma = 1$). We perform this experiment 10000 times for each value of ρ and multiple values of n . We show the results in Fig. 10. Note that except for very small n , the distributional approximation is very good for the partial magnitude correlation (of course it is exact for magnitude correlation).

S11 Additional application figures

The phase for the Barro Colorado Island data for the first analysis (*B. tovarensis*, *P. armata*, *U. pittieri* and gradient) is shown in Fig. 11. We see that for large values of the marginal spectra, they are close to zero as expected.

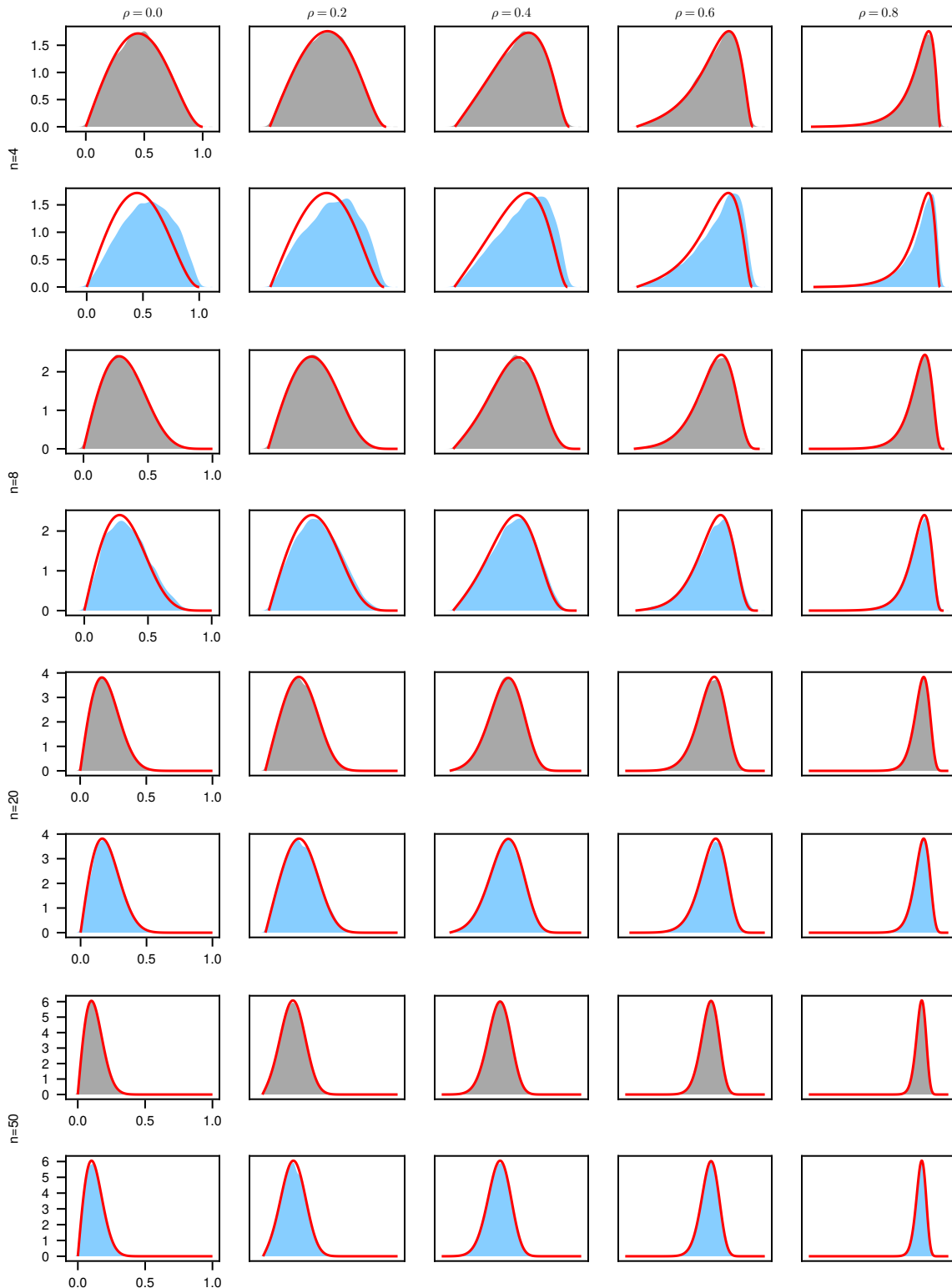


Figure 10: The empirical distributions of the magnitude correlation and partial magnitude correlation for normal random variables vs the truth (shown by the red line). Rows are organized so they alternate correlation (gray) and partial correlation (blue).

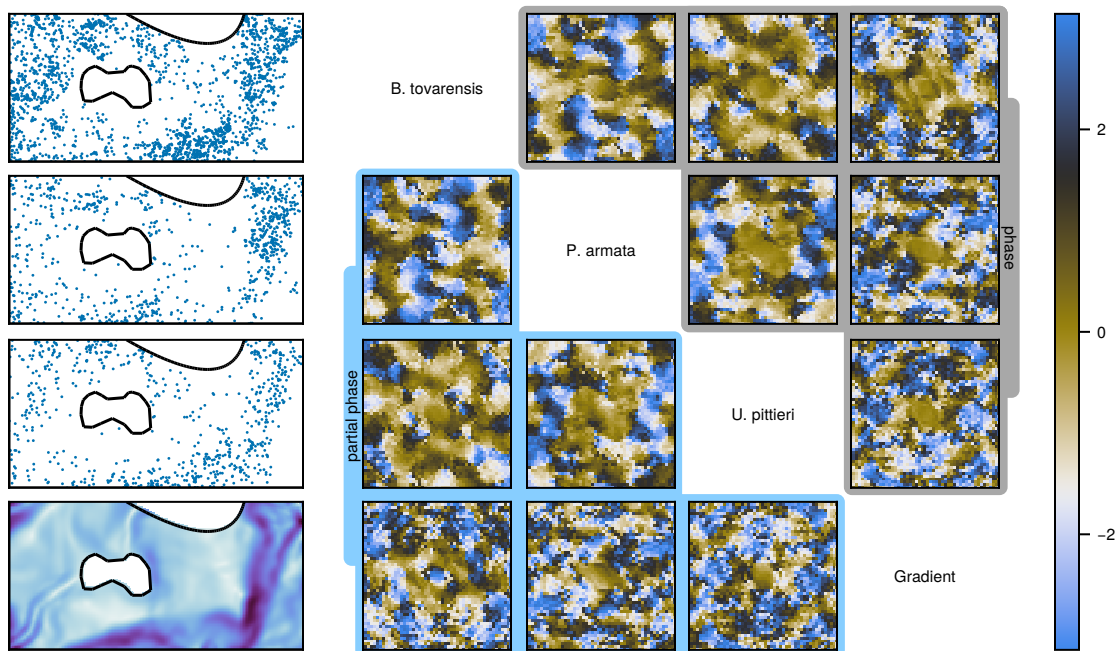


Figure 11: The phase (upper triangle of the plot matrix) and partial phase (lower triangle) of *B. tovarensis*, *P. armata*, *U. pittieri* and the gradient of the terrain. The spatial data has axes 0 to 1000 and 0 to 500, and the wavenumber domain plots ranging from -0.05 to 0.05 in both x and y axes.

References

Adler, R. J. (2010). *The Geometry of Random Fields*. SIAM.

Andén, J. and Romero, J. L. (2020). Multitaper estimation on arbitrary domains. *SIAM Journal on Imaging Sciences*, 13(3):1565–1594.

Baddeley, A. J., Møller, J., and Waagepetersen, R. (2000). Non-and semi-parametric estimation of interaction in inhomogeneous point patterns. *Statistica Neerlandica*, 54(3):329–350.

Bandyopadhyay, S. and Lahiri, S. N. (2009). Asymptotic properties of discrete Fourier transforms for spatial data. *Sankhyā: The Indian Journal of Statistics, Series A*, pages 221–259.

Barnett, A. H., Magland, J., and af Klinteberg, L. (2019). A parallel nonuniform fast Fourier transform library based on an “exponential of semicircle” kernel. *SIAM Journal on Scientific Computing*, 41(5):C479–C504.

Bartlett, M. S. (1963). The spectral analysis of point processes. *Journal of the Royal Statistical Society Series B: Statistical Methodology*, 25(2):264–281.

Bartlett, M. S. (1964). The spectral analysis of two-dimensional point processes. *Biometrika*, 51(3/4):299–311.

Biscio, C. A. and Coeurjolly, J.-F. (2016). Standard and robust intensity parameter estimation for stationary determinantal point processes. *Spatial Statistics*, 18:24–39.

Biscio, C. A. N. and Waagepetersen, R. (2019). A general central limit theorem and a subsampling variance estimator for α -mixing point processes. *Scandinavian Journal of Statistics*, 46(4):1168–1190.

Bonferroni, C. (1936). Teoria statistica delle classi e calcolo delle probabilità. *Pubblicazioni del R istituto superiore di scienze economiche e commerciali di firenze*, 8:3–62.

Brillinger, D. (1972). The spectral analysis of stationary interval functions. *Proceedings of the 6th Berkeley Symposium on Mathematical Statistics and Probability*, 1.

Brillinger, D. R. (1965). An introduction to polyspectra. *The Annals of Mathematical Statistics*, 36(5):1351–1374.

Brillinger, D. R. (1974). *Time Series: Data Analysis and Theory*. International series in decision processes. Holt, Rinehart, and Winston, New York.

Brillinger, D. R. (1982). Asymptotic normality of finite Fourier transforms of stationary generalized processes. *J. Multivariate Anal.*, 12(1):64–71.

Carter, G., Knapp, C., and Nuttall, A. (1973). Statistics of the estimate of the magnitude-coherence function. *IEEE transactions on audio and electroacoustics*, 21(4):388–389.

Carter, G. C. (1987). Coherence and time delay estimation. *Proceedings of the IEEE*, 75(2):236–255.

Condit, R., Pérez, R., Aguilar, S., Lao, S., Foster, R., and Hubbell, S. (2019). Complete data from the Barro Colorado 50-ha plot: 423617 trees, 35 years.

Cooley, J. W. and Tukey, J. W. (1965). An algorithm for the machine calculation of complex Fourier series. *Mathematics of computation*, 19(90):297–301.

Dahlhaus, R. (2000). Graphical interaction models for multivariate time series. *Metrika*, 51:157–172.

Daley, D. J. and Vere-Jones, D. (2003). *An Introduction to the Theory of Point Processes, Volume I: Elementary Theory and Methods*. Springer.

Daley, D. J. and Vere-Jones, D. (2007). *An introduction to the theory of point processes: volume II: general theory and structure*. Springer Science & Business Media.

Diggle, P. J., Gates, D. J., and Stibbard, A. (1987). A nonparametric estimator for pairwise-interaction point processes. *Biometrika*, 74(4):763–770.

Dutt, A. and Rokhlin, V. (1993). Fast Fourier transforms for nonequispaced data. *SIAM Journal on Scientific computing*, 14(6):1368–1393.

Eckardt, M. and Mateu, J. (2019a). Analysing multivariate spatial point processes with continuous marks: A graphical modelling approach. *International Statistical Review*, 87(1):44–67.

Eckardt, M. and Mateu, J. (2019b). Partial characteristics for marked spatial point processes. *Environmetrics*, 30(6):e2565.

Eckardt, M. and Mateu, J. (2019c). A spatial dependence graph model for multivariate spatial hybrid processes. *arXiv preprint arXiv:1906.07798*.

Eichler, M., Dahlhaus, R., and Sandkühler, J. (2003). Partial correlation analysis for the identification of synaptic connections. *Biological cybernetics*, 89(4):289–302.

Goodman, N. R. (1957). *On the Joint Estimation of the Spectra, Cospectrum and Quadrature Spectrum of a Two-Dimensional Stationary Gaussian Process*. Princeton University.

Gröchenig, K. (1996). An uncertainty principle related to the poisson summation formula. *Studia Mathematica*, 121(1):87–104.

Guillaumin, A. P., Sykulski, A. M., Olhede, S. C., and Simons, F. J. (2022). The debiased spatial Whittle likelihood. *Journal of the Royal Statistical Society Series B: Statistical Methodology*, 84(4):1526–1557.

Harms, K. E., Condit, R., Hubbell, S. P., and Foster, R. B. (2001). Habitat associations of trees and shrubs in a 50-ha neotropical forest plot. *Journal of ecology*, 89(6):947–959.

Hubbell, S. P. and Foster, R. B. (1983). Diversity of canopy trees in a neotropical forest and implications for conservation. In Whitmore, T., Chadwick, A., and Sutton, A., editors, *Tropical Rain Forest: Ecology and Management*, pages 25–41. The British Ecological Society, Oxford.

Hubbell, S. P. and Foster, R. B. (1986). Commonness and rarity in a neotropical forest: implications for tropical tree conservation. In Soule, M., editor, *Conservation biology: the science of scarcity and diversity*, pages 205–231. Sinauer Associates, Sunderland, MA.

Illian, J., Penttinen, A., Stoyan, H., and Stoyan, D. (2008). *Statistical Analysis and Modelling of Spatial Point Patterns*. John Wiley & Sons.

Kanaan, M., Taylor, P. C., and Mugglestone, M. (2008). Cross-spectral properties of a spatial point-lattice process. *Statistics & Probability Letters*, 78(18):3238–3243.

Masry, E. (1978). Poisson sampling and spectral estimation of continuous-time processes. *IEEE Transactions on Information Theory*, 24(2):173–183.

Masry, E. (2003). Alias-free sampling: An alternative conceptualization and its applications. *IEEE Transactions on Information Theory*, 24(3):317–324.

Matsuda, Y. and Yajima, Y. (2009). Fourier analysis of irregularly spaced data on \mathbb{R}^d . *Journal of the Royal Statistical Society Series B: Statistical Methodology*, 71(1):191–217.

Miller, K. S. (1980). *Hypothesis testing with complex distributions*. Krieger, Huntington - N.Y.

Møller, J., Syversveen, A. R., and Waagepetersen, R. P. (1998). Log Gaussian Cox processes. *Scandinavian journal of statistics*, 25(3):451–482.

Møller, J. and Waagepetersen, R. P. (2003). *Statistical Inference and Simulation for Spatial Point Processes*. CRC press.

Mrkvíčka, T. and Myllymäki, M. (2023). False discovery rate envelopes. *Statistics and Computing*, 33(5):109.

Mugglestone, M. A. and Renshaw, E. (1996a). The exploratory analysis of bivariate spatial point patterns using cross-spectra. *Environmetrics*, 7(4):361–377.

Mugglestone, M. A. and Renshaw, E. (1996b). A practical guide to the spectral analysis of spatial point processes. *Computational Statistics & Data Analysis*, 21(1):43–65.

Percival, D. B. and Walden, A. T. (1993). *Spectral Analysis for Physical Applications*. Cambridge University Press.

Rajala, T. A., Olhede, S. C., Grainger, J. P., and Murrell, D. J. (2023). What is the Fourier transform of a spatial point process? *IEEE Transactions on Information Theory*, 69(8):5219–5252.

Renshaw, E. (2002). Two-dimensional spectral analysis for marked point processes. *Biometrical Journal: Journal of Mathematical Methods in Biosciences*, 44(6):718–745.

Riedel, K. S. and Sidorenko, A. (1995). Minimum bias multiple taper spectral estimation. *IEEE Transactions on Signal Processing*, 43(1):188–195.

Schur, J. (1911). Bemerkungen zur theorie der beschränkten bilinearformen mit unendlich vielen veränderlichen. *Journal für die reine und angewandte Mathematik*, 1911(140):1–28.

Simons, F. J. and Wang, D. V. (2011). Spatiospectral concentration in the Cartesian plane. *GEM-International Journal on Geomathematics*, 2:1–36.

Stein, E. M. and Weiss, G. (1971). *Introduction to Fourier analysis on Euclidean spaces*, volume 1. Princeton university press.

Thomson, D. (1982). Spectrum estimation and harmonic analysis. *Proceedings of the IEEE*, 70(9):1055–1096.

Waagepetersen, R., Guan, Y., Jalilian, A., and Mateu, J. (2016). Analysis of multispecies point patterns by using multivariate log-Gaussian Cox processes. *Journal of the Royal Statistical Society: Series C (Applied Statistics)*, 65(1):77–96.

Walden, A. T. (2000). A unified view of multitaper multivariate spectral estimation. *Biometrika*, 87(4):767–788.

Whittaker, J. (2009). *Graphical Models in Applied Multivariate Statistics*. Wiley Publishing.

Yang, J. and Guan, Y. (2024). Fourier analysis of spatial point processes. *arXiv preprint arXiv:2401.06403*.